Stockholm University

C–H and Si–H functionalization using redox-active diazo compounds and decarboxylative coupling

Rajdip Chowdhury

Doctoral Thesis in Organic Chemistry at Stockholm University, Sweden 2022

C–H and Si–H functionalization using redox-active diazo compounds and decarboxylative coupling

Rajdip Chowdhury

Academic dissertation for the Degree of Doctor of Philosophy in Organic Chemistry at Stockholm University to be publicly defended on Friday 11 March 2022 at 10.00 in Magnélisalen, Kemiska övningslaboratoriet, Svante Arrhenius väg 16 B.

Abstract

The work presented in this thesis is based on two basic organic chemistry concepts: carbene catalysis and radical coupling reactions. Diazo compounds in the presence of transition-metal catalysts are known to be excellent reagents for the construction of C–X bonds (X = C, Si, N, O, etc.) under mild conditions. However, their applications are limited to conventional diazo compounds (e.g. diazoacetates, diazonitriles, diazoketones, etc.), where further modifications of the products after carbene transfer are not feasible. The thesis aims at the development of new methodologies using a diazo compound with a geminal radical precursor as methylene equivalent. In **Chapter 2** of this thesis, a unified C–H alkylation of indole using this redox-active diazo compound, NHPI-DA has been presented. This process includes a highly selective insertion of ruthenium-carbenes into C–H bond of indoles at the C2- and C3- positions. These products have been diversified into a variety of functionalized indoles (e.g. boryl, aryl, alkyl, alkenyl, etc.) at the C3-position. These unified alkylation conditions can be a potential alternative for late-stage functionalization of indoles. In **Chapter 3** of this thesis, decarboxylative radical couplings of redox-active *N*-hydroxyphthalimide (NHPI) esters with electron-poor olefins have been described. This methodology utilizes self-sensitized photoreductants, dihydronicotinamides to generate alkyl radicals from redox-active carboxylates in presence of blue light. This approach, unlike the typical photo-redox chemistry, is independent of using photocatalysts or inorganic reductants. Moreover, we have demonstrated that NADH which is a native cofactor in living organisms, can efficiently couple alkyl radicals with DNA-encoded Michael acceptors. The mechanism of the reaction has been established through detailed kinetic and photophysical studies. **Chapter 4** of this thesis focuses on the development of new syntheses of (borylmethyl)silanes. These compounds are unique due to the presence of orthogonal silicon and boron moiety at the same carbon atom and display significant applications for the synthesis of molecules of great synthetic value. This approach involves a ruthenium-catalyzed insertion of the NHPI-DA into Si–H bond and a subsequent decarboxylative borylation of the resulting redox-active esters. Interestingly, using this method a wide variety of silanes have been transformed into the corresponding (borylmethyl)silanes.

Keywords: *carbenes, radicals, redox-active esters, indoles, carboxylic acids, silanes, photochemistry.*

Stockholm 2022
http://urn.kb.se/resolve?urn=urn:nbn:se:su:diva-201458

ISBN 978-91-7911-776-4
ISBN 978-91-7911-777-1

Department of Organic Chemistry

Stockholm University, 106 91 Stockholm

C–H AND SI–H FUNCTIONALIZATION USING REDOX-ACTIVE DIAZO COMPOUNDS AND DECARBOXYLATIVE COUPLING

Rajdip Chowdhury

Stockholm University

C–H and Si–H functionalization using redox-active diazo compounds and decarboxylative coupling

Rajdip Chowdhury

ISBN print 978-91-7911-776-4
ISBN PDF 978-91-7911-777-1

Printed in Sweden by Universitetsservice US-AB, Stockholm 2022

To my father

'Where the mind is
without fear and the
head is held high
Where knowledge is
free...'

Rabindranath Tagore

Abstract

The work presented in this thesis is based on two basic organic chemistry concepts: carbene catalysis and radical coupling reactions. Diazo compounds in the presence of transition-metal catalysts are known to be excellent reagents for the construction of C–X bonds (X = C, Si, N, O, etc.) under mild conditions. However, their applications are limited to conventional diazo compounds (e.g. diazoacetates, diazonitriles, diazoketones, etc.), where further modifications of the products after carbene transfer are not feasible. The thesis aims at the development of new methodologies using a diazo compound with a geminal radical precursor as methylene equivalent. In **Chapter 2** of this thesis, a unified C–H alkylation of indole using this redox-active diazo compound, NHPI-DA has been presented. This process includes a highly selective insertion of ruthenium-carbenes into C–H bond of indoles at the C2- and C3- positions. These products have been diversified into a variety of functionalized indoles (e.g. boryl, aryl, alkyl, alkenyl, etc.) at the C3-position. These unified alkylation conditions can be a potential alternative for late-stage functionalization of indoles. In **Chapter 3** of this thesis, decarboxylative radical couplings of redox-active *N*-hydroxyphthalimide (NHPI) esters with electron-poor olefins have been described. This methodology utilizes self-sensitized photoreductants, dihydronicotinamides to generate alkyl radicals from redox-active carboxylates in presence of blue light. This approach, unlike the typical photo-redox chemistry, is independent of using photocatalysts or inorganic reductants. Moreover, we have demonstrated that NADH which is a native cofactor in living organisms, can efficiently couple alkyl radicals with DNA-encoded Michael acceptors. The mechanism of the reaction has been established through detailed kinetic and photophysical studies. **Chapter 4** of this thesis focuses on the development of new syntheses of (borylmethyl)silanes. These compounds are unique due to the presence of orthogonal silicon and boron moiety at the same carbon atom and display significant applications for the synthesis of molecules of great synthetic value. This approach involves a ruthenium-catalyzed insertion of the NHPI-DA into Si–H bond and a subsequent decarboxylative borylation of the resulting redox-active esters. Interestingly, using this method a wide variety of silanes have been transformed into the corresponding (borylmethyl)silanes.

Populärvetenskaplig sammanfattning

Organisk kemi är ett vetenskapsområde som vi studerar på skolan, men det är fortfarande kopplat till våra liv sedan vi föds. Från livräddande medicinerna till våra kläderna allt är tillverkning med begreppen av organisk kemi. C− H och Si− H bindnings funktionalisering är viktigaste teknikerna som används inom organisk kemi som har direkt inverkan i vårt dagliga liv. I denna doktorsavhandling beskriver arbetet användning av en redoxaktiv diazoförening med en ruteniumkatalysator och användning av kemin för dekarboxylering för att modifiera olika funktionaliserade produkter. **Kapitel 2** beskriver C−H-bindningsalkyleringen av indoler. Indoler finns i kärnan av många naturliga produkter och läkemedelskandidater. Kombinationen av NHPI-DA och en ruteniumkatalysator (RuPheox) gör det möjligt att syntetisera bibliotek av syntetiskt användbara organiska föreningar som innehåller olika funktionella grupper. Dessa viktiga klasser av indoler kan endast syntetiseras med specialdesignade reagenser, hårda reaktionsförhållanden och längre syntesvägar. I **Kapitel 3** beskrivs dekarboxylativa Giese-reaktioner av redoxaktiva NHPI estrar med elektronbristande olefiner med hjälp av biokompatibla fotoreduktanter och blått ljus. Tidigare har denna typ av reaktivitet utförts med användning av ytterligare fotokatalyter och/eller oorganiska reduktionsmedel. Omfattningen och användbarheten av detta arbete har illustrerats med användningen av NADH som fotodeduktant, vilket är en kofaktor i levande organismer. Dessutom har denna metod tillämpats i synteserna av DNA-kodade bibliotek, vilket visar den syntetiska användbarheten av arbetet. Rigorösa kinetiska och mekanistiska studier utförs för att fastställa mekanismen för denna foto-Giese-reaktion. I **Kapitel 4** av denna doktorsavhandling beskriver en enkärlssyntes av (borylmetyl)silaner via Si− H funktionalisering med användning av NHPI-DA och ruteniumkatalysatorn (RuPheox). Kiselorganiska föreningar har breda tillämpningar inom material- och medicinska vetenskaper även i vårt dagliga liv. Den ortogonala karbenradikala kemin har lett oss till att komma åt dessa föreningar från strukturellt olika silaner med milda reaktionsförhållanden snarare än att använda specialdesignade reagenser, hög temperatur och överskott av utgångsmaterial. I slutet har den syntetiska tillämpningen av denna kemi utvidgats till synteser av oxasilacyklopentaner via difunktionalisering av enolföreningar med användning av NHPI-DA.

List of Publications

This thesis is based on the following publications

***1. N*-Hydroxyphthalimidyl Diazoacetate (NHPI-DA): A Modular Methylene Linchpin for the C–H Alkylation of Indoles.**
Rajdip Chowdhury and Abraham Mendoza*
Chem. Commun., **2021**, *57*, 4532-4535.

***2.* Decarboxylative Alkyl Coupling Promoted by NADH and Blue Light.**
Rajdip Chowdhury,‡ Zhunzhun Yu,‡ My Linh Tong, Stefanie V. Kohlhepp, Xiang Yin and Abraham Mendoza*
J. Am. Chem. Soc. **2020**, *142*, 20143–20151.
‡ These authors contributed equally
This paper was featured in the cover of the journal

3. **Modular Synthesis of (Borylmethyl)silanes through C1 Difunctionalization**
Rajdip Chowdhury, Gabor Z. Elek and Abraham Mendoza* *(manuscript)*

Previous Documents Based on This Work

The thesis is partly based on the author's half-time report titled 'C–H functionalization with redox-active carbenes and related decarboxylative coupling reactions'(presented on March 4th, 2021).

Chapter 1 (*introduction*) of the thesis has been updated with more details about single carbon building blocks, carbenes and redox-active esters. References has been updated accordingly.

Chapter 2 (*paper I*) was present in the half-time report and has been modified both in terms of the texts and schemes.

Chapter 3 (*paper II*) was present in the half-time report and has been revised both in terms of the texts and schemes.

Chapter 4 (*paper III*) was not present in the half-time report and has been written entirely based on new experimental results.

Contents

Abbreviations

Abbreviations are used in agreement with the standards of the subject.* Additional abbreviations used in this thesis are given below:

ACBP	Axially chiral bipyridine
BDBMP	l,6-bis(dimethylamino)pyrene
BOX	Bisoxazoline
bpy	2,2’-Bipyridine
DCC	*N,N'*-Dicyclohexylcarbodiimide
DCM	Dichloromethane
DMF	*N,N*-Dimethylformamide
DMFDMA	*N,N*-Dimethylformamide dimethyl acetal
DMAc	*N,N*-Dimethylacetamide
DMSO	Dimethylsulfoxide
DOSP	Dodecylphenylsulfonyl)prolinato]dirhodium
DPEPhos	Bis[(2-diphenylphosphino)phenyl] ether
di-*t*Bubpy	4,4’di-*tert*-butyl-2,2’-bipyridine
equiv.	Equivalent
EDA	Electron donor acceptor
EDG	Electron donating group
EWG	Electron withdrawing group
HAT	Hydrogen atom transfer
NTTL	*N*-1,2-naphthaloyl-(*S*)-*tert*-leucine
NHPI	*N*-hydroxyphthalimide
OPC	Organo-photocatalyst
ppy	2-Phenylpyridine
pin	Pinacol
PC	Photocatalyst
r.t.	Room temperature
SET	Single electron transfer
SnAP	Sn (tin) amino protocol
SPA	Spiro phosphoric acid

TCSPC	Time-correlated single photon counting
THF	Tetrahydrofuran
TMHD	2,2,6,6-tetramethyl-3,5-heptanedionate
TMG	1,1,3,3-Tetramethylguanidine
TMEDA	Tetramethylethylenediamine
TPP	Tetraphenylporphyrin
TTN	Total turnover number

*The ACS Style Guide, 3rd Edition, American Chemical Society: Washington, DC, 2006

1. Introduction

1.1 Synthesis with Single Carbon Building Blocks

The design and the synthesis of custom targeted libraries through late-stage functionalization strategies is a major endeavour in organic synthesis. Despite the success achieved in recent years, the main drawback of this strategy is the need of synthesizing specific substrates and reagents that carry the different functionalities desired in the final products. The use of elementary carbon units to which different functions and molecular fragments can be attached, is a potential solution to streamline the synthesis of compound libraries. In particular, methylenes (–CH_2–) are common single carbon (C1) units in organic molecules such as natural products and pharmaceuticals. However, methylene synthetic equivalents are yet to be implemented in diversity oriented synthesis (DOS) due to the problematic identification of two or more orthogonal functionalization handles that can be set in the same carbon atom.[1]

In the past few decades, significant progress has been made in the chemistry of C1 building blocks (Figure 1.1). Most commonly explored C1 synthons in academic and industrial research are carbon monoxide,[2a,k] carbon dioxide,[2a,d,k] methane,[2a,k] methanol,[2l] formaldehyde[2b,n] and formic acid[2m] (Figure 1.1 A). The use of these materials has allowed the production of petrochemicals, clean-fuels and value-added organic chemicals for years. However, heavy comsumption of these materials slowly leads to depletion of fossil resources. In addition, some of these single carbon building units are hazardous gases, and relatively inert, thus hindering their activation.[2a] Despite the recent development of the halomethyltrialkyltin derivatives (known as SnAP reagents) they are specifically designed and suited for the synthesis of heterocycles in small scale (Figure 1.1 B).[2g,h] Bromoform has also been reported in the synthesis of ishwarane as a C1 building block (Figure 1.1 C).[2i] More recently, it has been reported that chlorodifluoromethane can be used as a C1 synthon connecting two different anilines but its broader potential is yet unknown.[2j]

There exists an ample ground for the exploration of new C1 equivalents that bears versatile and unique reactivity to complement current DOS strategies, and are sufficiently practical to maximize adoption. Advances in this area would enable access to compound libraries by a systematic assembly of different fragments to a central methylene unit. In this thesis, carbenes with a geminal radical precursor are explored as methylene equivalents in different connective processes as well as related methodological developments required for this purpose (Figure 1.1 D).

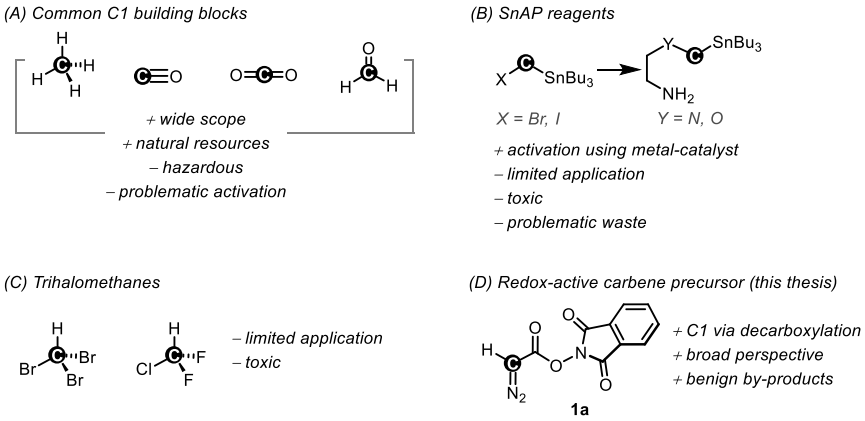

Figure 1.1: Progress in single carbon (C1) precursors in Organic Synthesis.[2]

1.2 Carbenes

1.2.1 History of Carbenes and Metal-Carbene Complexes

In 1855, Geuther and Hermann suggested that chloroform under basic medium leads to generation of a reactive intermediate, named dichlorocarbene ($:CCl_2$).[3,4a] This was proposed to be a short-lived, neutral, divalent and six-electron carbon intermediate bearing two unshared electrons. Later in 1897, Nef suggested the same reaction intermediate for the transformation of pyrrole to α -chloropyridine using chloroform.[4b] But it was only after the first synthesis of tropolones in 1953 (Scheme 1.1, top) that carbenes were widely recognized by the scientific community.[5a] Doering and Knox reported that the photochemical reaction between diazomethane and benzene proceeded *via* the formation of free methylene ($:CH_2$). The following year, they expanded the methodology by developing a cyclopropanation reaction using dibromocarbene generated from bromoform in basic medium (Scheme 1.1, bottom).[5b]

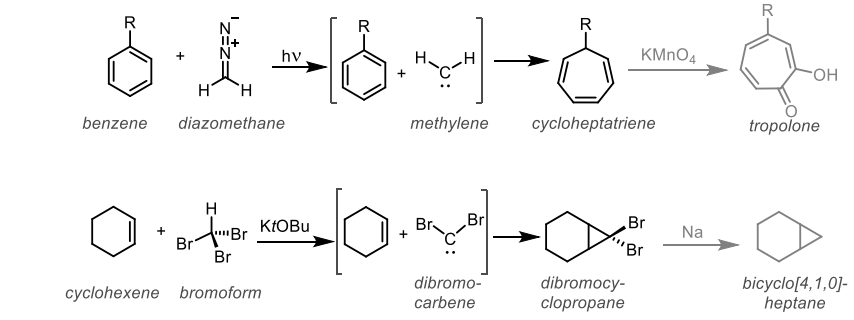

Scheme 1.1: Early discovery of carbenes.[5]

Depending on the electronic structure and reactivity carbenes are classified in two categories: singlet carbenes and triplet carbenes. In singlet carbene the carbenoid carbon is sp^2-hybridized, whereas triplet carbenes can be both sp^2- and *sp*-hybridized (Figure 1.2 A).

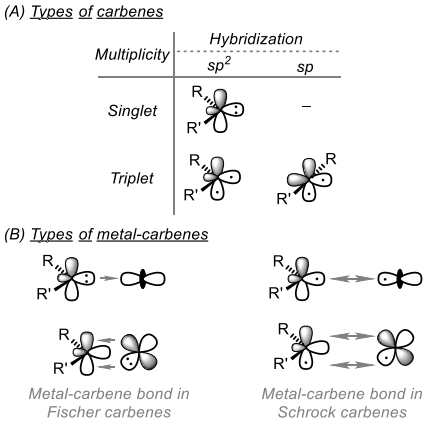

Figure 1.2: Reactivity of singlet and triplet carbenes.[6]

In 1964, Fischer and Maasböl synthesized the first metal-carbene complex using tungsten(0) pentacarbonyl as the supporting metal fragment.[6a,c] Unlike free carbenes, these so called Fischer-type carbene complexes are stable, featuring a carbenoid carbon in the singlet state and sp^2-hybridized. These complexes exhibit electrophilic character and are most common with middle or late transition-metals in low oxidation states (e.g. chromium(0), iron(0), manganese(0), etc.) and surrounded by π-acceptor ligands (Figure 1.2 B). In 1974, Schrock reported a different kind of carbene complex, where the carbenoid carbon is nucleophilic and sp^2-hybridized with triplet character.[6b,c] Schrock carbenes are common with early transition-metals in high oxidation state (e.g. titanium(IV), tantalum(V), etc.).

1.2.2 Reactivity of Metal-Carbene Complexes

Beyond stoichiometric reactions with transition-metal complexes, metal-carbenes are key intermediates in a wide range of catalytic reactions, and first examples were reported in 1958.[7] Initially, copper was employed in such transformations, before dirhodium tetracarboxylates became predominant catalysts in 1970s.[3c,d] Most commonly, metal-carbene complexes are prepared *in situ* when a diazo compound reacts with a transition-metal. These intermediates can react with a variety of organic substrates to generate valuable products *via* cycloadditions with π-systems (*i.e.* cyclopropanation, Büchner ring expansion, olefin-metathesis, Dötz-benzannulation) and insertion into X–H σ-bonds (X = C, N, Si, etc.) (Scheme 1.2 A). The insertion of metal-carbene species into X–H bonds are known to occur *via* two pathways: (1) the concerted mechanism, where the metal-carbene evolves through a single step insertion

(Scheme 1.2 B); and (2) the stepwise mechanism, where the insertion involves ylide formation and subsequent 1,2-proton shift (Scheme 1.2, C).[3e]

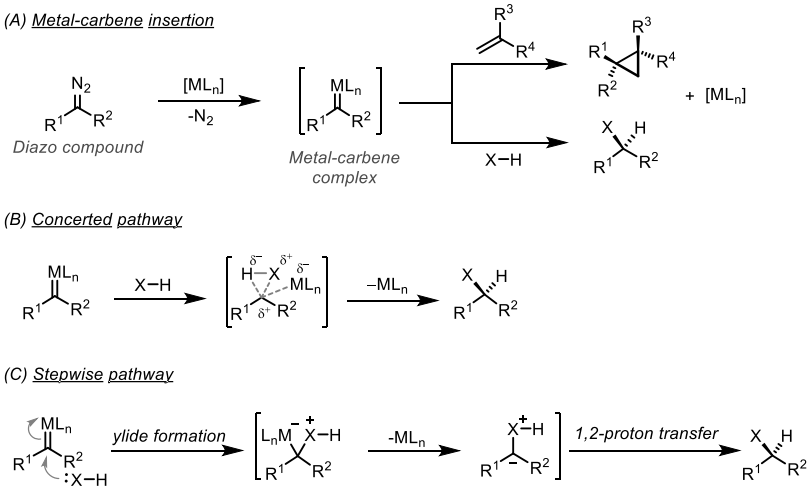

Scheme 1.2: (A) Insertion of metal-carbenes in organic molecules. (B) Concerted mechanism for the insertion in a general X–H bond. (C) Stepwise mechanism for the insertion in a general X–H bond.[3]

1.2.3 Carbene Precursors

Even though carbenes were initially generated through *α*-elimination reactions on haloforms, decades of research have resulted in new carbene sources with different properties. It is known that aryliodonium ylides can react with transition-metal complexes generating metal-carbenes,[8] and those can engage in different reactions, such as cyclopropanations, cycloadditions and intramolecular cyclizations (Scheme 1.3, Pathway A).[8] These hypervalent aryliodine(III) species can be readily obtained from compounds bearing acidic C–H bonds upon treatment with diacetoxyiodobenzene or equivalent reagents. Likewise, sulfonium and sulfoxonium ylides have also been used as metal-carbene precursors and their application in cylcopropanation and epoxidation and insertion reactions is well established (Scheme 1.3, Pathway B).[9] Despite these advances, these metal-carbene precursors suffer from several drawbacks, such as side-reactions, toxicity, poor atom economy and required waste management. In contrast, diazo compounds react with transition-metal catalysts to cleanly generate metal carbenes only producing inert nitrogen gas (Scheme 1.3, Pathway C).[3f] In addition, a wide variety of diazo compounds with different substitutions can be synthesized, thus providing access to a wider range of reactivity than other carbene precursors. As such, diazo compounds are probably the most common and versatile carbene sources currently used in organic synthesis.[3]

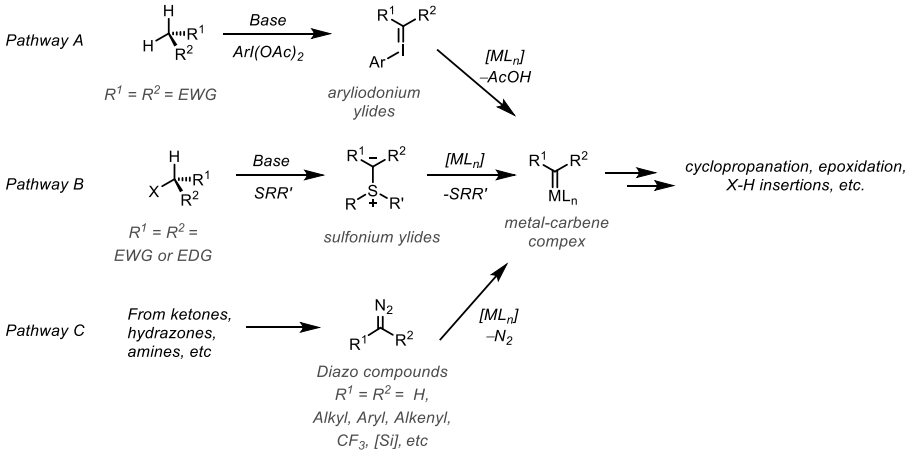

Scheme 1.3: Different types of metal-carbene precursors: (A) aryliodonium ylides, (B) sulfonium ylides; (C) diazo compounds.[3,8,9]

A major factor on the reactivity of metal-carbene complexes is the electronic properties of the two substituents at the carbenoid carbon. Depending on their electronic nature, metal-carbene complexes are classified into three categories: donor-acceptor (or *"push-pull"*), single acceptor and double acceptor carbene complexes (Figure 1.3).[10] Donor-acceptor metal-carbene complexes possess one electron-withdrawing group and one electron-donating group at the carbenoid carbon center. Donor-acceptor carbenes are more common due to their moderate reactivity and higher selectivity than that of other carbenes. Single acceptor carbenes with an electron-withdrawing group and a hydrogen atom at the carbene carbon are less stable (more reactive) towards organic substrates than donor-acceptor carbenes. On the other hand, double acceptor carbenes have two electron-withdrawing substituents at the carbon center that confer more electrophilicity and charge delocalization, thus resulting in more specialized applications than the other types of metal-carbenes.

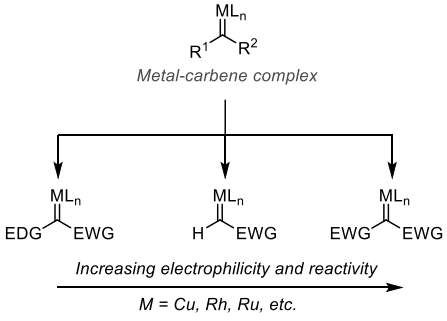

Figure 1.3: Types of metal-carbenes with respect to their substituents.[10]

Over decades, several transition-metal-catalyzed transformations have been developed using diazo compounds and copper, rhodium, or ruthenium catalysts. Copper complexes are inexpensive and have been widely used in many carbene insertion processes but these are not as effective as dirhodium (II) complexes.[3e] The dirhodium carbene complexes get additional stability through the assistance by the second rhodium atom, decreasing the activation energy of X–H insertion processes (X = C, N, O, Si, etc.).[3c] Ruthenium-carbene complexes are less electrophilic than their rhodium analogs and are most commonly employed in olefin metathesis,[11a] developed after seminal research on carbene complexes derived from phenyldiazomethane.[11b] Recently, ruthenium-carbene complexes have also been reported as efficient catalysts for the cyclopropanation of olefins but their overall impact in carbene transfer reactions is much lower than the copper and rhodium catalysts.[12]

1.2.4 Redox-Active Carbenes

Extensive studies on transition-metal-catalyzed diazo transfer reactions have led to the development of many valuable synthetic methods, such as cyclopropanation, C–H or Si–H bond functionalization and advanced cycloadditions.[3c-g] Despite the significant progress that has been made in this field, the scope and applications of such fundamental reactions are limited only to conventional stable diazo compounds, such as ethyl diazoacetate, α-aryl diazoacetates, diazonitriles, etc. Reactions with more advanced diazo compounds including versatile functionalization handles are limited by the stability of these precursors and the promiscous reactivity of the corresponding metal-carbene complexes. This way, it would be possible to introduce relevant functionalities by taking advantage of the powerful reactivity of carbenes.

Recently, Mendoza and co-workers have reported the development of redox-active carbenes and their use in enantioselective cyclopropanation reactions (Scheme 1.4).[13] These diazo compounds bear a redox-active *N*-hydroxyphthalimidyl ester functionality (see Section 1.3.2), which was found to be orthogonal to some geminal metal-carbenes. Moreover, it was discovered that these redox-active carbenes were more reactive and more selective than conventional diazoacetates. For example, *N*-hydroxyphthalimidyl diazoacetate (NHPI-DA; **1a**) proved to be efficient and enantioselective in the cyclopropanation of challenging aliphatic olefins.[13b] An important feature of these reagents is that after the cyclopropanation reaction, the resulting carbene transfer products were easily diversified into libraries of derivatives by taking advantage of the versatility bestowed by the redox-active ester handle in the diazo compound (see Section 1.3.2).[13] The increasing interest in new synthetic methods based on the reductive decarboxylation of these redox-active esters, continuously expand the opportunities presented by the synthetic intermediates produced after the carbene transfer.

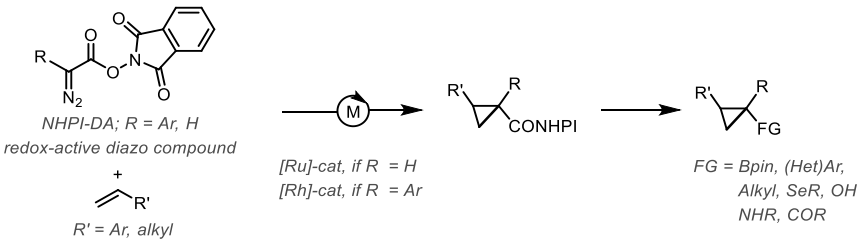

Scheme 1.4: Enantioselective cyclopropanation of unactivated olefins using redox-active carbenes.[13]

1.3 Redox-Active Esters as Radical Precursors

1.3.1 Carboxylic Acids as Radical Precursors

Carboxylic acids are highly abundant, cheap and stable organic substances that are found in alkaloids, terpenes, sugars, proteins, fatty acids and petrochemical feedstocks. Various core methods have been developed to convert them into derivatives such as acyl chlorides, esters, and amides. In 1962, Sir Derek Barton, for the first time used carboxylic acids as a source of alkyl radicals by transforming them to their xanthate derivatives.[14a] Thermolysis or photolysis of *O*-ethyl-*S*-phenylacetyl xanthate led to the generation of phenylacetyl and xanthate radicals. The former on decarbonylation resulted in the generation of a benzyl radical that was captured by the latter to form *S*-benzyl-*O*-ethyl xanthate (Scheme 1.5 A).

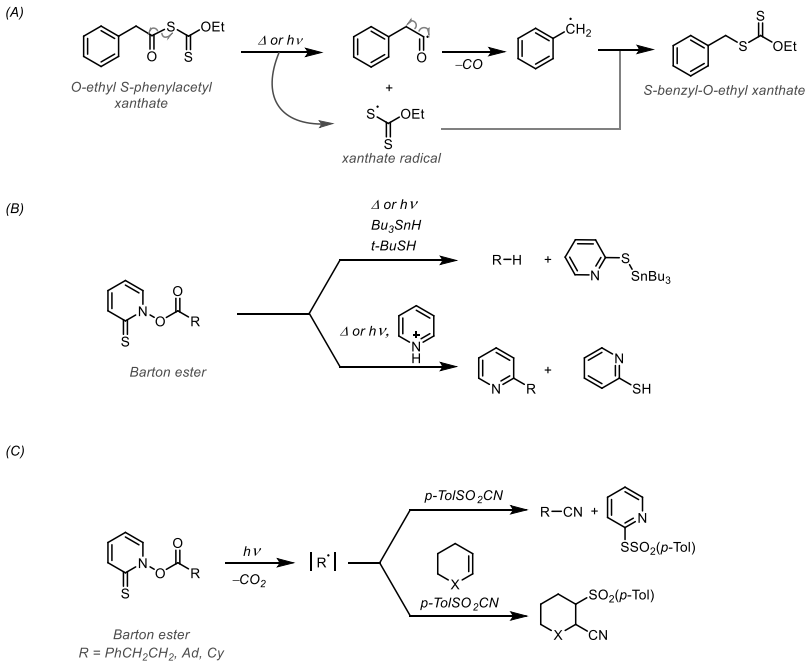

Scheme 1.5: Classical decarboxylation approaches using (A) xanthates and (B) Barton esters. (C) Synthesis of alkyl nitrile from Barton esters.[14]

Later in 1983, thermal fragmentation of 2-pyrithione derivative of carboxylic acids was developed further into a set of general methods (Scheme 1.5, B).[14b] These ester derivatives, often called Barton esters, underwent decarboxylation when refluxed in the presence of tributylstannane or upon irradiation with visible or UV-light, generating alkyl radicals which were reduced by suitable hydrogen atom donors, e.g., *tert*-butylthiol. The addition of alkyl radicals generated this way to protonated heteroaromatics had also been successfully achieved following a radical chain mechanism.[14c] In 1992, Barton and co-workers demonstrated photo-initiated synthesis of alkyl nitriles using these esters and sulfonyl cyanides or isothiocyanides (Scheme 1.5, C, top).[14d] In addition, they described that catalytic amount of acyl derivatives of *N*-hydroxy-2-thiopyridone (Barton esters) in the presence of tungsten lamp is highly effective for the difunctionalization of electron rich olefins (Scheme 1.5, C, bottom). However, this chemistry was fundamentally limited by the intrinsic instability of Barton esters and the competition of the thiopyridone by-product in the capture of the resulting alkyl radicals.

1.3.2 *N*-hydroxyphthalimide Esters as Radical Precursors

Carboxylic acids can be coupled with *N*-hydroxyphthalimide (NHPI) in the presence of DCC and DMAP to synthesize the corresponding esters.[15] Like other *N*-*O* esters used in peptide coupling (derived from *N*-hydroxysuccinimide, *N*-hydroxybenzotriazole, etc.), NHPI esters were reported to possess enhanced reactivity towards nucleophiles. For example, Tesser and co-workers, in 1961, reported the synthesis of protected dipeptide using these active esters.[15] In 1988, Okada and co-workers demonstrated that under UV-light irradiation *N*-hydroxyphthalimide esters undergo decarboxylation generating alkyl radicals.[16a] Upon irradiation of a mixture of *N*-hydroxyphthalimide esters and 1,6-bis(dimethylamino)pyrene (BDMAP) in ^{i}PrOH-water (95:5) the corresponding alkane was obtained in high yield (Scheme 1.6, A). Up to this point, this type of reactivity was classically achieved by Barton esters,[14a-d] (see Section 1.3.1) the thermolysis of peresters[14e-g] or by two-step conversion involving Hunsdiecker reaction and radical coupling of the resulting haloalkane.[17] Moreover, this new decarboxylative method effectively solved the problems associated with Barton esters, such as the requirement of anhydrous reaction conditions and their instability towards light and heat that can complicate their handling.[14]

In Okada's seminal study, it was proposed that the mechanism by which NHPI esters generate alkyl radicals is initiated by single electron reduction.[16b] The resulting radical anion fragments into the corresponding alkyl radical, expelling CO_2 and phthalimidate anion (Scheme 1.6, B). This is the reason why these compounds are often termed 'redox-active esters'. Therefore, the single electron reduction of NHPI esters represents a convenient alternative way to generate alkyl radicals from abundant carboxylic acid sources. This is complementary to the direct generation of alkyl radicals from carboxylate anions, which is driven by oxidants, and therefore controlled by the redox-potential of the carboxylate anion.

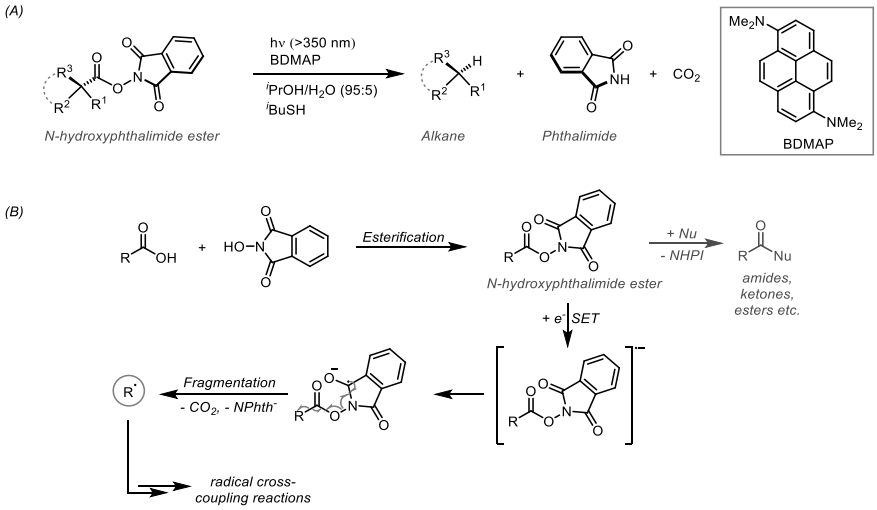

Scheme 1.6: (A) Initial discovery by Okada of NHPI esters as the source of alkyl radicals. (B) Fragmentation of NHPI ester *via* single electron transfer (SET) process.[16]

1.3.3 Decarboxylative Cross-Coupling Reactions

The cross-coupling reaction has played a central role at the core of organic chemistry for its capacity to systematically assemble functionalized arenes, alkenes and alkynes. However, the inherent instability of aliphatic organometallics species has limited the tolerance of cross-coupling methods towards alkyl substituents. In this context, there has been a recent increase in the development of radical cross-coupling reactions that aim to address this limitation.[18]Along this line, redox-active esters have emerged as an excellent source of alkyl (or aryl) radicals from abundant carboxylate precursors and take part in reductive processes (Scheme 1.7),[19] including C–C or C–X (X = N, O, B, Si, etc.) bond forming reactions which would be otherwise difficult to achieve. These reactions typically require transition-metals as catalysts or photocatalysts, while transition-metal free processes were rare at the onset of the work presented in this thesis.[19e,f,v,w,20]

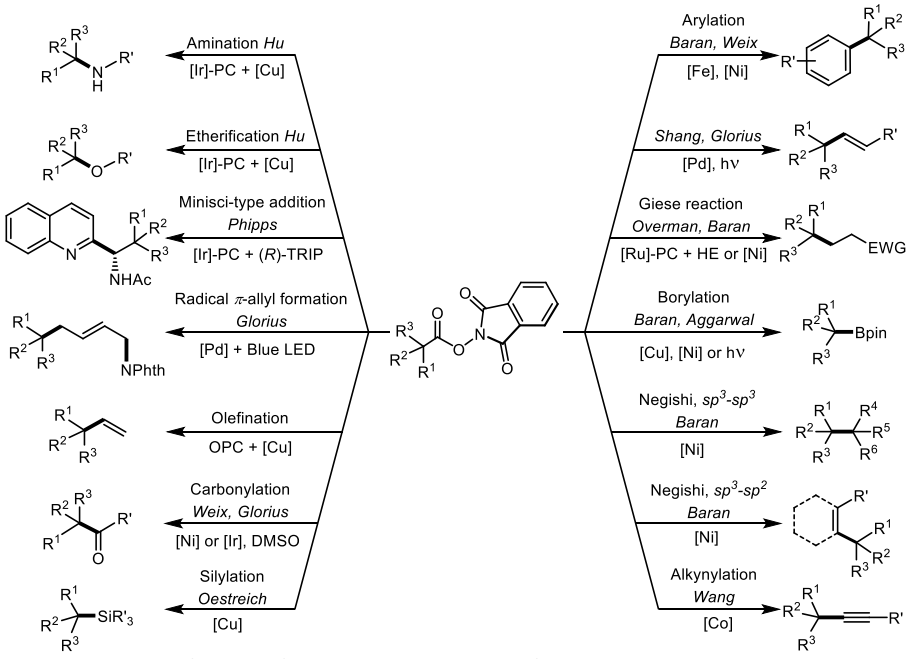

Scheme 1.7: State-of-the-art of cross-coupling reactions of redox-active NHPI esters; TRIP = 3,3′-bis(2,4,6-triisopropylphenyl)-1,1′-bi-2-naphthol cyclic monophosphate; OPC = *N*,*N*-diaryl dihydrophenazines.[19]

1.3.4 Decarboxylative Coupling on Biomolecules

Recently, decarboxylative alkyl ligation has received significant attention due to the unique features of radical reactions in the selective functionalization of biomolecules. In 2016, MacMillan and co-workers reported the decarboxylative peptide macrocyclization using visible light photoredox catalysis (Scheme 1.8, A). This technology has been used to cyclize peptides containing 3 to 15 amino acid units.[21a] The selective decarboxylation of the carboxylic group in the terminal aminoacid can be achieved due to a slight difference in its redox-potential in comparison to other carboxylates in the substrate. Two years later, Baran and co-workers demonstrated the coupling of redox-active esters with DNA-encoded Michael acceptors (Scheme 1.8, B).[21b] In this case, zinc nanoparticles were required to generate alkyl radicals from redox-active esters in a heterogeneous process. Another contribution to this field was described by Molander's group in 2019, with a related decarboxylative coupling of *β*-amino acids with DNA-tagged aryl halides through nickel and photoredox catalysis, allowing the syntheses of libraries of DNA-encoded benzylamines (Scheme 1.8, C).[21c] A similar technique was followed for the coupling of alkyl bromides with DNA-tethered aryl halides, leading to the synthesis of libraries of aryl-alkyl coupled products (Scheme 1.8, D).[21d] After the development of the work presented in Chapter 3 of this thesis, Molarder and co-workers have disclosed the hydroalkylation of trifluoromethyl substituted olefins using redox-active esters and the Hantzsch ester (Scheme 1.8, E). This reaction proceeds *via* the formation of an EDA-complex between NHPI esters and the Hantzsch ester, which then undergoes photo-induced electron transfer (PET) followed by fragmentation, ultimately generating an alkyl radical. Using this strategy, a series of DNA-encoded benzylic trifuoromethylated products have been synthesized.[21e] Despite these developments, all these reactions require complex transition-metal catalysts and photocatalysts, anhydrous solvents, anoxic conditions and/or insoluble inorganic reductants. These limitations are inherent to the respective principles of activation of these reactions. Therefore, further developments are required to unveil the full potential of decarboxylative alkyl ligation in chemical biology.

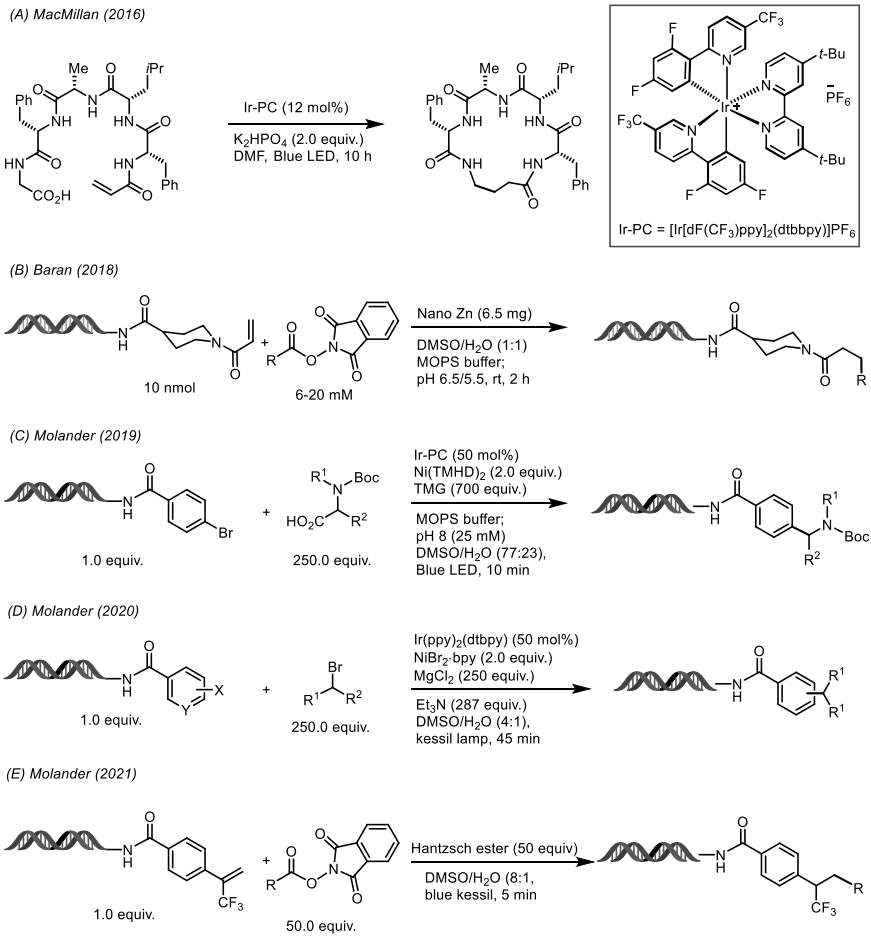

Scheme 1.8: Contribution by (A) MacMillan (B) Baran and (C) Molander towards decarboxylative couplings of redox-active esters on biomolecules.[21]

1.4 Objectives and Aims of the Thesis

The work presented in this thesis is based on both carbene catalysis and radical coupling reactions. Using these two basic organic chemistry concepts the thesis aims at the development of general C–H or Si–H alkylation strategies on important feedstock chemicals (e.g. indoles and silanes) using a single redox-active diazoacetate reagent (NHPI-DA; **1a**) and subsequent decarboxylative operations (Scheme 1.9). The redox-active diazoacetate reagent NHPI-DA is aimed to be used as single carbon linchpin reagent. Merging the rich chemistry of carbenes and decarboxylative coupling reactions would allow the syntheses of compounds carrying a wide range of functionalities connected by a common methylene unit. Cooperatively, this new approach focuses to overcome the limitations of the current synthetic methodologies that require custom manipulation of the reagents, harsh reaction conditions, excess starting materials, and often leads to poor selectivity on structurally complex substrates. Moreover, the work in this thesis emphasizes on the development of Giese-type reactions of redox-active esters using self-sensitized organic photoreductants, eliminating the need of external photocatalysts and/or inorganic reductants which is common in photoredox chemistry. In addition, the design of some of these reactions should be compatible with the reaction environments typical of biochemistry, where fast reaction times, air and moisture compatibility and high dilution are often required.

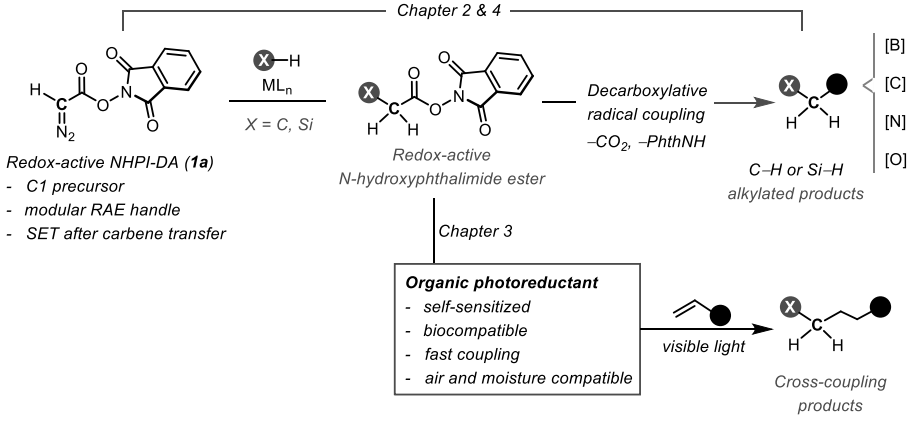

Scheme 1.9: Objective of this thesis.

2. Unified C–H Alkylation of Indoles Using *N*-hydroxyphthalimidyl Diazoacetate (NHPI-DA) as a C1 Precursor (Paper I)

2.1 Introduction

2.1.1 Indoles and Their Importance

Indoles are among the most studied heterocycles in organic chemistry.[22] Their ubiquitous presence in molecules with important biological activity has always attracted the attention of organic chemists. This structural motif is present in the naturally occurring amino acid *L-tryptophan*, the neurotransmitter *serotonin*, the plant growth hormone *auxin*, the psychoactive agent *lysergic acid*, and the drug candidate *catharanthine* for treatments towards hypertension, *indomethacin* for inflammation and *sumatriptan* for migraine (Figure 2.1). The breadth of their applications in medicinal chemistry have earned them to be highlighted as "privileged structures" in drug discovery.[23,24] Moreover, indole-based phosphines have produced highly active transition-metal catalysts utilizing their unique stereoelectronic properties.[25] Therefore, the synthesis and functionalization of indoles has remained as an important area of research in organic chemistry.[26]

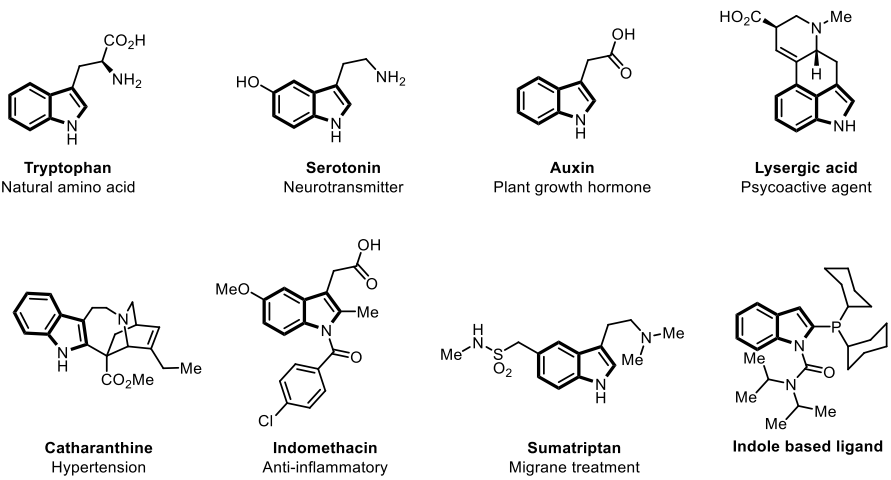

Figure 2.1: Indole as ubiquitous structural unit in natural products.[22]

1.3.1 Structure, Synthesis and Reactivity of Indoles

Indoles are π-excessive heterocycles with very low basicity due to high delocalization of the nitrogen lone pair into the extended aromatic system, making C3 its most electron rich carbon.[27] This is one of the reasons for the abundance of C3-functionalized indoles in alkaloids and natural products (Figure 2.2).

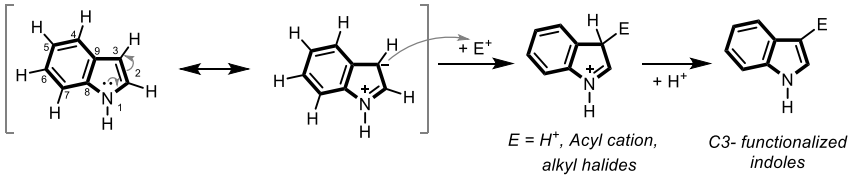

Figure 2.2: Resonance structure of indole describing its reactivity.[27]

Synthetic organic chemists have developed numerous methods to obtain and functionalize indoles **2** (Scheme 2.1). The Fisher indole synthesis[28a] starting from enolizable *N*-aryl hydrazones, the Gassman synthesis[28b] from *N*-halo-anilines, and the Madelung cyclization of *N*-acyl-*o*-toluidines are among the most classic procedures, and are still currently used widely in organic synthesis.[28c] Syntheses of indoles using the conditions developed by Bartoli,[28d] Bischler-Möhlau,[28e] Batcho-Leimgruber,[28f] and Larock[28g] are also widely applied.[26] As it can be deduced from the synthetic disconnections enabled by these methods, C3-functionalized indoles require starting materials bearing the desired functionality or custom manipulation of C3-unfunctionalized indoles.

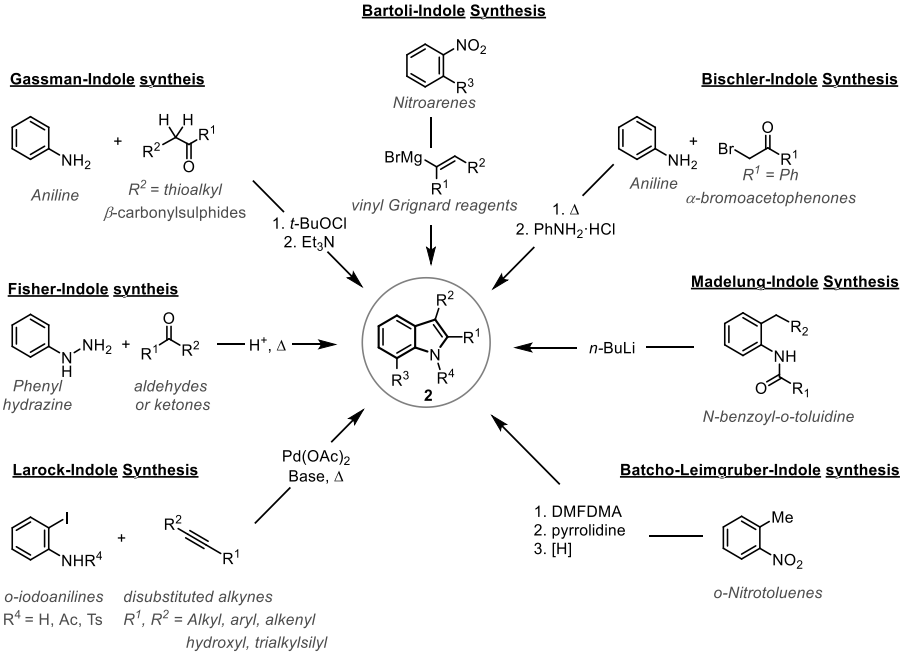

Scheme 2.1: Classic methods for the synthesis of indoles.[28]

2.1.3 Current Synthetic Strategies towards C–H Functionalization of Indoles

Synthetic techniques to install alkyl groups at the C3-position of indoles are particularly important due to the relevance of these products in natural and artificial bioactive compounds (see Section 2.1.1).[22,25] There are methods to obtain such molecules, but they require specific functionalities in the substrate and specific reagents depending on the functionality of the desired C3-alkyl product.[19e,29] For example, the synthesis of C3-benzylated indoles uses benzyl alcohol at 165 ˚C (Scheme 2.2 A),[29a] or benzyl bromide using microwave irradiation at 150 ˚C (Scheme 2.2 B).[29c] The introduction of more advanced methylboronates at C3-position is particularly illustrative of the current synthetic limitations as the required alkyl electrophiles (α-methylboronates) are not sufficiently stable at these temperatures to be used for this purpose. Instead, a recent method by Aggarwal uses a photo-decarboxylative approach for the borylation of redox-active esters derived from indole-3-acetic acid.[19e] However, the synthesis of the latter requires harsh reaction conditions with strong base and high temperature (250 ˚C) that are unsuitable for complex multifunctional indoles (Scheme 2.2 C).

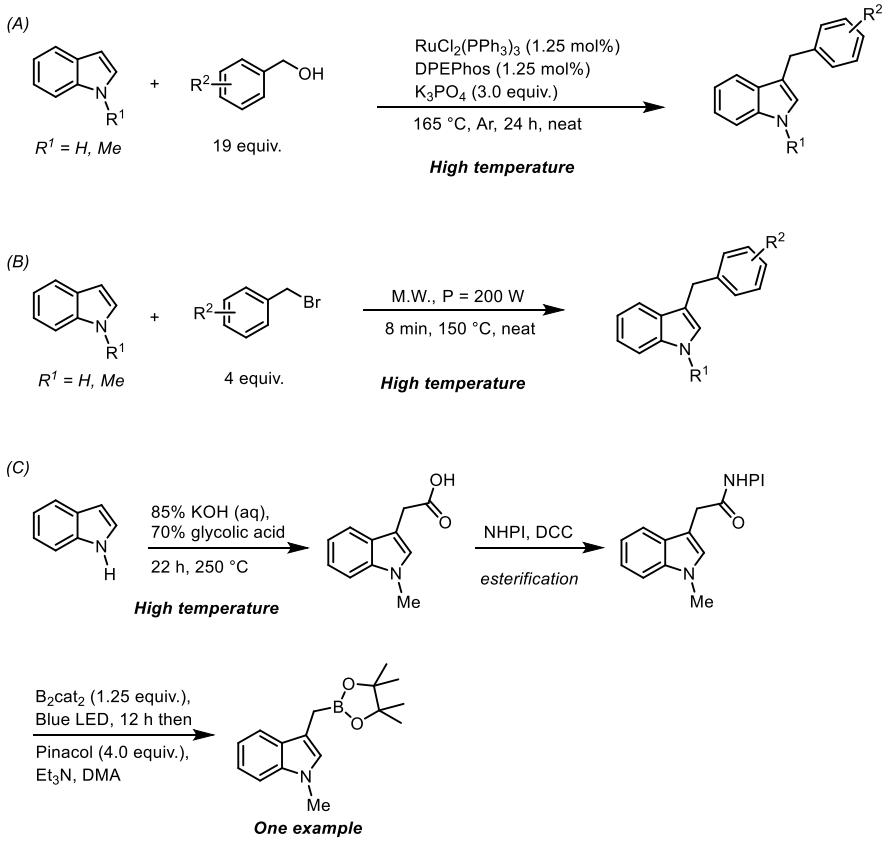

Scheme 2.2: Previous reports of syntheses of C3-functionalized indoles.[19e,29]

2.1.4 Transition-Metal Catalyzed C–H Functionalization of Indoles Using Diazo compounds

Transition-metal catalyzed C–H functionalization reactions have received increased attention of synthetic organic chemists in the late-stage modification of arenes and heteroarenes.[22,23,25,26] In particular, insertion reactions mediated by metal-carbene intermediates have been particularly attractive in the C–H functionalization of indoles **2** due to their mild reaction conditions (< 25 ˚C).[30-34] However, the high reactivity of these species make the insertion processes challenging to tame into efficient and selective reactions. In this area, it is well established that the substituent on the indole nitrogen atom has large influence on the regioselectivity of the products of the C–H insertion reactions. Indoles with an electron donating substituent at this position commonly favor C3-insertion products.[30,32] For these substrates, simple acceptor diazo compounds **3a**, in combination with Cu- and Rh-catalysts (Table 2.1; Entries 1,2) are most common,[30c-f] despite the recent developments of enzymes- and myoglobin- catalyzed conditions (Entries 3,4).[30b,g] Both base metal (Fe) and precious metal catalysts (*i.e.* Pd, Rh, etc.) have also been utilized for the insertion of α-substituted diazo compounds into C–H bonds of indoles (Entries 7,9,10).[32a,b,e] Insertions of α-aryl diazoacetates **3b** have been reported using a chiral Pd-catalyst to obtain C3-functionalized products with good yields and enantioselectivity.[32e] More recently, non-transition-metal catalysts such as boranes have been discovered to catalyze the C–H insertions using stabilized α-aryl diazoacetates (Entry 8).[32j] Moreover, functionalization of C–H bond of indoles using photo-excited diazo compounds have also been realized,[31a,32n] albeit only aryl-substituted reagents display good C3- selectivity,[32n] whereas simple ethyl diazoacetate provided mixture of C2- and C3- products[31a] (Entries 5,6).

Table 2.1: Insertion of conventional diazoacetate reagents into C–H bond of indoles at the C3-position.

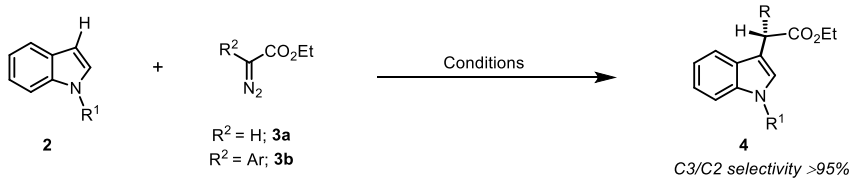

Entry	Conditions	R^1	R^2	Ref.
1	[**L1**Cu(NCMe)] (1 mol%), CH_2Cl_2, r.t.	Alkyl	H	*Pérez*[30d]
2	$[Rh_2(OAc)_4]$ (1-5 mol%), DCE, r.t.	Alkyl	H	*Bera*[30c]
3	*E. coli* cells, P411-HF variants, M9-N buffer, pH 7.4, r.t.	H	H	*Arnold*[30g]
4	*E. coli* cells, Myoglobin variant (0.8 mol%), KPi-buffer, pH 7, r.t.	H	H	*Fasan*[30b]
5[a]	$Ru(bpy)_3Cl_2$ (0.2 mol %), MeOH/H_2O (10:1), Blue LEDs, r.t.	Alkyl	H/Ar	*Gryko*[31a]
6	CH_2Cl_2, Blue LEDs, air, r.t.	Alkyl	Ar	*Davies*[32n]
7	$Fe(ClO_4)_2$ (1 mol%), TMEDA (1.2 mol%), NaBArF (1.2 mol%), DCE, r.t.	Alkyl	Ar	*Zhou*[32b]
8	$B(C_6F_5)_3$ (10 mol%), CH_2Cl_2, 45 ˚C	Alkyl	Ar	*Melen*[32j]
9	$[Pd(PhCN)_2Cl_2]$ (5 mol%), **L2** (5 mol%), 5 Å M.S., CH_2Cl_2, 30 ˚C	Alkyl	Ar	*Zhou*[32e]
10	$[Rh_2(S\text{-NTTL})_4]$ (0.5 mol%), toluene, -78 ˚C	Alkyl/aryl	Alkyl	*Fox*[32a]

[a] C3/C2 =3.2:1 to 11:1.

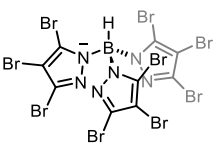

Tp^{Br3} (**L1**)

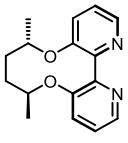

C_4-ACBP (**L2**)

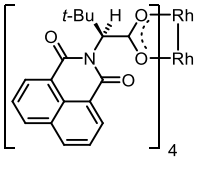

$Rh_2(S\text{-NTTL})_4$

2.2 Aim of the Project

Despite the success achieved in recent years in the C–H alkylation of indoles through carbene transfer reactions, these methods are still limited in the versatility of the diazo compounds. Addressing this limitation would unlock a mild and unified strategy to build libraries of decorated C3-alkyl indoles **6** from unfunctionalized indole materials **2**. An ideal approach to this problem would involve a single methylene equivalent reagent that would connect indoles and interesting functionalities. Methylenes are ubiquitous units in organic chemistry but rarely used connecting units in diversity-oriented synthesis.[1] This way, it will be possible to obtain systematically C–H alkylated indoles with distinct functionalities on the alkyl chain using a unified synthetic approach.[29]

In principle, these problems might be directly addressed by the insertion of advanced carbenes, like boryl,[35a] aryl,[35b] alkyl,[35c,d] alkenyl[35e] methylidenes **11a-d**. However, their inherent instability hinders their application in the C–H alkylation reactions.[30] Therefore, we envisaged a general two-step alkylation strategy of indoles **2**, where these functionalities in indoles would be introduced using a versatile carbene precursor **1a** (Scheme 2.3). To be successful, this reagent should allow the early-stage C–H insertion on feedstock indoles **2** and the late-stage diversification of the intermediate products **5**.[19] Recently, our group has discovered enantioselective cyclopropanation using redox-active *N*-hydroxyphthalimidyl diazoacetate (**1a**-NHPI-DA; see Section 1.2.4).[13] Broad substrate scope and very good enantioselectivity of this cyclopropanation method demonstrate the orthogonality of the NHPI moiety to the geminal carbenoid carbon. Encouraged by this study, we set out to explore the capacity of the redox-active diazo compound **1a** as a methylene linchpin reagent for the late-stage functionalization of indoles.

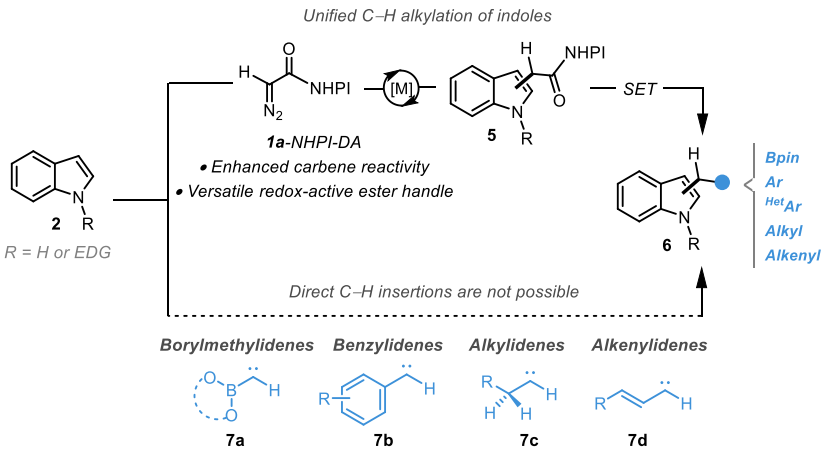

Scheme 2.3: Unified strategy for C–H alkylation of indoles using a versatile diazo compound, NHPI-DA.

2.3 Results and Discussion

In the beginning of our study, we took the opportunity to use the conventional dirhodium tetracarboxylates as catalysts for the insertion of the redox-active diazo compound **1a** on model *N*-benzylindole **2b** (Table 2.2). It is important to highlight that the insertion of NHPI-DA (**1a**) on indole **2b** often lead to poor mass balance due to the precipitation of **8** during the reaction and its very low solubility in deuterated chloroform used for NMR analysis. Despite the known success of similar catalytic conditions with simple diazoacetates, we obtained only poor yield of the C–H functionalized product **5b** using NHPI-DA (Entry 1). Several other rhodium carboxylates were also tested to improve the efficiency of the reaction, but none of them provided enhanced reactivity towards the formation of **5b** (Entries 2-5). Contrary to the results reported in the copper-mediated protocols developed by Perez and Chen,[30d,e] the performance of the NHPI-DA under similar conditions provided only low yield of **5b** (Entry 6). The use of Cu(I) catalysts in this C–H insertion process also failed to deliver the product in good yield (Entries 7,8). Several ligands **L1-4** were tested in combination with common Cu(I) precursor, but **5b** was obtained only in low yields along with the extensive decomposition of NHPI-DA (Entries 9-12). These include the *bis*-oxazoline (*S*)-Ph-BOX (Entry 9), bipyridines (Entries 10,12) and phenanthroline (Entry 11). Slow addition of the diazoacetate reagent *via* syringe pump (Entry 13) and slight increase of the temperature (Entry 14) failed to enhance the yield of the desired insertion product **5b**.

In the light of these results, we also focused on the application of less common catalysts used for C–H insertion of indoles. The Fe-based catalysts derived from tetraphenylporphyrin (TPP) only provided trace amount of **5b** (Entry 15), while iron phthalocyanine (**L5**) delivered the product **5b** in low yield (Entry 16). $[Ru(p\text{-cymene})_2Cl_2]_2$ which is a known catalyst for the insertion of α-aryl diazoacetates at the C2- position of *NH*- indoles,[33b] was found to be a potential alternative, yet obtained only in moderate yield (Entry 17). In contrast, the achiral metallacycle $[Ru\mathbf{L9}(MeCN)_4]PF_6$ produced the desired insertion product in very good yield (Entry 18).[36] Interestingly, the model indole substrate **2b** reached completion in just 15 min using only slight excess (1.25 equiv.) of NHPI-DA and without the requirement of any slow addition of the reagent (Entries 19,20). It is worth to mention that the redox-active ruthenium carbenoid species undergoes selective C–H insertion at the C3-position, despite the possibility of the competing insertion at the C2-position[31] or cyclopropanation of the double bond between C2- and C3.[34] This result demonstrates the efficiency and chemoselectivity of the insertion of the redox-active carbenes derived from a ruthenium metallacycle, which is rare when using α-unsubstituted diazo compounds.[30a,b,34c,e]

Table 2.2: Screening of the reaction parameters for the insertion of redox-active carbenes on indole **2b**.

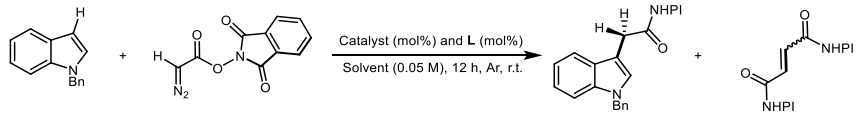

Entry	Catalyst/**L** (mol%)	Solvent	Yield (**5b**) (%)[a]	Yield (**8**) (%)[a]
1	$Rh_2(OAc)_4$ (2)	DCE	38	8
2[b]	$Rh_2(OAc)_4$ (2)	DCE	30	3
3	$Rh_2(piv)_4$ (2)	DCE	36	11
4	$Rh_2(TPA)_4$ (2)	DCE	23	12
5	$Rh_2(esp)_2$ (2)	DCE	33	13
6	$Cu(OTf)_2$ (10)	DCE	12	6
7	CuI (10)	DCE	4	3
8	$[Cu(CH_3CN)_4]PF_6$ (10)	DCM	33	5
9	$Cu(OTf)_2 \cdot C_6H_6$ (5) + **L3** (10)	DCM	24	1
10	$Cu(OTf)_2 \cdot C_6H_6$ (5) + **L4** (10)	DCM	27	3
11	$Cu(OTf)_2 \cdot C_6H_6$ (5) + **L5** (10)	DCM	23	3
12	$Cu(OTf)_2 \cdot C_6H_6$ (5) + **L6** (10)	DCM	35	3
13[b]	$Cu(OTf)_2 \cdot C_6H_6$ (5) + **L6** (10)	DCM	33	3
14[c]	$Cu(OTf)_2 \cdot C_6H_6$ (5) + **L6** (10)	DCM	23	3
15	Fe[**L7**]Cl (10)	DCE	<1	5
16	Fe**L8** (10)	DCE	30	6
17	$[Ru(p\text{-cymene})_2Cl_2]$ (1)	DCM	56	12
18	[Ru**L9**$(MeCN)_4]PF_6$ (1)	DCM	87	–
19[d,e,f,g]	[Ru**L9**$(MeCN)_4]PF_6$ (1)	DCM	95	–
20[d,g,h]	[Ru**L9**$(MeCN)_4]PF_6$ (1)	DCM	95	–

[a] Yields were determined by ^{1}H-NMR spectroscopy using 1,1,2,2-tetrachloroethane as internal standard. [b] 30 min addition of **1a**; [c] 60 ˚C; [d] 1.25 equiv. of **1a**; [e] 15 min addition of **1a**; [f] 2 h; [g] 0.1 M concentration; [h] 0.25 h; **L3** = (*S*)-Ph-BOX; **L4** = 2,2'-bipyridine; **L5** = 1,10-phenanthroline; **L6** = 4,4'-*di*-tert-butyl-2,2'-bipyridine; **L7 =** tetraphenylporphyrin; **L8** = phthalocyanine; **L9** = 4,4-dimethyl-2-phenyloxazolin-2'-yl.

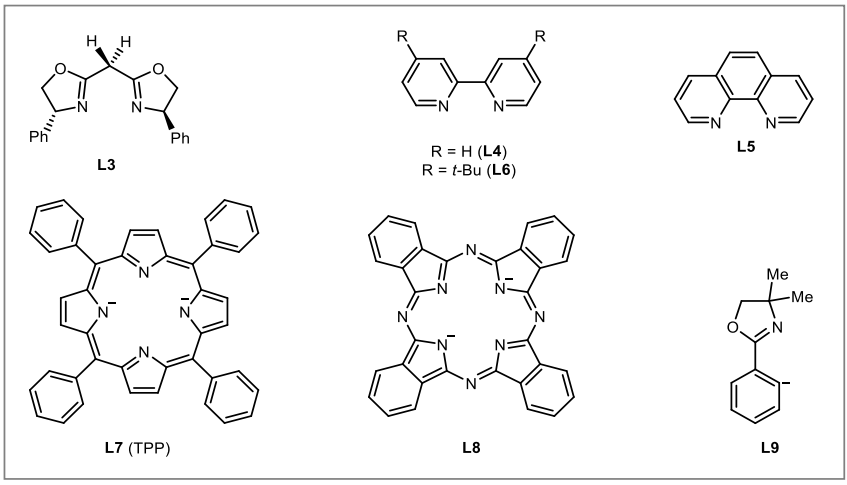

2.4 Scope Study

Given the structural diversity in bioactive indole compounds, an exhaustive substrate scope study was undertaken. In line with previous work in the area, it was found that the substituent on the nitrogen of the indole plays a vital role in controlling the chemoselectivity of the reaction (Table 2.3). The ruthenium-metallacyclic catalyst has been found to be highly active in a large series of indoles with different alkyls (**5a-j**), aryl (**5k**) or silyl (**5l**) substituents. Among those, *N*-methylindole **2a**, which is common in the structures of natural products, has been functionalized efficiently to furnish **5a**. Functionalities, like ketone (**5c**), bromo (**5d**), aryl (**5e**), ester (**5f**), ether (**5g**), or nitrile (**5h**) were all found to be compatible in the C–H functionalization processes with NHPI-DA (**1a**). Moreover, this C–H insertion proceeds in the presence of a strained cyclopropane (**5i**) or a reactive allyl substituent (**5j**). The latter demonstrates the chemoselectivity of this ruthenium-mediated C–H insertion process over the competing cyclopropanation of the aliphatic alkene.[13a] *N*-aryl indole could also be used in this reaction to obtain the corresponding C3- alkylated product in good yield (**5k**). Silyl functionality (**5l**) on the heterocyclic nitrogen atom is also well tolerated under the standard reaction conditions, thus enabling easy access to functionalized *NH*-indoles after deprotection.

Table 2.3: Scope of the insertion of the NHPI-DA (**1a**) on different *N*-alkyl indoles.[a]

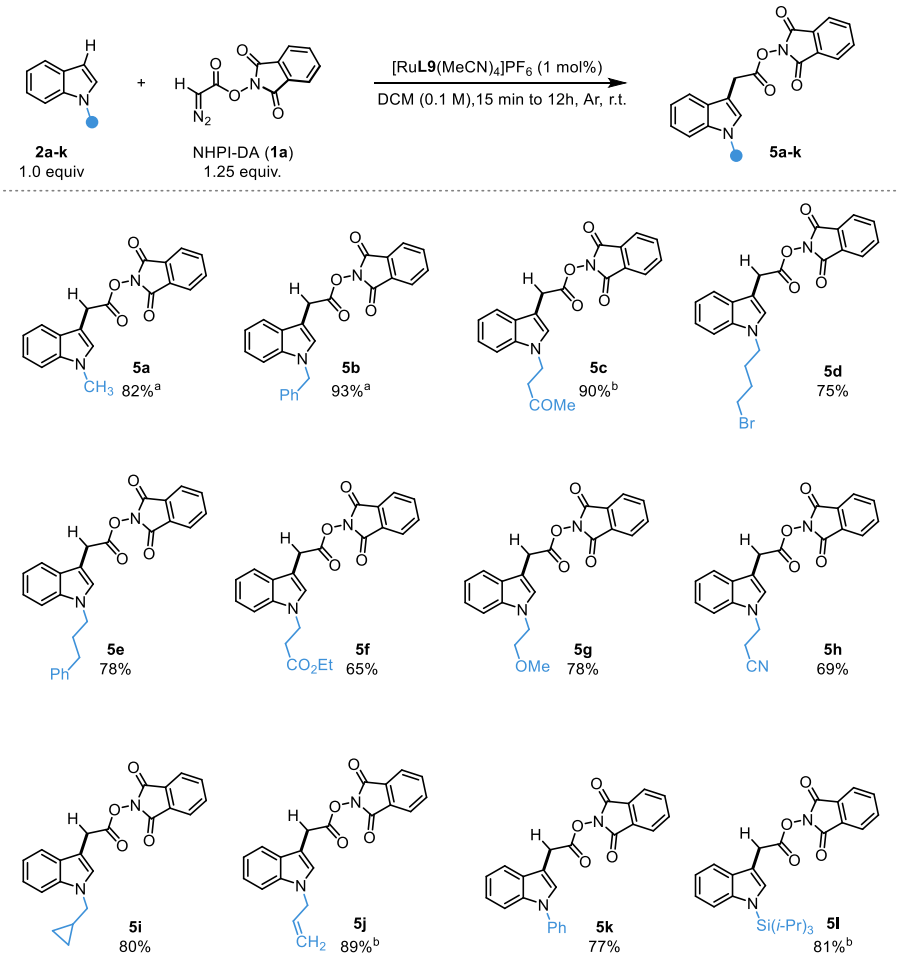

[a] Reaction conditions: **2** (0.2-0.3 mmol), **1a** (1.25 equiv.), [Ru**L9**(MeCN)$_4$]PF$_6$ (1 mol%), CH_2Cl_2 (0.1 M), 0.25 -14 h, r.t. Isolated yields are reported. [b] Slow addition of **1a** over a period of 2 h using syringe pump.

It is well established that the substituent at the C2-position of indoles ring has prominent role in controlling the overall reactivity towards metal-carbenes, and therefore we evaluated the system in this regard (Table 2.4). To our delight, aryl substituents with different electronic nature displayed high efficiency in this insertion process, which includes the strongly electron-withdrawing CF_3 group (**5o**) and an extended aromatic system (**5p**). Aliphatics, such as methyl and a bulky *tert*-butyl groups can also be accommodated at the C2-position, delivering the desired products in acceptable yields (**5q,r**). It is important to highlight that in the case of the hindered 2-*tert*-butyl substrate (**5r**), a controlled addition over a period of 12 h of the NHPI-DA (**1a**)

was essential in order to avoid decomposition and dimerization of the diazoacetate reagent.

Table 2.4: Scope of the insertion of the NHPI-DA (**1a**) on *N*-alkyl indoles with substituents at the C2-position.[a]

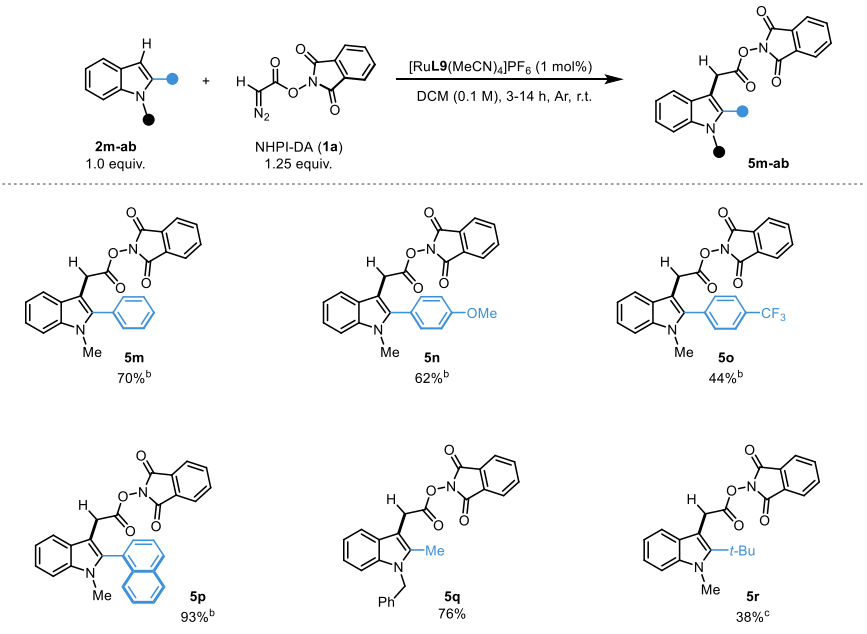

[a] Reaction conditions: **2** (0.2-0.3 mmol), **1a** (1.25 equiv.), [Ru**L9**(MeCN)$_4$]PF$_6$ (1 mol%), CH_2Cl_2 (0.1 M), 0.25 -14 h, r.t. Isolated yields are reported. [b] 2 h addition of **1a**; [c] 12 h addition of **1a** using syringe pump.

The effects of the substituents in the fused-benzene ring of indoles were also scrutinized (Table 2.5). Indoles with different halides **5s-u**, electron donating substituent **5v**, a pinacolboronate ester **5w**, extended aromatic (e.g., naphthyl; **5x**) and heteroaromatics (e.g., thiophene; **5y**) at the C4- and C5- positions engaged seamlessly under the standard conditions. Chloro (**5s**), bromo (**5t**) and iodo (**5u**) substituents that are found in marine natural products performed well and delivered the C–H functionalized products in good yields. Interestingly, these redox-active ester products can be used as potential starting materials in two different kinds of cross-coupling reactions, (e.g. Suzuki-type cross-coupling with the aromatic halide and decarboxylative coupling with the redox-active ester handle), thus illustrating the synthetic potential of this strategy. Similarly, the tolerance of the pinacolboronate ester towards the redox-active carbene insertion process (see **5w**) is remarkable in terms of the potential of the corresponding product for further modifications. Selective insertion of the NHPI-DA (**1a**) at the C3-position of indole in presence of a thiophene unit further demonstrates the chemoselectivity of this system in the presence of other nucleophilic heterocycles.

The effects of the substituents at C7- and C8- positions were also studied. This includes *p*-tolyl group (**5z**) at C7-, methyl and aldehyde functionalities (**5ab,ac**) at C8-position, which delivered uneventfully the insertion products.

Table 2.5: Scope of the insertion of the NHPI-DA (**1a**) on different *N*-alkyl indoles with substituents on fused-benzene ring.[a]

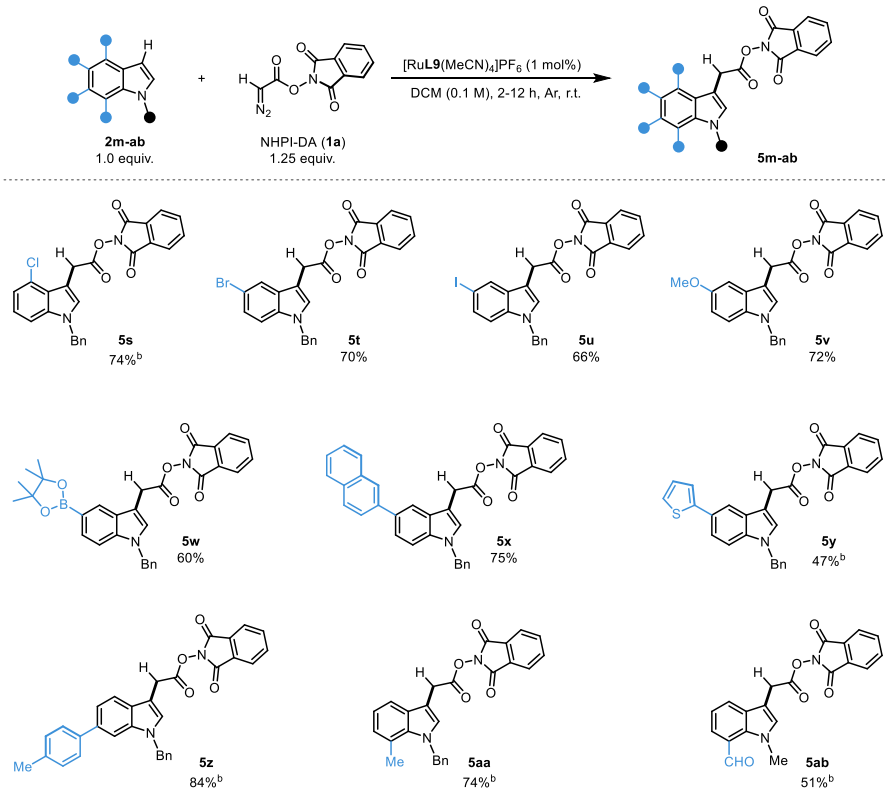

[a] Reaction conditions: **2** (0.2-0.3 mmol), **1a** (1.25 equiv.), [Ru**L9**(MeCN)$_4$]PF$_6$ (1 mol%), CH_2Cl_2 (0.1 M), 0.25 -14 h, r.t. Isolated yields are reported. [b] Slow addition of **1a** over a period of 2 h using syringe pump.

Selective C–H functionalization of unprotected indoles remains a frontier in this context due to the abundance of these products in bioactive small molecules and proteins. However, the optimal catalyst for *N*-protected indoles [Ru**L9**(MeCN)$_4$]PF$_6$, failed to provide any C–H functionalized product when reacted with *NH*-indoles, rather extensive decomposition and dimerization of the diazo compound was observed. To our surprise, [Ru(*p*-cymene)$_2$Cl$_2$]$_2$ was efficient for this purpose (Table 2.6). This catalyst is known to be suitable only for the insertion of more stabilized α-aryl diazoacetate reagents at the C2-position of indoles.[33b] Interestingly, NHPI-DA (**1a**) reacted successfully with 3-methylindole (**5ac**) and 3-methyl-5-bromoindole (**5ad**) to deliver the desired products in very good yields. Methyl esters of indole 3-acetic acid and *L*-

tryptophan were also subjected to this reaction protocol, albeit 4 mol% catalyst loading was essential for these substrates to perform moderately (**5ae,af**). Unfortunately, these products proved to be unstable during various types of chromatographic purification, which complicated isolation in pure form.

Table 2.6: Scope of the insertion of the NHPI-DA (**1a**) on *NH*-indoles.[a]

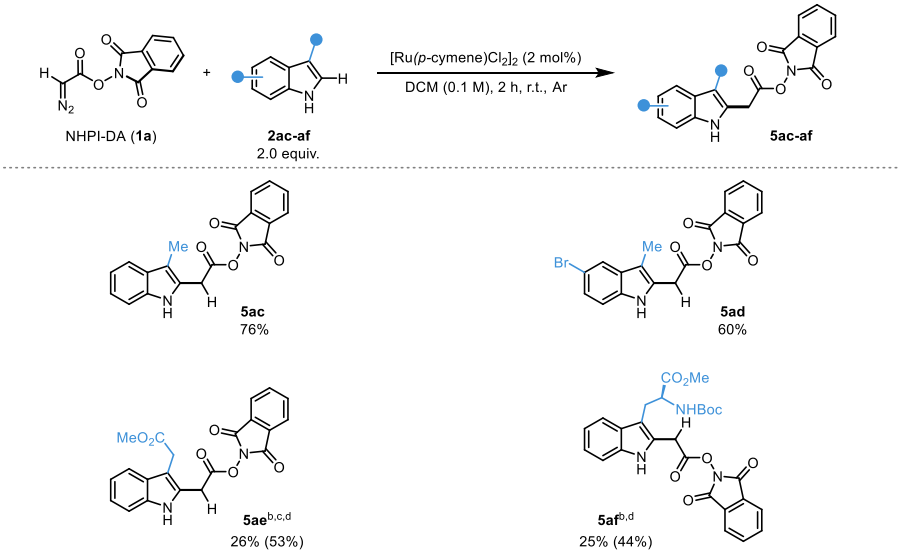

[a] Reaction conditions: **1a** (0.3 mmol), **2** (2.0 equiv.), [Ru(*p*-cymene)Cl_2]$_2$ (2 mol%), CH_2Cl_2 (0.1 M), 2 h, r.t., Ar. Isolated yields are reported. In parenthesis are the crude yields determined by ^{1}H-NMR spectroscopy using 1,1,2,2-tetrachloroethane as internal standard. [b] 4 mol% of [Ru(*p*-cymene)Cl_2]$_2$ was used; [c] 4 h reaction time; [d] Due to instability the product could not be isolated in pure form.

Overall, the C–H functionalization of indoles using redox-active ruthenium carbenoids highlights the unusual chemoselectivity, efficiency and functional group tolerance of these intermediates. These properties enable new opportunities to access versatile indole intermediates through late-stage functionalization of simple indole materials instead of longer routes based on the functional group manipulations on more complex indole sources.

2.5 Diversification of the Redox-Active Ester Products

2.5.1 One-Pot C3-Methylborylation of Functionalized Indoles

Insertion of borylmethylidenes into C–H bond of indoles would allow the synthesis of valuable methylborylated indoles that are boronic analogs of the auxin plant-growth hormone, and useful synthetic intermediates due to the rich chemistry of boron. However, borylmethylidenes are known to be unstable already at extremely low temperatures,[19e] thus limiting its application in metal-catalyzed insertion processes. We hypothesized that the C–H insertion of redox-active carbenes into indoles (Section 2.3, 2.4) followed by a decarboxylative borylation of the resulting products could address this issue.[19e] This approach compares favourably to the previously described longer routes to these compounds, where it requires to pre-synthesize the starting carboxylic acids from unfunctionalized indoles using harsh reaction conditions.[29b]

In recent years, several strategies to borylate NHPI esters have been reported.[19b,e,f,37] Among those, our preliminary evaluation demonstrated that the nickel-catalyzed conditions developed by Baran and co-workers were most effective in our indole-containing substrates.[19b] Moreover, it was found that the borylation reaction could be telescoped from the unfunctionalized indoles without isolating the intermediate insertion products in a one-pot process. This way, the solvent was evaporated after the insertion step and the components for the borylation were added over the crude mixture to obtain methylborylated indoles without isolating any intermediates.

The scope of this formal methylborylation process was explored using indoles with several alkyl substituents at the heterocyclic nitrogen (**6a-f**), which have the most profound effect in the putative radical intermediates involved in these reactions (Table 2.7). This includes methyl (**6a**), benzyl (**6b**) and aliphathics bearing an ester (**6c**), nitrile (**6d**), ether (**6e**) and phenyl (**6f**) functionalities, providing the desired methylborylated indoles in moderate to good yields. The comparison of the crude and isolated yields evidenced the instability of the products during chromatographic purification. The indoles with aryl and silyl substituents at the nitrogen atom (**6g,h**) were also found to be effective towards the combined C–H insertion and borylation approach, delivering the methylborylated products in moderate to good yields.

Table 2.7: One-pot methylborylation of indoles using NHPI-DA (**1a**) as methylene linchpin reagent.[a]

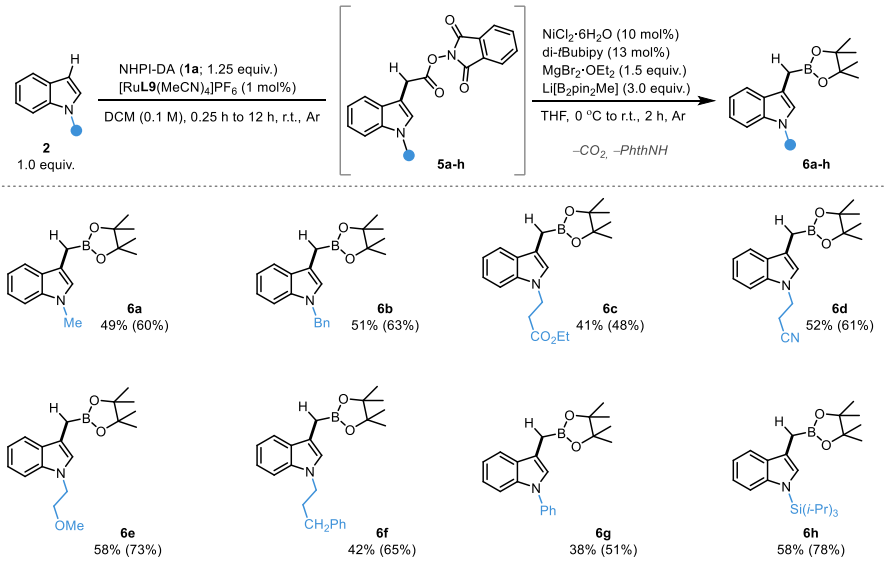

[a] Isolated yields are reported. In parenthesis are the crude yields determined by ^{1}H-NMR spectroscopy using 1,1,2,2-tetrachloroethane as internal standard. Reaction conditions: **2** (0.3 mmol), **1a** (1.25 equiv.), [Ru**L9**(MeCN)$_4$]PF$_6$ (1 mol%), CH_2Cl_2 (0.1 M), 0.25 -14 h, r.t., then $NiCl_2{\cdot}6H_2O$ (0.10 equiv.), 4,4'-*di*-*t*-Bubipy (0.13 equiv.), $MgBr_2{\cdot}OEt_2$ (1.5 equiv.), B_2pin_2 (3.0 equiv.), MeLi (3.3 equiv.), 0 ˚C to r.t., 2 h, Ar.

The effects of this one-pot methylborylation protocol with different substituents in various positions of the indole substrate were tested (Table 2.8). Alkyl (**6i**) and aryl (**6j**) substituents were tolerated providing the desired products in moderate yields. Substitutions of the benzo-fused ring at C4- (**6k**), C6- (**6l**) and C7- (6**m**) were also deemed viable. It is important to highlight that the isolated yields of some of these methylborylated indoles are significantly lowered by their instability on silica during the chromatographic purification.

Table 2.8: One-pot methylborylation of indoles using NHPI-DA (**1a**) as methylene linchpin reagent.[a]

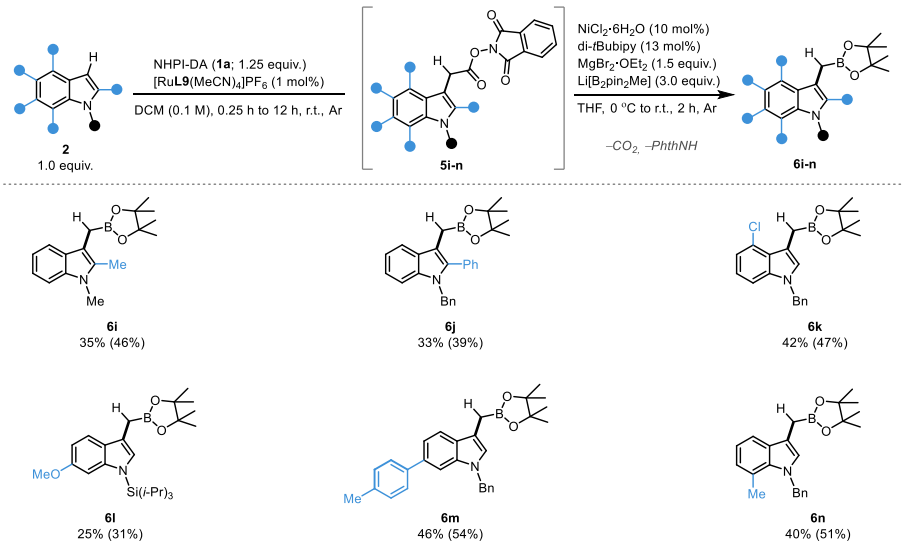

[a] Isolated yields are reported. In parenthesis are the crude yields determined by ^{1}H-NMR spectroscopy using 1,1,2,2-tetrachloroethane as internal standard. Reaction conditions: **2** (0.3 mmol), **1a** (1.25 equiv.), [Ru**L9**(MeCN)$_4$]PF$_6$ (1 mol%), CH_2Cl_2 (0.1 M), 0.25 -14 h, r.t., then $NiCl_2$·$6H_2O$ (0.10 equiv.), 4,4'-*di*-*t*-Bubipy (0.13 equiv.), $MgBr_2$·OEt_2 (1.5 equiv.), B_2pin_2 (3.0 equiv.), MeLi (3.3 equiv.), 0 ˚C to r.t., 2 h, Ar.

2.5.2 Unified C–H Alkylation of Indoles at Room Temperature

Currently, the C–H alkylation of indoles often requires harsh reaction conditions and specific reagents that incorporate the desired functionality of the alkyl chain, which need to be synthesized independently[29] (see Section 2.1.3). A unified approach that uses a single but versatile diazo compound precursor would overcome some of the limitations associated with benzylidene, alkenylidene, and alkylidene intermediates. These carbenes are generally sourced in unstable diazo compounds, and are prone to take part in side-reactions like Büchner ring-expansion, cyclopropanation or β-hydride elimination. It was found that arylation, alkenylation and alkylation of the indole redox-active esters can be performed with slight modifications on the conditions recently developed for decarboxylative couplings[19a,c,d,k] (Table 2.9). Diorganozinc reagents were used as sources of the corresponding carbon fragments, which were prepared using the conditions reported in the literature.[19c,d,k] A nickel-catalyzed system was used to couple the indole NHPI esters (**5b**/**l**) with several diarylzinc reagents, allowing the mild syntheses of C3-benzyl indoles. This way, difluorophenyl (**6o**), naphthyl (**6p**) and *m*-tolyl (**6q**) groups were introduced in high efficiency from a common intermediate. Olefins can also be incorporated to yield non-conjugated C3-allyl derivatives including cyclohexenyl (**6r**), propenyl (**6s**) and styrenyl (**6t**) groups. A

variety of dialkylzinc reagents allow further elongation of the alkyl chain at C3- position of indoles incorporating functionalities, such as ether (**6u**), morpholine (**6v**), chloride (**6w**), olefin (**6x**), cyclopropyl (**6y)** and the simple ethyl (**6z**), all in moderate to excellent yields.

Table 2.9: Unified C–H alkylation of indoles using NHPI-DA (**1a**) as methylene linchpin reagent.[a]

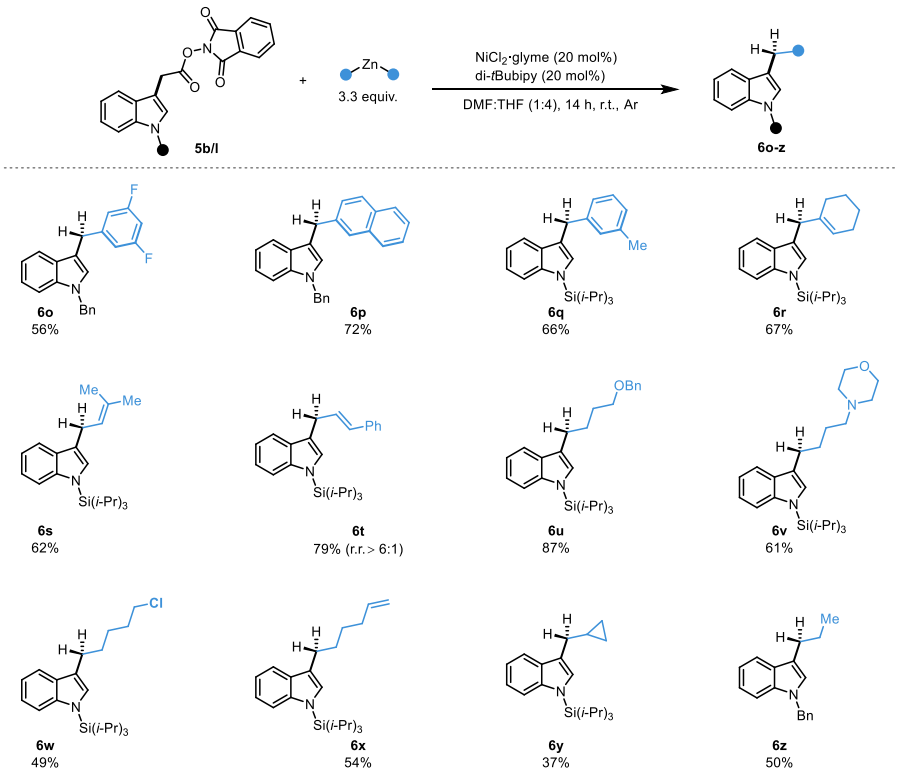

[a] Reaction conditions: **5b/l** (0.2-0.3 mmol), dialkylzinc (3.3 equiv.), $NiCl_2$·glyme (20 mol%), 4,4'-*di*-*t*-butyl-2,2'-bipyridine (20 mol%), DMF:THF (1:4; 0.1 M), 14 h, r.t.

2.5.3 Giese Reaction of Redox-Active Esters of Indoles with Michael Acceptors

A milder alternative to create aliphatic linkages through radical coupling is the Giese reaction, which involves the conjugate addition of an alkyl radical into an electrophilic olefin. The decarboxylative coupling of the indole redox-active esters and Michael acceptors was explored using zinc as reductant and a nickel catalyst as reported by Baran and co-workers.[19u] Several electron-poor olefins were coupled to obtain products **6aa-ac**, such as methyl vinyl ketone (**6aa**), acrylonitrile (**6ab**) and benzyl acrylate (**6ac**), thus enabling further decoration of the C3-alkyl chain in indole (Table 2.10). A new approach towards these Giese-type reactions discovered in our group will be discussed in depth in Chapter 3 of this thesis.

Table 2.10: Giese reaction of redox-active ester products of indoles.[a]

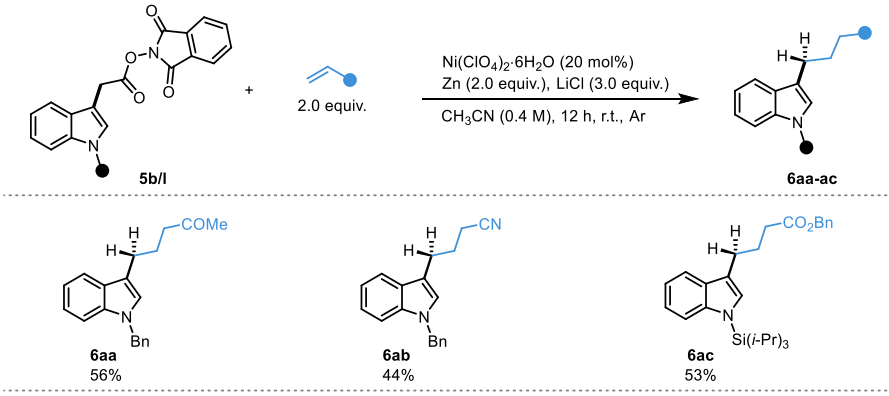

[a] Reaction conditions: **5b/l** (0.2 mmol), Michael acceptor (2.0 equiv.), $Ni(ClO_4)_2 \cdot 6H_2O$ (20 mol%), Zn (2.0 equiv.), LiCl (3.0 equiv.), CH_3CN (0.4 M), 12 h, r.t.

2.6 Conclusion

In summary, it has been demonstrated that redox-active ruthenium carbenes undergo highly selective insertion reactions into C–H bond of indoles at the C2- and C3-positions. The reactivity and selectivity bestowed by these redox-active carbenes are remarkable in the context of related insertions with simple diazoacetate reagents. The resulting products have been further transformed into variety of boryl-, aryl-, alkyl-, and alkenyl functionalized indoles through a unified strategy. Collectively, these results form a new platform for the C–H alkylation that is mild and can complement existing methods when harsh conditions and functional group tolerance may prove problematic. Overall, these transformations are equivalent to the formal insertions of the unstable and problematic carbenoids that cannot engage in direct insertion. Importantly, all these formal insertion processes are accomplished using a single versatile redox-active diazoacetate reagent (NHPI-DA).

3. Decarboxylative Giese Reactions of Redox-Active Esters Promoted by Biocompatible Photoreductants and Blue Light (Paper II)

3.1 Introduction

3.1.1 Decarboxylative Giese Reactions

Giese reactions are the conjugate addition of carbon radicals into electron-deficient olefins resulting in the construction of aliphatic C–C bonds.[38] Originally, these radicals were generated by the direct abstraction of halides from alkyl halides upon treatment with trialkyltin reagents in the presence of UV-light.[38a,b] However, these processes have many drawbacks, such as the use of halogen compounds which results in the production of halogen containing waste. Furthermore, trialkyltin reagents are very toxic.[38c] Over the years, significant progress has been made in the discovery of wide range of alkyl radical precursors. Particularly, carboxylic acids have emerged as source of carbon radicals and their abundance has impacted the C–C bond forming chemistry through Giese reactions (see Sections 1.3.2, 1.3.3).[38d] In 2014, MacMillan demonstrated that carboxylic acids **8** in the presence of Ir(III)-photocatalyst undergo single electron oxidation, which results in the formation of alkyl radicals extruding CO_2 as gas. The alkyl radical generated this way attacks the electron-poor olefins **9** to form the C–C bond, and the resulting radical is then reduced by Ir(II) to deliver the product **10** after proton transfer (Scheme 3.1).[38e]

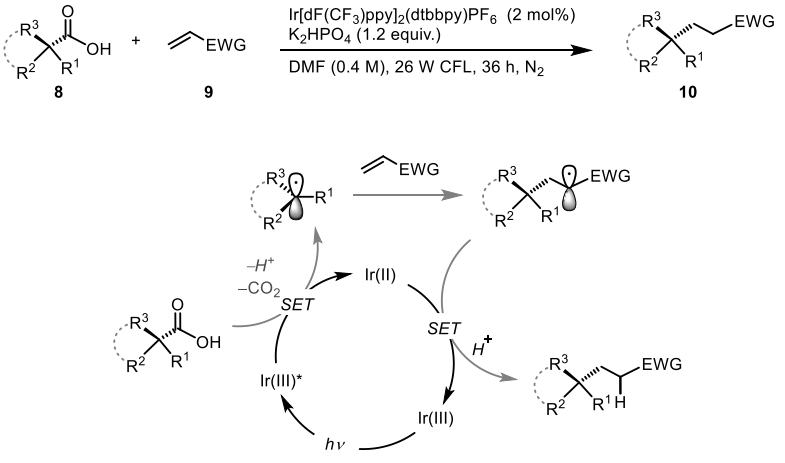

Scheme 3.1: Giese reaction using carboxylic acid as radical precursor in the presence of Ir-photocatalyst.[38e]

Carboxylic acids can be coupled with *N*-hydroxyphthalimide (NHPI) in the presence of DCC and DMAP to synthesize the corresponding *N*-hydroxyphthalimide esters (see

section 1.3.2). In 1988, Okada and co-workers discovered that these esters have redox-active properties and they can be transformed into the corresponding alkanes under UV-irradiation in the presence of a photosensitizer.[16a] In 1991, the same group demonstrated a coupling reaction between ester **11** and Michael acceptors **9** using $[Ru(bpy)_3]Cl_2$ as photocatalyst, and *N*-benzyl nicotinamide (**12a**) as reductant.[16b] It was proposed that the excited photocatalyst, $Ru(II)^*$ undergoes a single electron transfer (SET) process with **12a** generating the reduced photocatalyst Ru(I) and dihydronicotinamyl radical cation **A**, which upon losing a proton leads to the formation of a dihydronicotinamyl radical **B** (Scheme 3.2). It was postulated that the reduced Ru(I) photocatalyst is required to reduce the redox-active ester **11** generating alkyl radical **C** with the extrusion of phthalimidate anion (**D**) and CO_2. Upon capture by the Michael acceptor **9**, the resulting carbon-centered radical **E** undergoes a subsequent hydrogen atom transfer process (HAT) leading to the product **10** and dihydronicotinamyl radical **B**. The latter then reduces another molecule of the redox-active ester *via* SET and propagates the radical chain. In addition to primary, secondary and tertiary carboxylic acids NHPI esters, a series of Michael acceptors were tolerated in this reaction to form cross-coupling products.

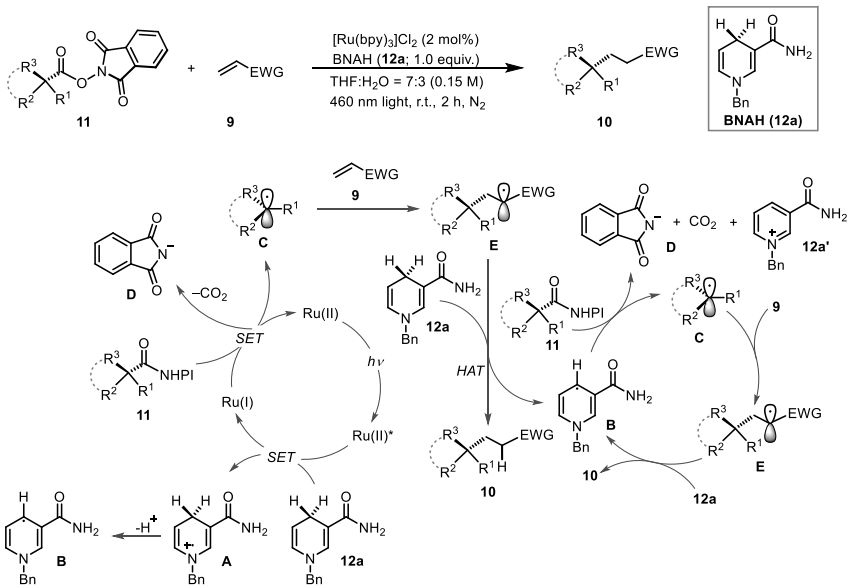

Scheme 3.2: Okada's decarboxylation of *N*-hydroxyphthalimide esters using BNAH (**12a**) as reductant.[16b]

3.1.2 Modern Giese Reactions with Redox-Active Esters

Built on Okada's seminal work and initially inspired by a total synthesis project, Overman and co-workers in 2015 reported construction of quaternary carbon centers from *N*-hydroxyphthalimide esters.[39a] In this particular case, the Hantzsch ester (H.E.) was used as reductant in the presence of a similar ruthenium photocatalyst and Hünig's base (Scheme 3.3 A). The mechanism of this reaction was proposed to have a similar pathway as that studied by Okada and co-workers (Scheme 3.2). Using this protocol it was possible to couple a variety of tertiary acid substrates with a series of Michael acceptors, which strengthened the synthetic potential of this reaction in the late stage construction of quaternary carbon centers. In later studies, they reported that in some substrates the photocatalyst was not required, and the Hantzsch ester could promote the photo-reaction on its own.[39a] In 2019 during the development of the research presented herein, Shang and co-workers expanded the substrate scope of this type of decarboxylative coupling using the Hantzsch ester as reductant without using a photocatalyst (Scheme 3.3 B).[39b] In this work, they proposed that an electron donor-acceptor complex (EDA) between the Hantzsch ester and the NHPI ester was formed and excited by visible light to undergo the activation. The alkyl radicals produced were subsequently captured by a suitable olefin, and quenched *via* hydrogen atom transfer (HAT) to form the desired product **10**. Both electron poor and rich olefins were efficiently coupled with a variety of primary, secondary and tertiary carboxylic acid derivatives using the Hantzsch ester as the only required reagent. Interestingly, when the reaction was carried out in the absence of olefin, hydrodecarboxylated products could also be obtained.

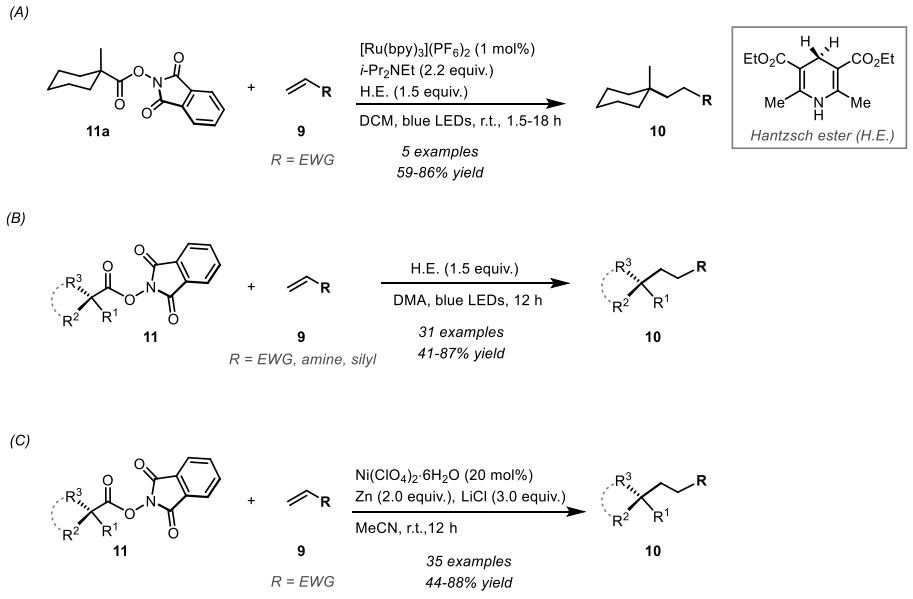

Scheme 3.3: (A) Overman's contribution to photo-Giese reaction. (B) Shang's decarboxylative Giese reaction without using photocatalyst. (C) Baran's nickel-catalyzed Giese reaction of NHPI esters.[19u,39]

Along with the development of visible light promoted Giese reactions of redox-active esters, alternative methods have been reported where transition-metal catalysts have been used. In 2017, Baran and co-workers reported decarboxylative coupling of these esters with Michael acceptors in the presence of nickel as catalyst and zinc as sacrificial reductant (Scheme 3.3, C).[19u] This method is applicable for the coupling of wide range of primary, seconday and tertiary radical precursors in excellent yields, and it has been applied for the macrocyclization towards cyclopeptides. More recently, the same group has demonstrated the application of zinc nanoparticles in the coupling of redox-active esters with DNA-encoded Michael acceptors (see Section 1.3.4).[21b]

3.2 Aim of the Project

Carboxylic acids are widely available and cheap feedstock chemicals that are particularly attractive starting materials for radical cross-coupling reactions.[21,40] In recent years, the decarboxylative C–C bond forming reactions have emerged as an important research area in the field of organic chemistry, and they have proven to be particularly suitable for the coupling of polar biomolecules (Section 1.3.4). However, these reactions have been reported to require photocatalysts, transition-metal catalysts and/or inorganic reductants that complicate their application in chemical biology.[21,40,41] Moreover, in the case of biomolecules the selective activation of a carboxylic acid in the presence of other carboxylates is always a challenge due to their similar oxidation potentials.[40c-e] To overcome these limitations, *N*-hydroxyphthalimidyl esters **11** could be used as an alternative and potential starting materials in the presence of soluble organic photoreductants, which upon irradiation with visible light would trigger the coupling with Michael acceptors **9**. In contrast to the existing methods, this Giese reaction would be activated externally using visible light in more biocompatible conditions. In this sense, the toxicity of the the photoreductant and the by-products, the concentration threshold, and the speed of the intermolecular coupling are key challenges that would need to be overcome (Scheme 3.4).

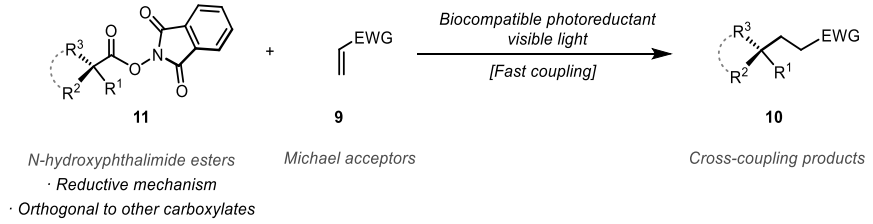

Scheme 3.4: Aim of the project.

3.3 Results and Discussion

The recent development of a diazo compound reagent, NHPI-DA (**1a**) by our group demonstrated the orthogonality of the *N*-hydroxyphthalimidyl group to a geminal carbenoid, and its enhanced reactivity and selectivity in cyclopropanation reactions (see Section 1.2.4).[13] The resulting redox-active ester products engage in versatile decarboxylative functionalization reactions, given the prowess of these substrates in cross-coupling (see Section 1.3.2). During the studies on our cyclopropane substrate **13**, we observed low yields in the Giese reactions using ruthenium- and iridium-based photocatalysts reported by Overman and Okada (Table 3.1, Entry 1-4).[16,39a,40e] Given the similar yields observed with different photocatalysts (Entries 3,4), we decided to run a control experiment without photocatalyst and realized that the reaction could be performed identically in that case (Entry 5). We reasoned that the dihydronicotinamide, BNAH (**12a**) has insufficient oxidation potential, (E_{ox} {**12a**} = 0.57 V vs Ag/Ag^+) to reduce redox-active esters (E_{red} {**7**}= –1.1 ± 0.1 V vs Ag/Ag^+).[42] However, these dihydronicotinamides are known to become potent single-electron reductants in their excited state, (E_{ox} {**12a**}* = –2.60 V vs Ag/Ag^+)[43,44] and will be capable of reducing a series of organic molecules, like redox-active esters.

Table 3.1: Preliminary exploration of the Giese reaction of NHPI ester of cyclopropane substrate.

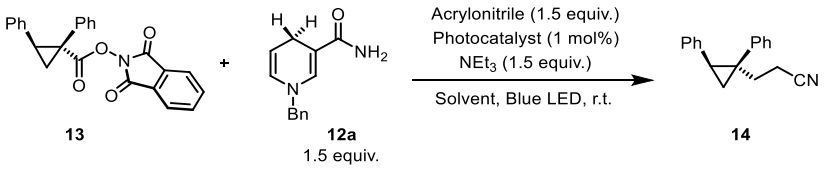

Entry	Photocatalyst	Solvent	Yield **14** (%)[a]
1	$[Ru(bpy)_3](PF_6)_2$	CH_3CN	25
2	$[Ru(bpy)_3](PF_6)_2$	Toluene	24
3	$[Ru(bpy)_3](PF_6)_2$	DCM	36
4	$[Ir(dtbbpy)(ppy)_2]PF_6$	DCM	36
5	none	DCM	30

[a] Yields were determined by ^{1}H-NMR spectroscopy using 1,1,2,2-tetrachloroethane as internal standard.

To further explore this coupling reaction, redox-active ester **11a** and Michael acceptor **9a** were chosen as model substrates in the presence of the dihydronicotinamide BNAH (**12a**) and blue light. Our preliminary optimization concluded that the reaction without photocatalyst performed best in polar solvents (DMF, 81%; MeCN, 65%; DMA, 75%), among which DMSO was optimal (92%; for details see Publication II Supporting Information). Moreover, it was observed that changing the concentration and slight increase of the temperature did not affect the efficiency of the reactions (Table 3.2, Entries 1-4). Furthermore, it was also possible to decrease the time of the reaction without a big impact on the overall performance (Entries 5,6). To our surprise 66% of the desired product **10a** was obtained when the reaction was carried out only for 30 min in DMSO as solvent (Entry 7). As expected, when the reaction was carried out in the dark no conversion of the starting materials was observed (Entry 8).

Table 3.2: Effects of concentration, temperature and other reaction parameters.

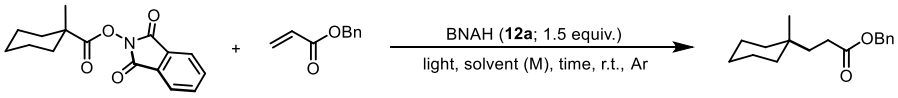

11a
0.1 mmol

9a
1.5 equiv.

10a

Entry	Solvent (M)	Light source	Time (h)	Yield (**10a**) (%)[a]
1	DMSO (0.2 M)	450 nm LED	24	89
2	DMSO (0.1 M)	450 nm LED	24	89
3	DMSO (0.05 M)	450 nm LED	24	91
4[b]	DMSO (0.1 M)	450 nm LED	24	89
5	DMSO (0.1 M)	450 nm LED	16	99
6	DMSO (0.1 M)	450 nm LED	2.5	93
7	DMSO (0.1 M)	450 nm LED	0.5	66
8[c]	DMSO (0.1 M)	No irradiation	16	0

[a] Yields were determined by ^{1}H-NMR spectroscopy using 1,1,2,2-tetrachloroethane as internal standard. [b] The reaction was performed at 40 ˚C; [c] the reaction was performed in vial wrapped in aluminium foil.

3.3.1 Exploration of Different Photoreductants at Low Concentration

Encouraged by the rapid coupling observed without photocatalyst in our conditions in 30 min (Table 3.2, entry 7), we set out to explore different dihydronicotinamide derivatives and study their relative performance (Table 3.3). It was observed that *N*-benzylnicotinic acid (**12b**) provided less than 5% of the coupling product (Entry 2),

and *N*-aryl dihydronicotinamides (**12c,d**) only provided poor yield of **10a** (Entries 3,4). These results underlined the importance of the substituent on the nitrogen and the dihydropyridine ring for the activation of the redox-active esters.

Table 3.3: Screening of different photoreductants and other reaction parameters.

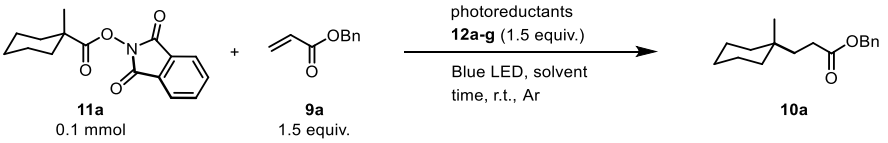

Entry	Solvent	Photoreductant	Time	Yield (**10a**) (%)[a]
1	DMSO (0.1 M)	**12a**	30 min	66
2	DMSO (0.1 M)	**12b**	2 h	< 5
3	DMSO (0.1 M)	**12c**	36 h	36
4	DMSO (0.1 M)	**12d**	36 h	26
5	DMSO (0.1 M)	**12e**	30 min	84
6	DMSO (0.1 M)	**12f**	5 min	99
7	DMSO (1 mM)	**12f**	20 min	87
8	1:1 H_2O/DMSO (1 mM)	**12f**	60 min	72
9[b]	1:1 H_2O/DMSO (1 mM)	**12f**	60 min	79
10	DMSO (10 mM)	**12g**	60 min	63
11[c]	1:1 H_2O/DMSO (1 mM)	**12g**	60 min	69

[a] Yields were determined by ^{1}H-NMR spectroscopy using 1,1,2,2-tetrachloroethane as internal standard. [b] Air instead of Ar and 3.0 equiv. of **12f** was used; [c] 10.0 equiv. of **12g** was used.

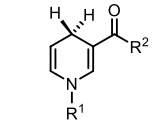

12a R^1 = Bn, R^2 = NH_2
12b R^1 = Bn, R^2 = OH
12c R^1 = Ph, R^2 = NH_2
12d R^1 = *p*-BrPh, R^2 = NH_2
12f R^1 = *n*-Bu, R^2 = NH_2

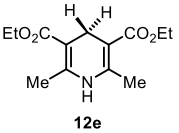

12e

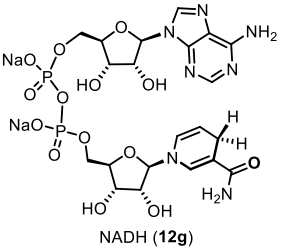

NADH (**12g**)

As reported in the literature, the Hantzsch ester (**12e**) was also effective and provided good yield of the desired product (Entry 5).[39b] Employing the *N*-butyl dihydronicotinamide (**12f**), which is slightly more reductive than the corresponding *N*-benzyl analogue **12a**,[45] we were delighted to obtain **10a** in 99% yield in just 5 min (Entry 6). Nevertheless, the photocoupling product **10a** was obtained in similar efficiency when performed under dilution (1 mM) (Entry 7). Moreover, we were surprised by the fact that this reaction works efficiently in a mixture of 1:1 water and DMSO as solvent, albeit longer time was needed for the completion of the reaction (Entry 8). Interestingly, the reaction can also be performed under air providing **10a** in very good yield with slightly higher loading of the photoreductant (Entry 9). The reduced nicotinamide adenine dinucleotide (NADH; **12g**) which is a native cofactor and closely structurally related to BuNAH (**12f**), was found to promote this cross-coupling reaction in good yield even in 10 mM concentration (Entry 10). But due to the challenging photophysics and shorter excited state lifetime (τ {**12g***} $\sim$ 0.4 ns)[46-49] it was essential to use higher loading of the NADH under inert atmosphere to carry out the coupling reaction in aqueous media at 1 mM concentration for optimal performance (Entry 11).

3.4 Scope Study

The simple reaction conditions of the coupling using BuNAH (**12f**) or NADH (**12g**) and the remarkable reactivity under dilution invited for a detailed scrutiny of the scope of this reaction under three different conditions: (A) the preparative conditions, where BuNAH (**12f**) was used as photoreductant in DMSO (100 mM) under argon; (B) the diluted coupling conditions, where BuNAH (**12f**) was used as photoreductant in 50% H_2O in DMSO (1 mM) under air; and (C) the diluted coupling conditions with the NADH (**12g**) as photoreductant in 50% H_2O in DMSO (1 mM) under argon. We started the scope with prototypical Michael acceptors (Table 3.4). Different electron-withdrawing substituents on the olefin were accommodated under these reaction conditions. Aromatic or aliphatic esters (**10a,c**) were coupled effectively, α-substituted electron poor olefin (**10b**) could also be used but lower yield of the desired product was obtained in case of the NADH reaction. Acrylamide (**10d**) was also found to be highly effective even under dilute aqueous conditions, whereas acrolein (**10e**) was sensitive towards the more challenging reaction conditions B and C. Methyl vinyl ketone and acrylonitrile were successfully coupled with **11a** to furnish the corresponding products **10f,g** in excellent yields. A sulphone could also be accommodated with high efficiency under different reaction conditions. The maleimide could also be used as Michael acceptor with minimal adjustment of the reaction conditions to deliver the corresponding product **10i** in high yield. Interestingly, dihydropyridine derivative **12e** failed to provide the cross-coupling product **10i** when the maleimide was used as Michael acceptor,[39b] which demonstrates the superior performance of the dihydronicotinamides (**12f,g**) in the photocoupling reaction.

Table 3.4: Scope of the alkyl photo-ligation reactions with different Michael acceptors.[a]

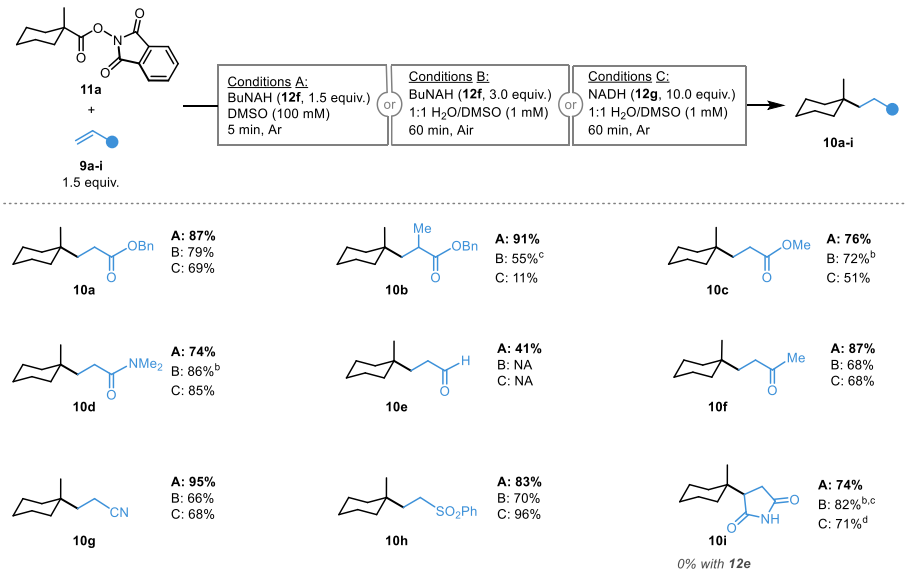

[a] Reaction conditions: (A) **11a** (1.0 equiv.), **9a-i** (1.5 equiv.) **12f** (1.5 equiv.), DMSO (100 mM), 5 min, Ar; (B) **11a** (1.0 equiv.), **9a-i** (1.5 equiv.) **12f** (3.0 equiv.), 50% H_2O in DMSO (1 mM), 60 min, Air; (C) **11a** (1.0 equiv.), **9a-i** (1.5 equiv.) **12g** (10.0 equiv.), 50% H_2O in DMSO (1 mM), 60 min, Ar. [b] Ar atmosphere; [c] DMSO; [d] DMSO (20 mM), 75 min.

After exploration of the coupling with a handful of Michael acceptors, we were interested in the behaviour of different radical precursors in the photo-Giese reaction (Table 3.5). First, we tested a variety of NHPI esters of tertiary carboxylic acids, that includes bicyclic (**10j**), adamantyl (**10k**), piperidine (**10l**), cyclopropane (**10m**) and oxetane (**10n**) scaffolds. Both BuNAH (**12f**) and the NADH (**12g**) were found to be excellent photoreductants to effectively connect these radicals with the Michael acceptors **9a**,**h** under diluted aqueous conditions. Secondary radical precursors were also successfully engaged in this coupling process to synthesize the corresponding alkylated products (**10o-q**), albeit no product formation was observed when the NADH was used as reductant for the indane derivative **10p**. The reason for the formation of **10q,q'** can be explained by a norbornenyl-nortricyclyl radical equilibrium[50] before the corresponding norbornenyl radical is trapped by the Michael acceptor **9h**. We were delighted to find out that a series of primary carboxylates (**10r-u**) could also be coupled under these reaction conditions. Interestingly, the indole derivative **10r** could be synthesized in good yield even in pure water as solvent. This result illustrates the capacity of these couplings to be combined with the C–H insertion of indoles using redox-active diazo compound, NHPI-DA (**1a**) (see Chapter 2). A protected sugar unit and the redox-active ester derived from *D*-biotin can be conjugated (**10s**) using the NADH as reductant with slight tuning of the other reaction parameters. The fatty acid **10t** and

a basic heterocyclic derivative (**10u**) could be obtained in moderate yields, although the pyridine carboxylate did not perform well in the aqueous conditions (B,C).

Table 3.5: Scope of the alkyl photo-ligation reactions with different redox-active esters.[a]

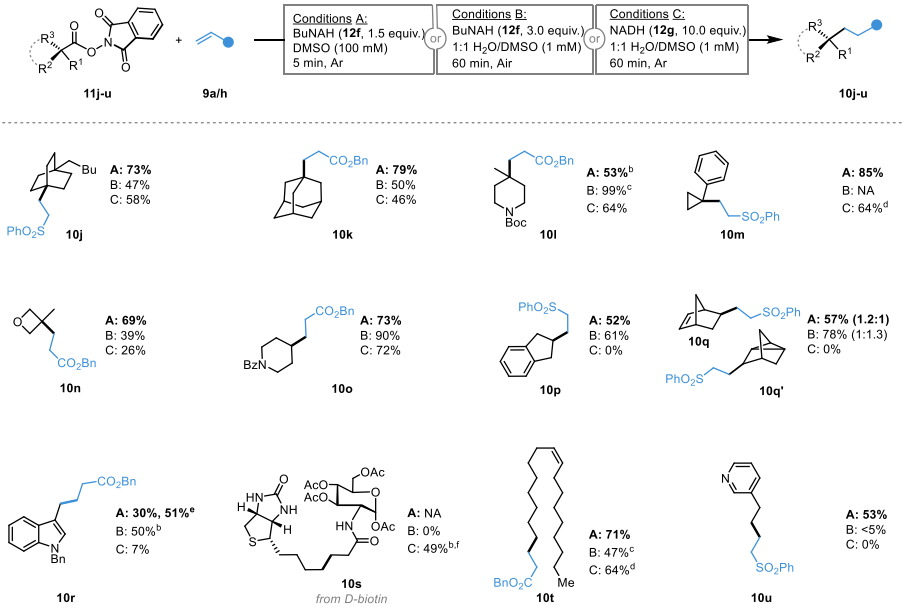

[a] Reaction conditions: (A) **11j-u** (1.0 equiv.), **9a/h** (1.5 equiv.) **12f** (1.5 equiv.), DMSO (100 mM), 5 min, Ar; (B) **11j-u** (1.0 equiv.), **9a/h** (1.5 equiv.) **12f** (3.0 equiv.), 50% H_2O in DMSO (1 mM), 60 min, Air; (C) **11j-u** (1.0 equiv.), **9a/h** (1.5 equiv.) **12g** (10.0 equiv.), 50% H_2O in DMSO (1 mM), 60 min, Ar. [b] Ar atmosphere; [c] DMSO; [d] DMSO (20 mM), 75 min; [e] 100% H_2O; [f] NADH (1.5 equiv.), DMSO (0.05 M), 14 h; NA = not applicable.

After screening a variety of different redox-active esters, we evaluated these systems on more complex substrates (Table 3.6). The gemfibrozil acid derivative was coupled with benzyl acrylate to obtain the corresponding product **10v** in high yield. To our surprise, the same radical precursor can also be used for the C−C bond construction using a Michael acceptor that bears an acid function (**10w**). Moreover, the aqueous or the NADH reaction conditions were equally effective for this particular substrate, demonstrating the orthogonality of the redox-active esters to carboxylates in intermolecular coupling. This is not possible with the oxidative methods using polycarboxylate subtrates due to the similar oxidation potentials of these functional groups that hinder their selective activation. Interestingly, the dipeptide model derived from alanine could also be coupled to synthesize the product **10x** in 60% yield even when pure water was used as solvent. The radical precursor derived from abietic acid could also participate under the standard reaction conditions furnishing good yield of **10y**. Unfortunately, the NADH reaction conditions were found to be unsuitable in these last

cases. It is worth to mention that the redox-active ester derived from 18ß-glycyrrhetinic acid could be selectively functionalized in the presence of unprotected carboxylic acids to deliver the product **10z**, which displays the orthogonality of the NHPI moiety over carboxylates in intramolecular fashion. The radical precursors derived from ketopinic acid (**10aa**), oleanoic acid (**10ab**) and 18ß-glycyrrhetinic acid (**10ac**) were seamlessly coupled with Michael acceptors providing the corresponding alkyl-ligated products with high efficiency under the standard reaction conditions, although understandably lower performance in the aqueous media was observed.

Table 3.6: Application of the alkyl photo-ligation reactions in the synthesis of medicinal compounds and natural products.[a]

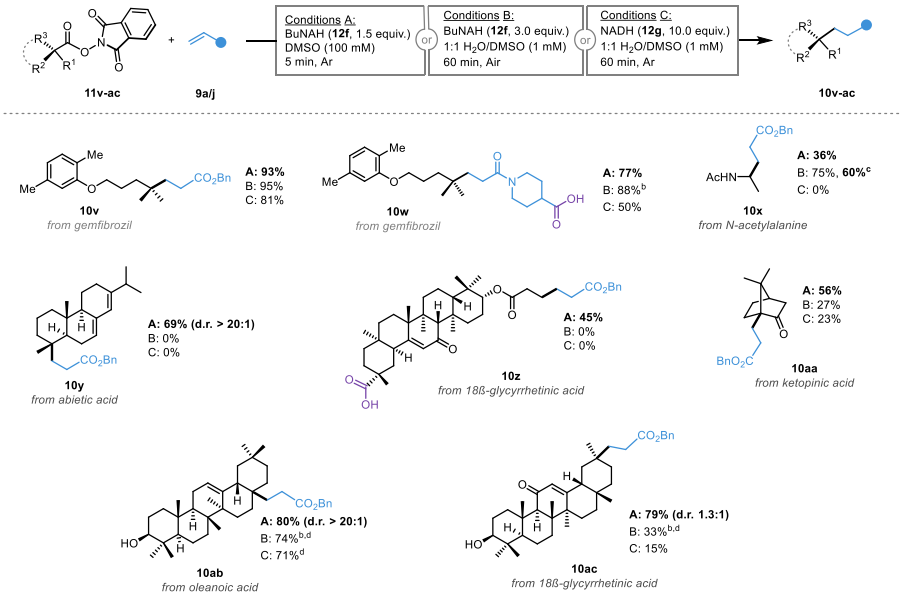

[a] Reaction conditions: (A) **11v-ac** (1.0 equiv.), **9a/j** (1.5 equiv.) **12f** (1.5 equiv.), DMSO (100 mM), 5 min, Ar; (B) **11v-ac** (1.0 equiv.), **9a/j** (1.5 equiv.) **12f** (3.0 equiv.), 50% H_2O in DMSO (1 mM), 60 min, Air; (C) **11v-ac** (1.0 equiv.), **9a/j** (1.5 equiv.) **12g** (10.0 equiv.), 50% H_2O in DMSO (1 mM), 60 min, Ar. [b] Ar atmosphere; [c] H_2O was used as solvent; [d] DMSO was used as solvent.

Encouraged by the water and moisture tolerance of this system and their robustness at very low concentration, we applied this technology for the C–C coupling of redox-active esters with DNA head-pieces [21,40] The efficiencies obtained were comparable to the related coupling reactions reported by Baran and co-workers,[21b] but with the advantage of fast coupling (1 h) and the use of a homogeneous light-triggered system. This way the synthesis of a series of DNA-coupled products **10ad-am** using both BuNAH and NADH was demonstrated (Scheme 3.5; see manuscript II for details).

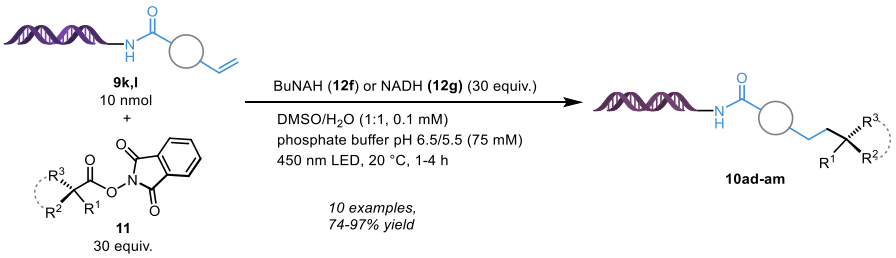

Scheme 3.5: Photo-ligation of redox-active esters with DNA-tagged Michael acceptors**.** Studies performed by Dr. My Linh Tong.

3.5 Kinetic Studies

Encouraged by the unusual fast rate of this photocoupling, we set out to explore the detailed reaction kinetics of this system. No-*D* NMR technology was utilized to monitor the progress of the reaction.[51] From the figures below it is evident that the standard photocoupling reaction reaches completion in less than 5 min (Figure 3.2 right, grey).[40c-f]

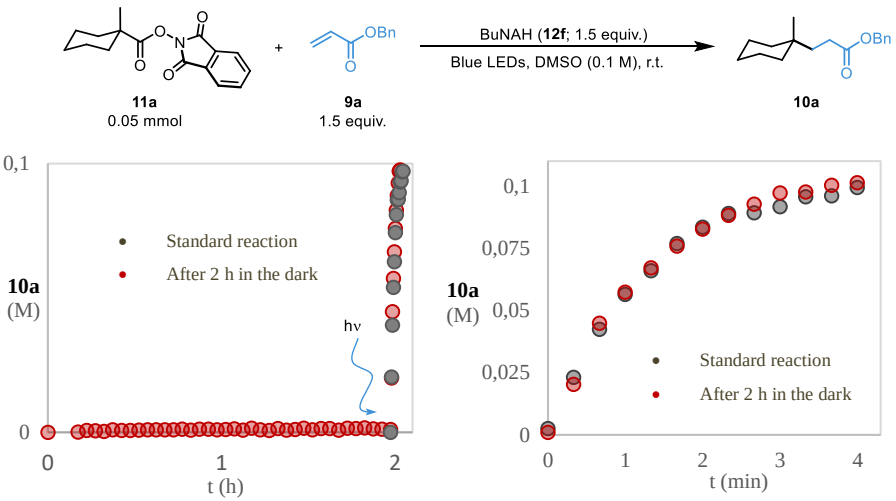

Figure 3.2: Left: Overlay of the reaction profiles of the standard reaction and the reaction after 2 h in the dark. Right: Time-shifted overlay of the standard reaction and the reaction after 2 h in the dark**.** Studies performed by Dr. Stephanie V. Kohlhepp.

To gain further knowledge about the background of the reaction, we monitored the conversion of the redox-active ester **11a** in the absence of light. In order to do this we set up the standard reaction inside a NMR tube excluding any adventitious light. Interestingly, we found out that during the dark period of 2 h there was no formation of the product **10a**. However, upon illumination with blue light after 2 h in the dark, the reaction reaches completion in less than 5 min (Figure 3.2 left, red). Moreover, from Figure 3.2 right, it can be seen that the progress of this experiment has very similar

profile to that of the standard reaction. This demonstrates the absence of any static deactivation of the reacting components in the dark, which could be a useful feature when other equilibriums would need to be established before triggering the C−C photocoupling.

3.5.1 Kinetic Study under Dilution

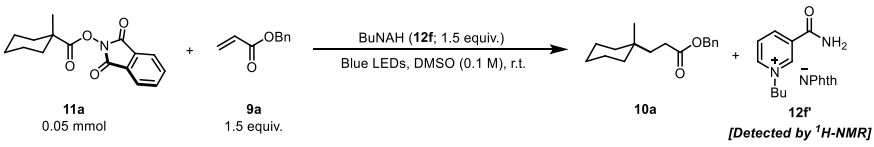

11a 0.05 mmol | **9a** 1.5 equiv. | **10a** | **12f'** *[Detected by ^{1}H-NMR]*

The concentration effect of this photocoupling reaction is an important aspect to study by kinetics. The progress of this reaction was monitored in three different initial concentrations of the starting redox-active ester **11a** inside NMR tubes. Interestingly, it was observed that the reactions at low concentrations (1-10 mM) are surprisingly faster than the standard reaction (Figure 3.3). At 1 mM concentration, the yield of the desired product **10a** was 97% in just 65 seconds, which was remarkable in terms of efficiency and robustness. To rationalize the much faster coupling rate at lower concentrations, a fourth experiment was performed at the least favourable concentration (100 mM) in a thinner NMR tube (diameter, φ = 1.25 mm) to minimize the light path of the system. The kinetics of this reaction was substantially accelerated and turned out to have a very similar profile to the ones at low concentration, i.e., 1-10 mM (Figure 3.3, orange). Thus, the acceleration in the coupling rate can be attributed to inner filter effect.[52] In the case of the reactions at lower concentration the light can be absorbed more efficiently throughout the reaction mixture, and this is also the case at higher concentration provided the reactor is thinner.

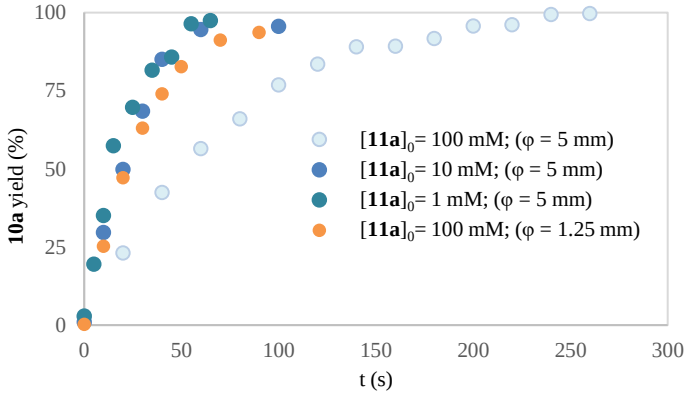

Figure 3.3: Kinetic study of the photocoupling reaction under dilution and inner filter effect. These experiments were performed by Dr. Stephanie V. Kohlhepp.

3.5.2 Profiling of Photo-Ligation using the NADH (**12g**) as Reductant by ^{1}H-NMR

The remarkable efficiency of the NADH (**12g**) as a photoreductant towards the alkyl photo-ligation reaction drew our interest to study the kinetics of the reaction with the redox-active ester **11k**. Conveniently, the reaction was performed in deuterated DMSO (DMSO-d_6) at micro-molar scale. We were delighted to find out that the desired coupling product **10k** can be obtained in 82% yield in less than 25 min of irradiation with 450 nm light and reaches completion in 73 min (Figure 3.4). The reactivity of the NADH (**12g**) in this photocoupling reaction is unusual despite its molecular complexity, unfavourable photophysics and low concentration of the medium.

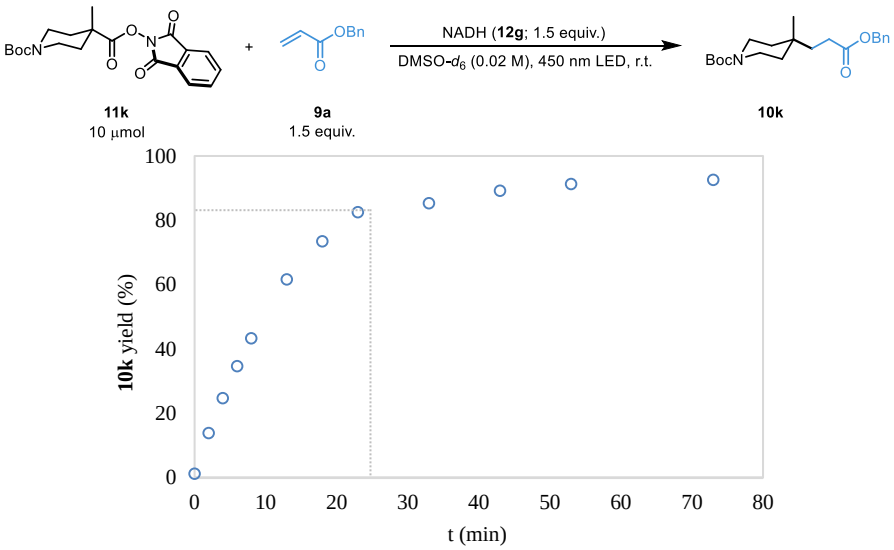

Figure 3.4: Kinetic study of the photocoupling reaction using NADH (**12g**) as reductant.

3.6 Mechanistic Studies

3.6.1 Determination of the Quantum Yield of the Photo-Giese Reaction

Intrigued by the surprisingly high rate of these coupling reactions under the demanding conditions, we set out to study its mechanism. Initially, the average quantum yield of the reaction was determined to get information on the possibility of a radical chain mechanism.[53] The quantum yield of a photochemical reaction is defined as the number of moles of the product formed per einstein of photons absorbed (Equation 1).[53] The quantum yield of the BuNAH (**12f**) mediated photocoupling reaction (Scheme 3.9) was determined using the procedure reported by Yoon and co-workers.[53]

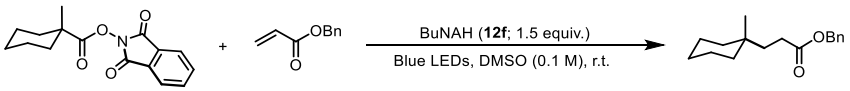

11a 0.24 mmol + **9a** 1.5 equiv. → **10a**

Scheme 3.9. Model reaction used to determine the quantum yield.

$$Quantum\ yield, \Phi = \frac{mol\ of\ \mathbf{10a}}{photonflux * t * f} \qquad (1)$$

In our case, the quantum yield is calculated using the expression above (eq. 1), where 't' is the time of the coupling reaction and 'f' is the fraction of the light absorbed by the reaction mixture at 450 nm.

$$f = 1 - 10^{-A} \qquad (2)$$

$$Photon\ flux = \frac{mol\ of\ Fe^{2+}}{\Phi * t * f} \qquad (3)$$

Normally, the fraction of the light absorbed (f) is estimated from the absorbance measurements at the wavelength used to activate the reactions (eq. 2). The absorbance (A) of the standard reaction mixture at λ = 450 nm is 1.99, and therefore f = $1–10^{–1.99}$ = 0.9897. The photon flux of the light source in the spectrophotometer was determined by standard potassium ferrioxalate actinometry (eq. 3).[53] In the reference system used, the quantum yield for the potassium ferrioxalate actinometer (ϕ = 1.01),[53] the time of irradiation (t) is expressed in seconds, and the fraction of light absorbed at λ = 450 nm by potassium ferrioxalate (f = 0.99833).[53] After triplicate measurement, the photon flux of the spectrophotometer was determined to be 4.53×10^{-9} einstein.s^{-1} at this wavelength which is in agreement with the literature values under similar conditions.[53]

The progress of our model reaction was monitored by three separate experiments (Table 3.7). After the error propagation analysis, the average quantum yield of the photo-Giese reaction was determined to be $\bar{\Phi} = 2.9 \pm 0.5$, which suggests the involvement of a radical chain mechanism.

Table 3.7: Quantum yield calculation of the photo-Giese reaction.

Entry	Irradiation time (s)	**10a** (mol×10^{-5})[a]	Quantum yield(ϕ)	(Δϕ)
1	3720	5.04	3.02	0.51
2	3720	4.68	2.80	0.48
3	4500	5.76	2.85	0.48

[a] The yield of **10a** was determined by ^{1}H-NMR spectroscopy with 1,1,2,2-tetrachloroethane as an internal standard.

3.6.2 UV-Vis Study

UV-Vis study of the BuNAH (**12f**), redox-active ester **11a**, and the mixture of **12f** and **11a** at different concentrations were conducted to have knowledge about the photo-physical properties of the reactants and any molecular interaction between them. When the study is performed at low concentration (Figure 3.5, left), no change in the absorbance of BuNAH (**12f**) was observed upon mixing with the redox-active ester **11a**. On the other hand, at higher concentration the absorbance of BuNAH (**12f**) increases slightly at 450 nm in the presence of **11a** (Figure 3.5, right). This may indicate the formation of an electron donor-acceptor complex (EDA), as earlier proposed by Shang and co-workers in a related system.[54,55]

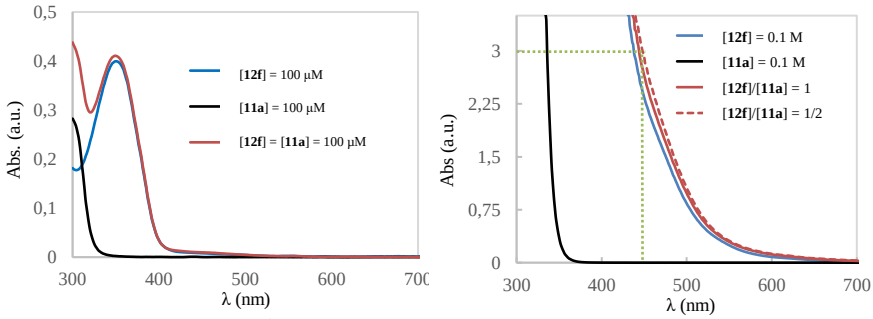

Figure 3.5: UV-Vis studies. Left: at low concentration; indicates no change in the absorbance upon mixing of **11a** with **12f**. Right: at higher concentration; indicates formation of an EDA-complex between **12f** and **11a**.

Based on these UV-Vis studies, we aimed to observe a discrete excitation profile for the putative EDA-complex. However, the excitation studies of pure BuNAH (**12f**) and the mixture of **12f** and the redox-active ester **11a** did not reveal any evident spectroscopic features for alternative excitations (Figure 3.6).

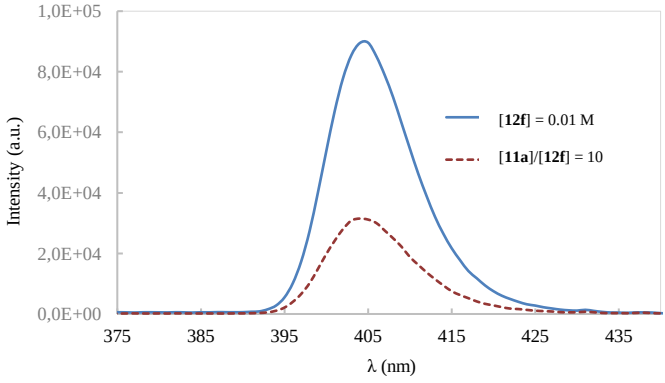

Figure 3.6: Excitation profiles of BuNAH (**12f**) and mixture of **12f** with redox-active ester **11a**; no new excited species is detected.

3.6.3 Stern-Volmer Quenching Study

Furthermore, steady-state fluorescence quenching experiment of BuNAH (**12f**) in the presence of different amount of redox-active ester **11a** indicates a linear decrease of the luminescence intensity (Figure 3.7, left). A linear Stern-Volmer quenching plot on steady state luminescence was not sufficient to prove the operative quenching mechanism (Figure 3.7; right, blue).[56] Thus, the lifetime of the excited state of BuNAH (**12f***) was measured using Time-Correlated Single Photon Counting (TCSPC), obtaining a value for τ_0 = 1.08 ns that decreased linearly in the presence of increasing concentrations of **11a**. However, the slope of the lifetime quenching plot (Figure 3.7; right, red) was significantly lower than that of the steady-state quenching plot (Figure 3.7; right, blue).

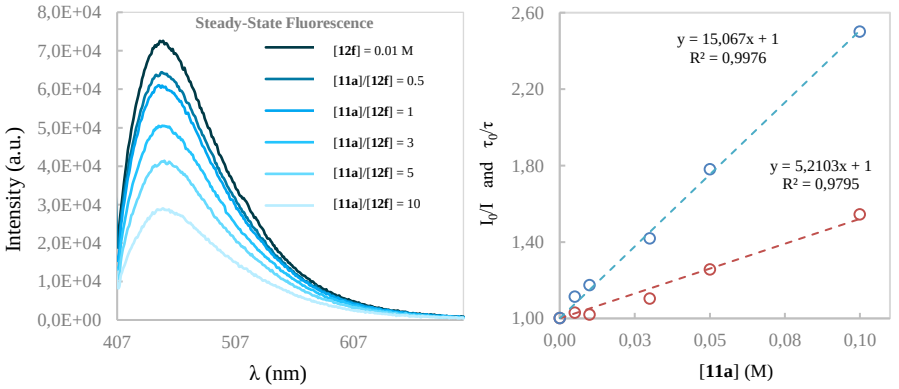

Figure 3.7: Left: Steady-state fluorescence quenching of **12f** with different concentration of **11a**. Right: Stern-Volmer plots of steady-state and lifetime fluorescence quenching of **12f** with **11a.**

The two different quenching constants calculated from the steady state and lifetime data (k_{sv} and k_q) is a typical scenario for a static-dynamic quenching mechanism (Figure 3.8, left).[56b]According to this model, the photoreductant **12f** can be promoted to its excited state **12f*** and is dynamically quenched by the redox-active ester **11a**, as demonstrated by the progressive decrease of the excited state lifetime with increasing concentrations of **11a**. On the other hand, the photoreductant **12f** in its ground state may exists in equilibrium as a complex (EDA) with the redox-active ester **11a**, whose emission quantum yield is much lower than that of **12f***or at least barely detected by the spectrophotometer. Therefore, the formation of an EDA-complex (**12f**·**11a**) effectively results in a more pronounced decrease in the emission intensity than could be ascribed to the dynamic quenching alone ($k_{SV} > k_q$). The steady state and lifetime data can be fitted in this model (Figure 3.8, right).to estimate the corresponding equilibrium constant ($K_{eq} \sim 7$).[56b] In our view, this case exemplifies how steady state Stern-Volmer data with a high linear correlation may easily be misinterpreted as proof for an operative dynamic quenching mechanism, and how the corresponding lifetime data is essential to obtain a complete picture.

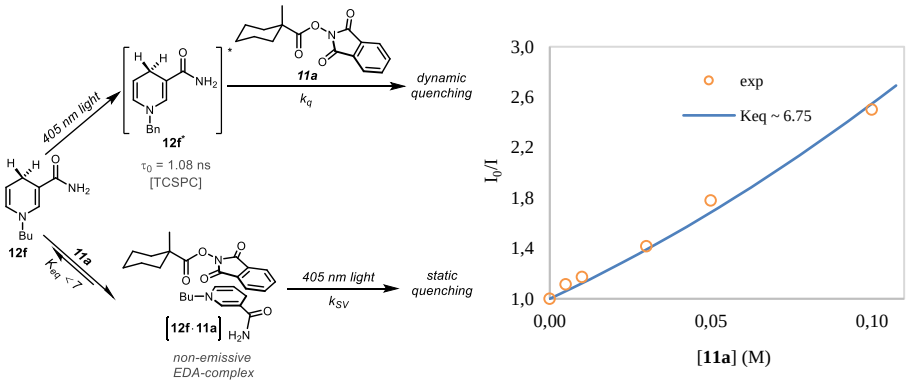

Figure 3.8: Left: Static-dynamic quenching model of BuNAH (**12f**) with redox-active ester **11a**. Right: Fitting of the steady state and lifetime data.

3.7 Mechanistic Model

Based on the average quantum yield obtained ($\varphi = 2.9 \pm 0.5$),[53] and further experimental details from the deuterium labelling and radical clock experiments (see publication II for details) we propose a mechanistic model below for the photo-Giese reaction (Figure 3.9). Our proposed mechanism is consistent with the electron-proton-electron manifold that is common in SET processes with the dihydropyridine photoreductants.[16b,c,39a,43,47,57,58] The excited photoreductant (**12f*** or **12g***) transfers an electron and a proton to the redox-active ester **11** to generate the alkyl radical **C** and the dihydronicotinamyl radical (**B**)[16b] forming phthalimide and CO_2 as by-products. Subsequently, the radical **C** is captured by a Michael acceptor **9** leading to the generation of carbon-centered radical **E**. Finally, the radical **E** undergoes a hydrogen atom transfer (HAT) process with a second molecule of the photoreductant (**12f** or **12g**) to yield the desired product (**10**).[16b,39a,57] This process also lead to the generation of the dihydronicotinamyl radical (**B**), which keeps propagating the radical chain,[16b,55] leaving the pyridinium salt (**12'**) and CO_2 as by-products. The latter were confirmed to be formed in the no-*D* NMR monitoring studies (see Section 3.5).

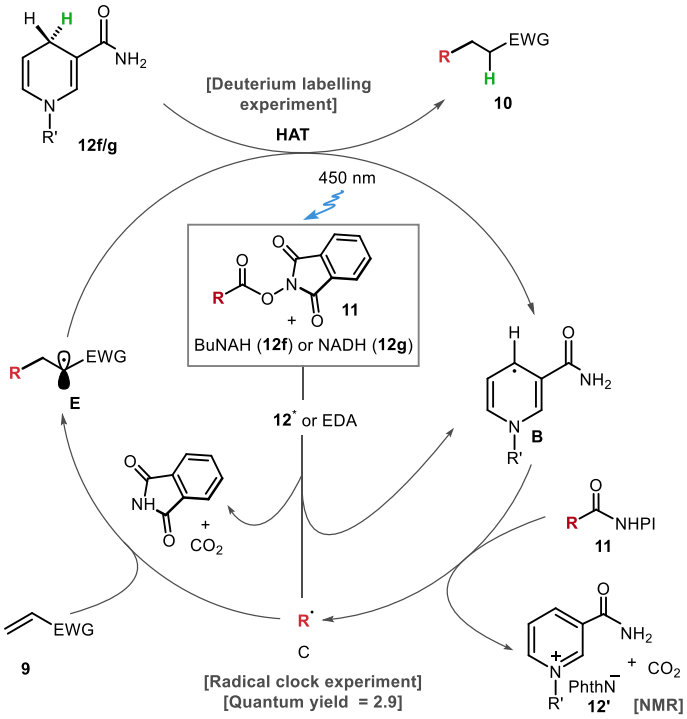

Figure 3.9: Proposed mechanism of the photo-Giese reaction.

3.8 Conclusion

To conclude, redox-active esters have been used in a new photo-triggered C−C coupling reaction promoted by NADH, a native cofactor in biological systems. We have demonstrated high functional group tolerance of these coupling reactions and its efficiency at very low concentrations. NADH has also been applied as reductant to forge C−C bond between redox-active esters and DNA-encoded electron-poor olefins. These reactions proceed without the need of any external photocatalyst and are very efficient when performed in the presence of air and water, making this coupling reaction relevant for further applications in chemical biology. This photo-Giese coupling has no background reactivity as established through extensive kinetic experiments. The kinetic and photophysical studies on the reaction have established the activation and propagation mechanism of this rapid photodecarboxylative coupling reaction.

4. Exploration of the Reactivity of α-Silyl Radicals Using the Redox-Active Diazo Compound (NHPI-DA) (Paper III)

4.1 Introduction

4.1.1 Organosilicon Compounds and Their Importance

In 1823, Swedish chemist Berzelius first isolated silicon by passing metallic potassium vapours over red-hot silica.[59] The residue obtained on treatment with water produced silicon as an amorphous solid with the evolution of hydrogen gas. Later in 1863, Friedel and Crafts reacted silicontetrachloride with diethylzinc to synthesize the first organosilicon compound, tetraethylsilane.[59] Besides the extensive applications of organosilicon compounds in material science and daily life, some silicon containing organic molecules also exhibit biological activity.[60] For example, *Si-Pc4* is used in laser photodynamic therapy towards cancer treatment,[60c] *flusilazole* is used as an antifungal agent, and *karenitecin* a silicon analogue of the anticancer natural product *campothecin* was evaluated in human trials for cancer treatment due to the increased lipophilicity of silicon.[60a] The silicon containing protein *NS5A* shows activity against hepatitis C virus (HCV) and *silafluofen* is used as an insecticide (Figure 4.1).[60c]

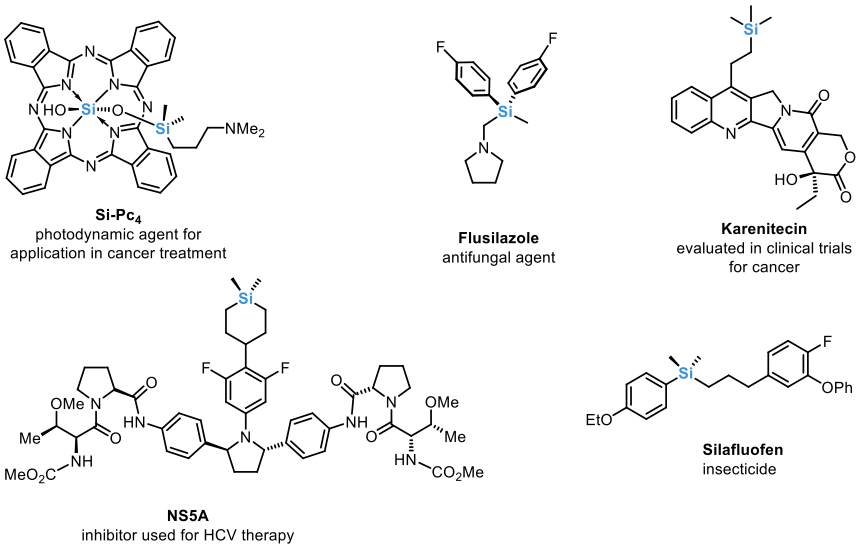

Figure 4.1: Silicon containing bioactive organic compounds.[59,60]

4.1.2 Structure, Synthesis and Reactivity of Silanes

Although organosilicon compounds are isoelectronic to carbon analogues, they exhibit properties that are very different from conventional organic molecules. It is known that a carbanion α-position to the silicon is better stabilized than the corresponding carbon counterpart is (α-silyl effect). This extra stability of α-silyl carbanions can be explained in terms of hyperconjugative effect, where Si-atom disperses the negative charge over three methyl groups of TMS (Figure 4.2 A).[61] Similarly, a carbocation in the β-position with respect to the silicon is more stable than the corresponding carbon analogue (β-silyl effect). This extra stabilization can be explained by the interaction of the filled σ(Si–C) orbital with the empty *p* orbital of the carbocation (Figure 4.2, B).[59,61]

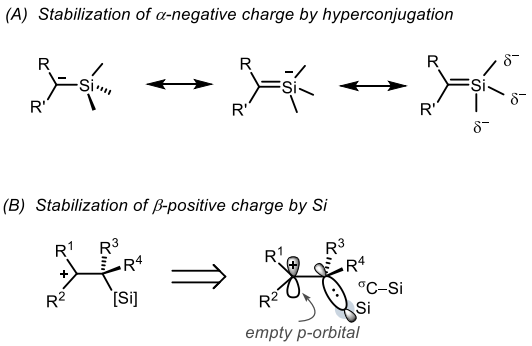

Figure 4.2: α- and β-silyl effects of silicon.[59,61]

4.1.3 α-Silyl Radicals and Their Application in Organic Synthesis

Like α-silyl carbanions, α-silyl radicals are known to be more stable than the corresponding carbon counterparts and do not undergo rearrangement to form silyl radicals.[62,63]These α-silyl radicals are reluctant to undergo rearrangements due to many factors, such as the less stability and high reactivity of silyl radicals in comparison to carbon radicals and the involvement of strained three-membered transition state (C–Si–C bond angle is *ca*. 48˚) during 1,2-migration of the carbon substituents. The generation of α-silyl radical was first realized in 1963 by Connolly and Urry.[62a] They described that (trimethylsilyl)methyllithium rapidly reacts with (chloromethyl)trimethylsilane and forms mainly 2,2,5,5-tetramethyl-2,5-disilahexane and tetramethylsilane along with trace amount of 2,2,4,4-tetramethyl-2,4-disilahexane after the usual 1,2-methyl shift (Scheme 4.1, A). Later in 1965, Wilt and Kolewe reported thermal decarbonylation of β-triphenylsilyl aldehyde in the presence of di-*tert*-butyl peroxide (DTBP) obatining methyltriphenylsilane in 52% yield (Scheme 4.1, B).[62b] On the other hand, they did not obtain similar product after the thermolysis of the corresponding carbon-counterpart. Further progress was made in this field and it was established that the generation of α-silyl radicals and their homocoupling can also take

place in the presence of silver bromide or *via* Kharasch-Grignard reaction (Scheme 4.1, C,D).[62c-f]

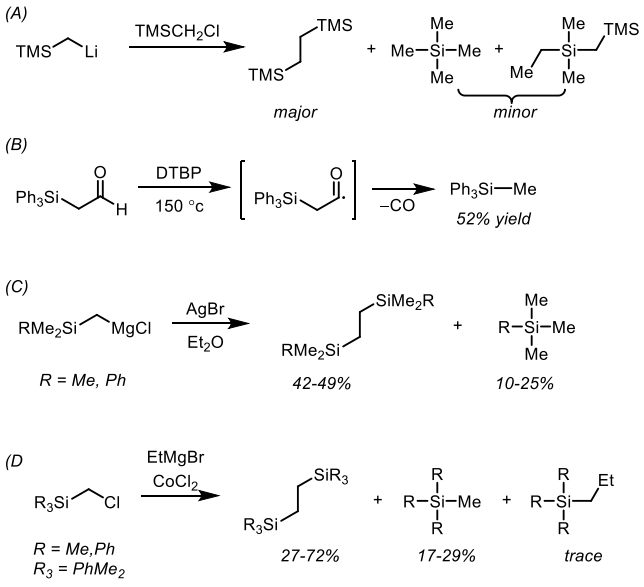

Scheme 4.1: Early discovery of α-silyl radicals.[62]

In 2017, Baran and co-workers reported iron-catalyzed cross coupling of alkenylsilanes with Michael acceptors to obtain six examples of alkylsilanes (Scheme 4.2, A).[63a] It has been proposed that this cross-coupling reaction proceeds *via* the transfer of a hydrogen atom from a transient iron(III)-hydride species to form a stabilized α-silyl radical in the presence of phenylsilane. More recently, Zhang and co-workers reported a radical-polar crossover reaction utilizing the stability of α-silyl radicals. In this case, an iridium photocatalyst has been used to oxidize halomethylsilicates in the presence of blue LEDs, generating alkyl radicals which are then captured by vinylsilanes. A number of alkylsilanes and cyclopropylsilanes have been synthesized using this methodology (Scheme 4.2, B).[63b]

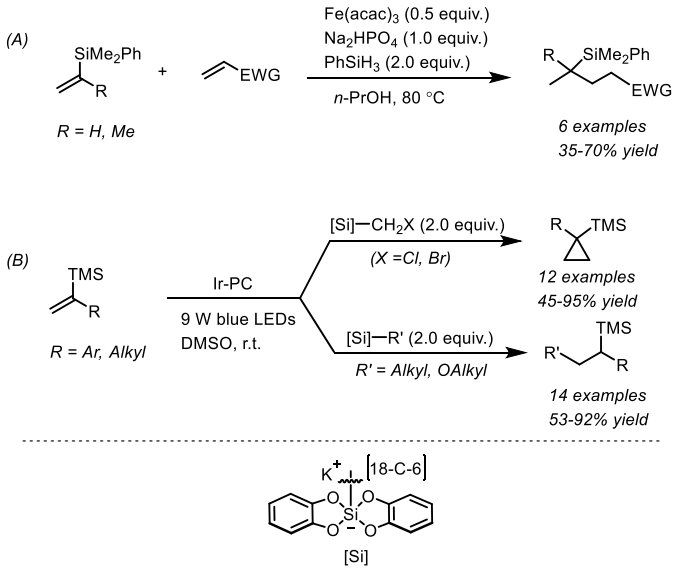

Scheme 4.2: Recent applications of α-silyl radicals in organic synthesis.[63] Ir-PC = $Ir[dF(CF_3)ppy]_2(dtbbpy)PF_6$

A number of organosilicon compounds are synthesized by reacting a carbon- or oxygen-based nucleophile with silicon halides (Scheme 4.3, A).[59] Also, hydrosilylation of alkenes or alkynes using a transition-metal catalysts is a commonly used approach towards organosilicon compounds. Depending on the metal catalyst used, the hydrosilylation can take place either *via* oxidative addition of the silicon hydride to the metal center or *via* the formation of Si−C bond through σ-bond metathesis (Scheme 4.3, B).[64] A typical hydrosilylation takes place according to the mechanism below as proposed by Chalk and Harrod in 1965 (Scheme 4.3, C).[64] This mechanistic scheme follows conventional oxidative addition, migratory insertion and reductive elimination steps, leading to the hydrosilylated product with *anti*-Markovnikov regioselectivity.

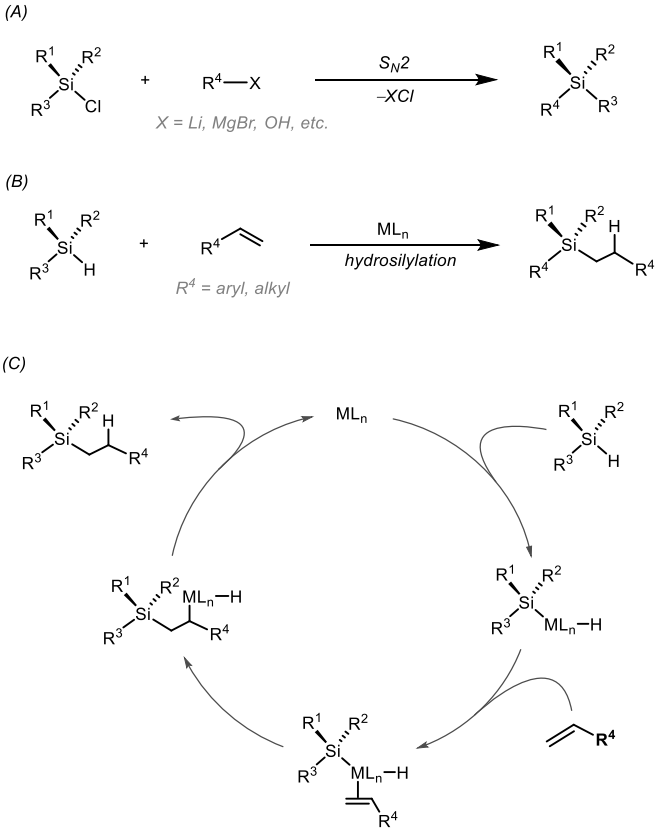

Scheme 4.3: Synthesis of organosilicon compounds through (A) classical S_N2 approach, and (B) transition-metal catalyzed hydrosilylation. (C) Mechanism of the hydrosilylation reaction proposed by Chalk and Harrod.[64]

According to the pioneering work by Kipping in 1904 silanediols undergo condensation to form silicones even though he characterized them as "sticky messes of no particular use" (Scheme 4.4).[65] The polymerization of silicones without silicon catenation can be attributed to the higher stability of the Si–O bond than Si–Si bond, which result in the proliferation of O–Si–O linkages. These silicon polymers possess different physical properties and today are routinely obtained as fluids or rubbers for countless applications.[59,66]

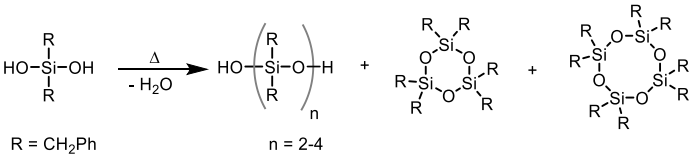

Scheme 4.4: Synthesis of silicones from silanediols through condensation.[65]

The higher affinity of silicon towards oxygen makes also silyl groups very important in the synthetic organic chemistry, particularly in the carbohydrate chemistry where protection and deprotection of polar functional group are among the key processes.[67] The synthetic utility of silyl moiety can be illustrated in the synthesis of 6-gingerol (Scheme 4.5), a phenol which is an ingredient responsible for the pungent smell in ginger oil.[59]

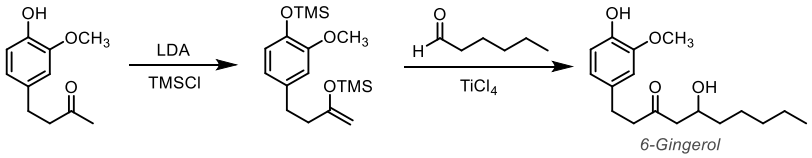

Scheme 4.5: Synthesis of 6-gingerol using silyl protecting groups.[59]

4.1.4 (Borylmethyl)silanes and Their Importance

Organosilicon compounds are considered as an important class of organic molecules due to their application in daily life, organic synthesis and material science.[66] Therefore, the development of reagents for the synthesis of organosilicon compounds is an interesting area of research for organic chemists.[66] Particularly, the chemistry of (trimethylsilyl)methylboronic acid is of interest due to the presence of orthogonal silicon and borane moiety at the same carbon atom.[68] In an early study by Matteson and Majumdar the synthetic usefulness of (borylmethyl)silanes was displayed through the synthesis of vinyl boronates from carbonyl compounds (Scheme 4.6).[68a] Further studies by Matteson and several other groups displayed significant application of this silaborane reagent in several organometallic processes as well as in Suzuki-type cross-coupling reactions in order to synthesize molecules of high synthetic value.[68b-h] This includes the synthesis of decorated (borylmethyl)silanes from alkyl halides, α-silyl ketones from aromatic esters, vinylsilanes from chiral epoxides, allyl silanes from vinyl halides, and benzylsilanes from *ortho*-aminoacetophenones. Recently, the synthetic usefulness of this reagent has been extended for the synthesis of complex tertiary aliphatic boronates from mesityl hydrazones.[68h] Despite the broad application, the exploration of more advanced chemistry of organosilaboranes requires more efficient and systematic assembly of these compounds from accessible materials.

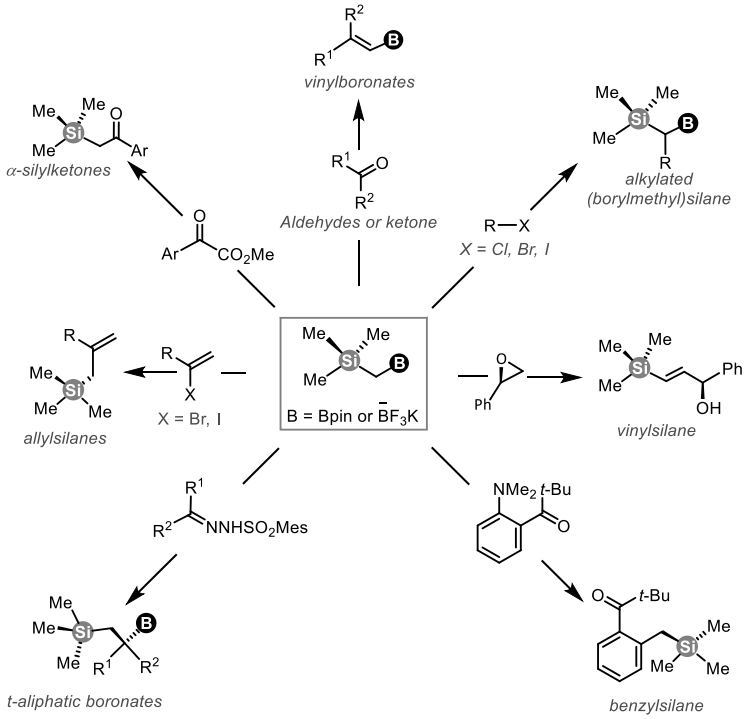

Scheme 4.6: Synthetic applications of (borylmethyl)silanes.[68]

4.1.4 Current Synthetic Strategies towards (Borylmethyl)silanes

Given the prowess of this class of compounds in organic synthesis, it is important to know the detailed background of the synthetic methods available to obtain them. In a seminal study in 1946, Whitmore and Sommer developed the first synthesis of (trimethylsilyl)methylboronic acid by reacting (trimethylsilyl)methylmagnesium chloride with trimethylborate (Scheme 4.7, A).[69b] The corresponding pinacol ester was synthesized by Matteson and Majumdar in 1980 by a similar approach.[69d,e] After almost three decades, in 2010 Ihara and Suginome reported a ruthenium-catalyzed Si−H functionalization strategy using a modified methylboronic acid, MeB(pza) affording five examples of (borylmethyl)silanes (Scheme 4.7, B).[69g] In a subsequent study by Ohmura and Suginome, an iridium-catalyzed C−H borylation of methylchlorosilanes was demonstrated towards the syntheses of (borylmethyl)silanes.[69h] Due to poor stability in moisture the resulting intermediate products were transformed to the corresponding isopropoxysilanes by the treatment with isopropanol and triethylamine (Scheme 4.7, C). In a recent study by Aggarwal and Shu, a metal-free photo-induced approach has been described for the C−H borylation of methylsilanes. It has been demonstrated that the reaction is initiated by violet light and *N*-alkoxyphthalimide based oxidant, using chlorine atom for the key hydrogen atom transfer (HAT) event (Scheme 4.7, D).[69k] Despite all these advances these methods posses several drawbacks, such as the use of excess starting materials and high temperature which is not optimal in cases where

sensitive functionalities are present. Therefore, development of more general and convenient methods for the syntheses of (borylmethyl)silanes is still highly sought after.

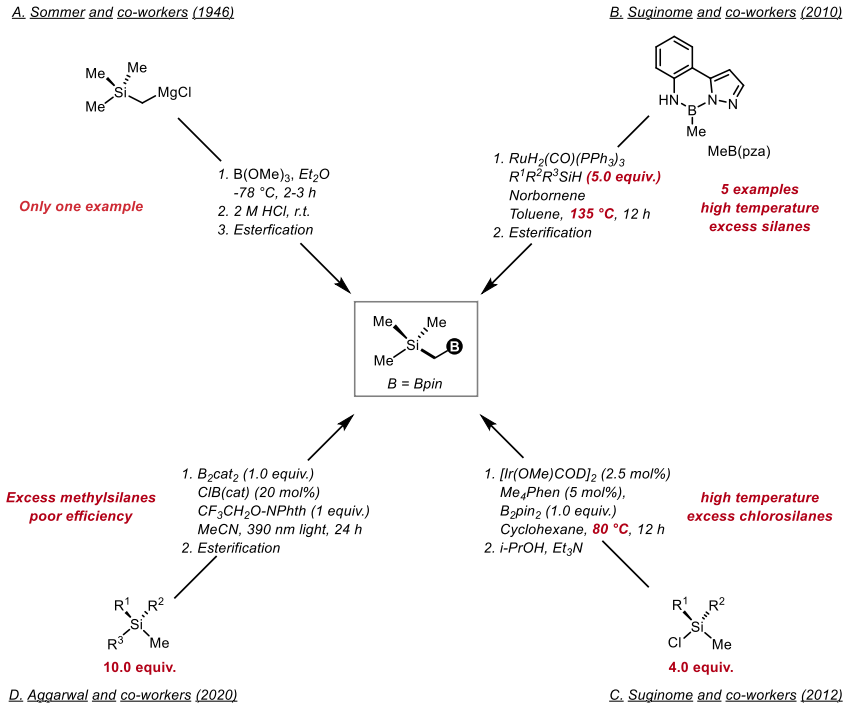

Scheme 4.7: (Borylmethyl)silanes: state-of-the-art and synthetic challenges.[69]

4.1.5 Si–H Functionalization of Silanes Using Diazo Compounds

Synthesis of organosilicon compounds *via* insertion of carbenes into Si–H bond was discovered by Kramer and Wright in 1963.[70] However, the limitations with the selectivity of the carbene Si–H insertion initially limited their application. Over the years, transition-metal-catalyzed Si–H functionalization reactions through carbene transfer has evolved systems for the insertion of different types of diazo compounds, including asymmetric methods.[3,71-74] In 1988, Doyle and co-workers first reported the insertion of rhodium carbenoids into Si–H bond for the synthesis of α-silyl esters and α-silyl ketones (Table 4.1, Entry 1).[72a] The first asymmetric Si–H insertion reaction was reported by Landais in 1994 using rhodium tetracarboxylates as catalyst and a diazo compound containing camphor-derived chiral auxiliaries, albeit poor stereoselectivity was obtained.[73a] In 1997, Davies used chiral rhodium(II) (*S*)-*N*-(arylsulfonyl)prolinate catalyst for the enantioselective synthesis of benzyl- and allylsilanes (Entry 6).[73g] Since then many different metal catalysts including Fe, Cu, Ag, Ru have been employed for this kind of diazo transfer reactions (Entries 2-4,7).[72,73] Important break-

throughs with α,α'-aryl trifluoromethyl[73h] and α,α'-diaryl diazo compounds[73k] in combination chiral copper and rhodium catalysts have been achieved (Entries 8,9). More recently, artificial enzymes have been developed for this purpose (Entry 5).[72d]

Table 4.1: Insertion of conventional diazoacetate reagents into Si–H bond.

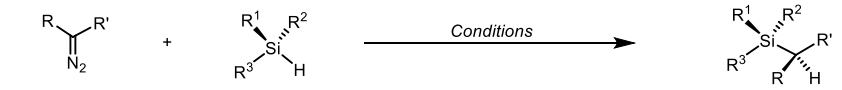

*Diazo compounds (**3**)* *Silanes (**15**)* *Si–H insertion products (**16**)*

Entry	Diazo compound (R,R')	Silane (R^1,R^2,R^3)	Conditions (equiv.)	Yield 16 (%)
1	R = H R' = CO_2Et or COPh	$R^1 = R^2 = R^3$ = Ar, alkyl	Silane (1.0-2.0), $Rh_2(OAc)_4$ (0.01)	85-94
2	R = H R' = CO_2Et	$R^1 = R^2$ = alkyl R^3 = H/Ar	Silane (12.0), [Ag**L1**] (0.2)	10-84
3	R = H R' = CO_2Et	$R^1 = R^2 = R^3$ = alkyl	Silane (1.1), $Cu(OTf)_2$ (0.08), **L10** (0.1)	70-92
4	R = Ar R' = CO_2Me	$R^1 = R^2 = R^3$ = alkyl	Silane (4.0), $Fe(OTf)_2$ (0.05)	65-99
5	R = alkyl R' = CO_2Et	$R^1 = R^2$ = alkyl, R^3 = Ar	Silane (2.0), *R. marinus cyt c*, M9-N buffer (pH 7.4), $Na_2S_2O_4$ (1.0)	47-6080[a]
6	R = Ar, alkenyl R' = CO_2Me	$R^1 = R^2$ = alkyl, R^3 = Ph	Silane (1.1), $Rh_2(DOSP)_4$ (0.01)	50-77
7	R = alkyl R' = CO_2R	$R^1 = R^2$ = alkyl, R^3 = Ph	Silane (2.0), [Ru**L9**$(MeCN)_4$]PF_6 (0.01)	53-95
8	R = Ar R' = CF_3	$R^1 = R^2 = R^3$ = alkyl	Silane (2.1), $[Cu(MeCN)_4]PF_6$ (0.05), **L11** (0.05), NaBArF (0.05)	61-99
9	R = R' = Ar	$R^1 = R^2$ = alkyl R^3 = Ar, alkynyl	Silane (1.2), $Rh_2(DOSP)_4$ (0.001)	37-93

[a] yield is expressed in total turnover number (TTN)

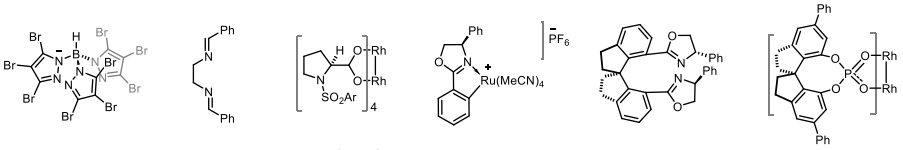

Tp^{Br3} (**L1**) *Schiff-base* (**L10**) *Ar = p-$C_{12}H_{25}C_6H_4$ $Rh_2(DOSP)_4$* *[Ru**L9**$(MeCN)_4$]PF_6* *spiro bis*-oxazoline (**L11**) *$Rh_2(SPA)_4$*

4.2 Aim of the Project

Despite the success achieved in recent years in the synthesis of (borylmethyl)silanes the existing methods possess many drawbacks in terms of efficiency, limited scope and harsh reaction conditions (see Section 4.1.4). Additionally, these synthetic routes often require excess starting materials, longer reaction period, and 5-10 mol% of precious iridium catalysts. Moreover, in the case of direct C–H borylation of methylsilanes, the competition between aliphatic and aromatic C–H bonds is another challenge yet to be solved. Therefore, the development of alternative methodology for the synthesis of (borylmethyl)silanes is of high importance. Ideally, the new methods should address the use of readily available hydrosilanes in minimal excess, offer milder and quicker coupling, and expand the scope to new organosilicon derivatives containing alkyl, aryl, heteroaryl and alkoxy groups.

In the previous studies by our group (see Chapter 2), we have demonstrated the orthogonality of the *N*-hydroxyphtalimide (NHPI) esters in carbene transfer processes.[13] The development of *N*-hydroxyphthalimidyl diazoacetate (NHPI-DA; **1a**) allowed formal insertion of unstable methylidenes (:CHR) into indoles and olefins. Based on these studies, we hypothesized that the functionalization of Si−H bond of silanes using the redox-active carbene precursor, NHPI-DA could provide a versatile entry towards α-silyl redox-active ester products, which could be the direct precursors of (borylmethyl)silanes through decarboxylative borylation (Scheme 4.8).

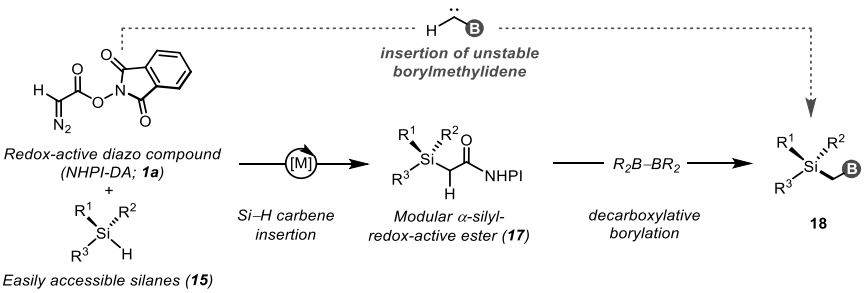

Scheme 4.8: Aim of the project.

4.3 Results and Discussion

4.3.1 Optimization of the Reaction Conditions for Si−H Insertion using NHPI-DA

Although, the insertion of the redox-active NHPI-DA (**1a**) into silanes is unprecedented, the abundant literature in this field gave us ample possibilities of metal precatalysts to start the optimization of the required insertion process (Table 4.2).[71-74] Initially, the conditions developed by Doyle and co-workers[72a] using rhodium carboxylate catalysts were applied for the insertion of the NHPI-DA (**1a**) into Si−H bond of model triisopropylsilane (**15a**) (Entries 1-2). Unfortunately, with our unusual diazo compound we obtained only 21% yield of **17a**. Copper-based catalysts, initially introduced for this purpose by Landais in 1995,[72c] also failed to provide enhanced reactivity (Entries 3-4). Several ligands, such as bipyridine (**L4**) and (*S*)-*i*-Pr-BOX (**L7**) were also tested in combination with commercial Cu(I) and Cu(II) sources, but only poor reactivity towards **17a** was obtained. Despite the success achieved in recent years with these catalytic systems,[72,73] in our case extensive decomposition of the NHPI-DA and significant amount of the carbene dimerization product was observed under similar conditions. Iron catalysts, which are known to be successful in silane insertions of *α*-aryl diazoacetates,[73j] were also scrutinized using phthalocyanine (**L8**) and tetraphenylporphyrin (**L7**) as ligands, but **17a** was obtained only in trace amounts (Entries 7-8). Encouraged by the performance of [Ru(*p*-cymene)Cl_2]$_2$ in catalyzing the insertion of NHPI-DA (**1a**) at the C2-position of *NH*-indoles (see Section 2.4), we explored this ruthenium carbenoid in this reaction, obtaining significantly better yield of **17a** (Entry 9). In line with our previous studies in cyclopropanation and indole insertion, the metallacyclic-ruthenium complex [Ru**L9**$(MeCN)_4$]PF_6 proved to be an excellent catalyst in this context. Using 2.0 equiv. of the model substrate **15a** and 5 mol% of [Ru**L9**$(MeCN)_4$]PF_6 97% yield of **17a** was obtained. This catalyst was originally developed by Iwasa[37] for the Si−H functionalization using diazopropionate reagents.[74] To our surprise, we found out that only 1.1 equiv. of triisopropylsilane (**15a**) and 1 mol% of the catalyst was an ideal composition to obtain optimal yield of the desired insertion product **17a** in just 30 minutes.

Table 4.2. Optimization of the Si−H insertion reaction using NHPI-DA (**1a**).

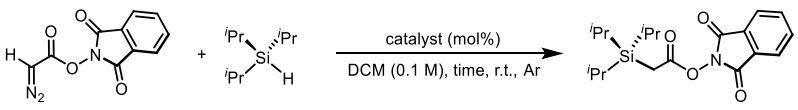

NHPI-DA (**1a**) 1.0 equiv. + **15a** (2.0 equiv.) → **17a**

Entry	Catalyst (mol%)	Time (h)	Conv. (1a) %[a]	Yield (17a) %[a]
1	$Rh_2(OAc)_4$ (1)	14	> 99	21
2	$Rh_2(piv)_4$ (1)	14	> 99	9
3	$Cu(OTf)_2$ (10)	14	32	13
4	$[Cu(OTf)]_2 \cdot C_6H_6$ (10)	14	> 99	15
5	$[Cu(MeCN)_4]PF_6$ (10) + **L4** (10)	14	> 99	15
6	$[Cu(MeCN)_4]PF_6$ (10) + **L12** (10)	14	> 99	18
7	Fe**L8** (10)	14	5	n.d.
8	Fe**L7**Cl (10)	14	10	5
9	[Ru(*p*-cymene)Cl_2]$_2$ (2.5)	14	> 99	39
10	[Ru**L9**$(MeCN)_4$]PF_6 (5)	14	> 99	97
11[b]	[Ru**L9**$(MeCN)_4$]PF_6 (1)	0.5	> 99	95

[a] Conversions and yields were determined by ^{1}H-NMR spectroscopy using 1,1,2,2-tetrachloroethane as internal standard; [b] 1.1 equiv. of **15a** was used; **L4** = 2,2'-bipyridine; **L7** = tetraphenylporphyrin; **L8** = phthalocyanine; **L9** = 4,4-dimethyl-2-phenyloxazolin-2'-yl; **L12** = (*S*)-*i*-Pr-BOX; n.d. not detected.

4.3.2 Scope of the Si−H Insertion Reaction using NHPI-DA

The performance of this catalytic system was elaborated in a wide range of diversely substituted silanes (Table 4.3). Initially, different triakylsilanes were evaluated, which includes isopropyl (**17a**), ethyl (**17b**), and benzyl substituents (**17c**), furnishing the desired insertion products in excellent yields. Aliphatic substrates with different functionalities, such as alkene (**17d**), chloro (**17e**) and benzyloxy (**17f**) provided the Si−H insertion products in high yields. To our surprise, silanes with pendant alkenes afforded exclusive formation of the Si–H insertion products (**17d,g**), despite the possibility of competing cyclopropanations that were not observed. Similar reactivity and selectivity were obtained with an arylsilane containing an alkynyl substituent (**17l**). Several other functionalized arylsilanes (**17h-k**), including triphenylsilane (**17m**) also engaged efficiently in the reaction.

Table 4.3: Scope of the Si–H insertion reaction of alkyl and arylsilanes using NHPI-DA (**1a**).[a]

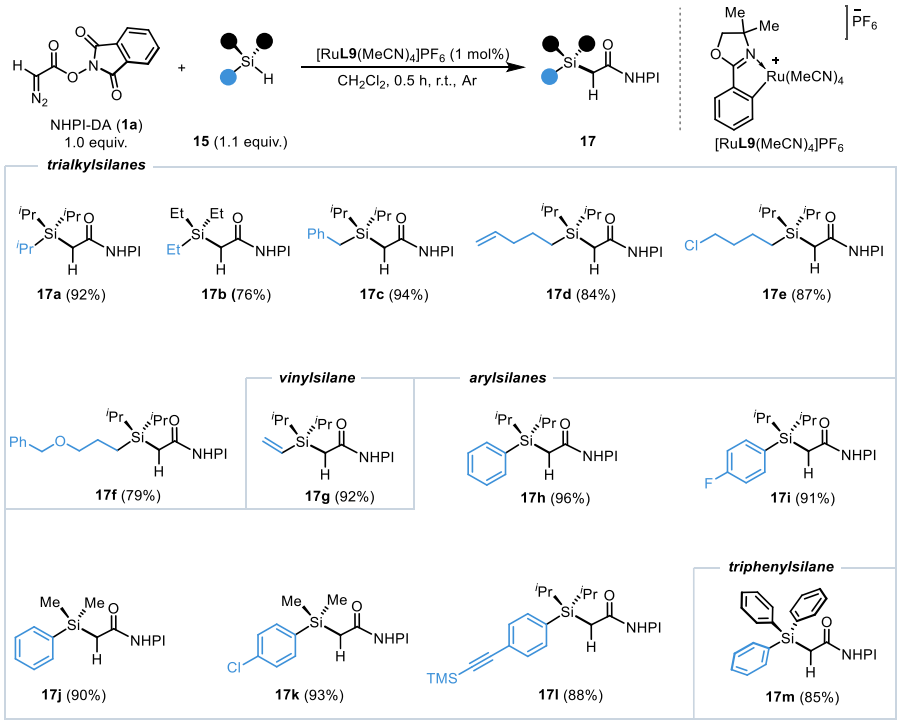

[a] Reaction conditions: **1a** (0.3 mmol), **15** (1.1 equiv.), and 1 mol% [Ru**L9**(MeCN)$_4$]PF$_6$, CH_2Cl_2 (0.1 M), 0.5 h, r.t., Ar.

Additionally, a heteroaryl silane also participated in this reaction to provide very good yield of the product (**17n**), despite the presence of the nucleophilic thiophene ring (Table 4.4). Interestingly, diphenylsilane bearing two Si–H bonds engages in this insertion process furnishing the *mono*-functionalization product (**17o**) predominantly along with the formation of 5% *double*-insertion product. Alkoxy silanes (**17p-x**) which are more sensitive and rarely explored substrates in this context were also studied.[75] As a result, the redox-active ester products decorated with phenoxy (**17p**) and benzyloxy (**17q**) substitutions were synthesized in high yields. Taking into account the orthogonality of these insertions to olefins, a silane with a pending cyclohexenol (**17r**) could also be reacted selectively at its Si–H bond. This type of products offers the possibility for a cascade cyclization after the expected decarboxylation process, leading to the synthesis of bicyclic 2-oxa-1-silacyclopentane derivatives.[76] Likewise, the silanes derived from several naturally-occurring alcohols could also be functionalized efficiently. These include menthol (**17t**), lactic acid (**17u**), indole (**17v**), geraniol (**17w**), and serine (**17x**). Importantly, organosilicon substituents are also tolerated in the transformation, as evidenced in the functionalization of supersilane to afford

17y in 88% yield. Toward the end of this study, diethylsilane and tetramethyldisiloxane were reacted under the given conditions in order to obtain the corresponding *mono*- and *double*-insertion products. Although the use of 2 mol% of the ruthenium catalyst and 2 equiv. of the diazo compound afforded the *double*-insertion products (**17z,aa**) in excellent yields, the *mono*-insertion prodcuts could not be obtained selectively in these cases. Overall, this ruthenium-catalyzed Si−H insertion method has proven to be robust and highly useful pathway to install the redox-active ester handle in many structurally diverse silanes, allowing for further diversification.

Table 4.4: Scope of the Si−H insertion reaction of diverse silanes using NHPI-DA (**1a**).[a]

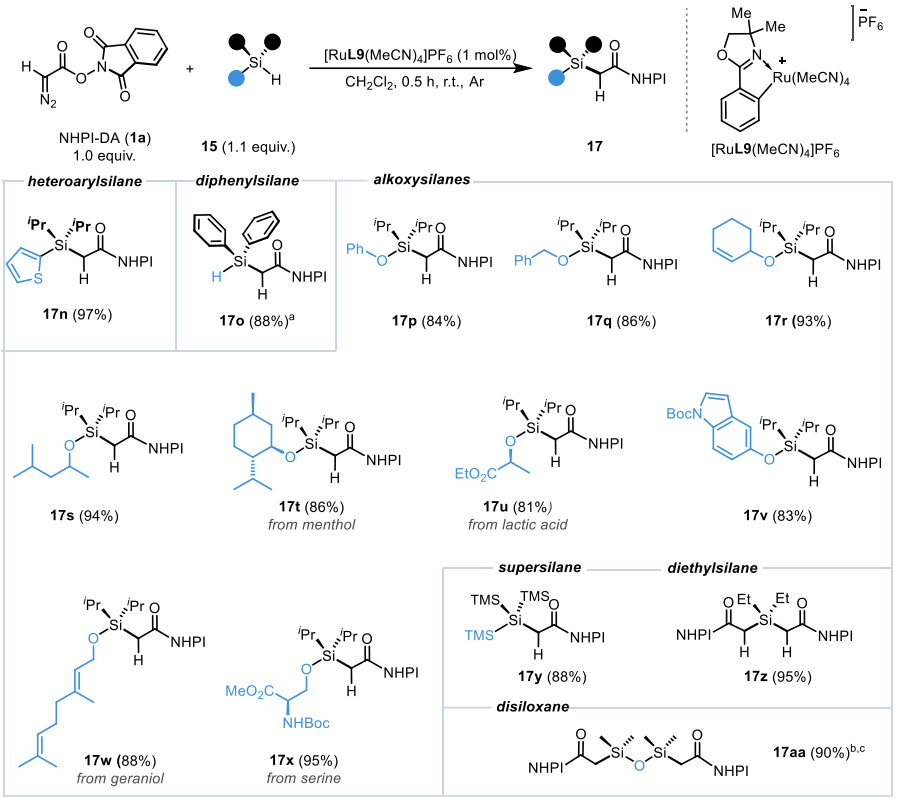

[a] Reaction conditions: **1a** (0.3 mmol), **15** (1.1 equiv.), and 1 mol% [Ru**L9**(MeCN)$_4$]PF$_6$, CH_2Cl_2 (0.1 M), 0.5 h, r.t., Ar; [a] *mono*:*di*-functionalization = 17:1; [b] ^{1}H-NMR yield is reported using 1,1,2,2-tetrachloroethane as internal standard; [c] 2 mol% [Ru**L9**(MeCN)$_4$]PF$_6$ and **15** (0.5 equiv.) were used.

4.3.2 Optimization of the Decarboxylative Borylation Conditions of *α*-Silyl Redox-Active Esters

With the satisfactory scope of the Si−H insertion reaction and given the importance of (borylmethyl)silanes (see Section 4.1.3), we set out to find a suitable condition to modify the redox-active ester products (**17**) into corresponding boronates. In the last few years decarboxylative borylation of redox-active esters has been intensely studied by many research groups.[15b,e,32a] Nevertheless, the borylation of α-silyl redox-active esters is unprecedented as far as we are aware. Actually, only one example of decarboxylative functionalization of α-silyl redox-active esters is known.[77] Among many other borylation protocols developed in the past decade, we were particularly interested in the conditions developed by Baran[19b,39a] and Aggarwal[19e] because of practical reasons and their vast generality. To begin with, five different redox-active esters **17a,b,j,m,s** with a variety of substituents at the silicon center were subjected to a set of three different borylation conditions A-C. Conditions A were developed by Aggarwal and co-workers using a photo-induced method is based on bis(catecholato)diboron (B_2cat_2) as the boron source.[19e] Condions B were introduced by Baran and co-workers, where a nickel-catalyzed protocol is used along with B_2pin_2·MeLi complex without light.[19b] Conditions C were developed later by Baran and Blackmond using copper catalyst and B_2pin_2 resulting in rapid and more convenient borylations.[39a] It was observed that the reactivity of the redox-active esters **17a,b,j,o,s** towards borylation depends largely on the substituents at silicon (Table 4.5). The photo-induced method developed by Aggarwal and co-workers is suitable for substrates containing smaller substituents, e.g. ethyl and methyl (Entry 2,3), and provided no reactivity towards borylation with comparatively larger substituents, e.g. isopropyl (Entry 1). On the other hand, a very different reactivity trend was observed for the nickel- and copper-catalyzed protocols presented by Baran and co-workers (Conditions B,C), favouring the substrates with bulkier substituents (Entry 1-3). Notably, the triphenylsilane substrate **17m** afforded the desired coupling product only in moderate yield with conditions C (Entry 4). The alkoxysilane substrate **17s** was also subjected to different borylation conditions and it was observed that only the nickel- and copper-catalyzed methods provided some of the borylmethylated product (Entry 5). With these results, we concluded that the copper-catalyzed method (Condition C) was suited for the substrates containing comparatively bulkier alkyl and aryl substitutents. In contrast, the light-promoted method (Conditions A) is suitable for converting the dimethylsilyl substrates to the corresponding (borylmethyl)silanes.

Table 4.5: Optimization of the decarboxyative borylation conditions of the insertion products **17**.

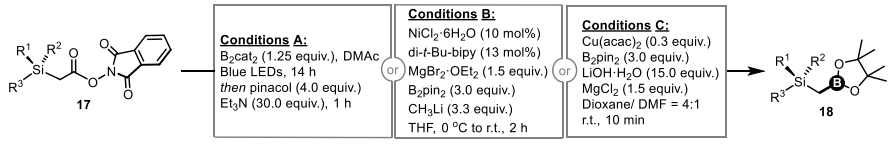

Entry	Substrate	Substituents			Yield (**18**) %[a]		
		R^1	R^2	R^3	A	B	C
1	**17a**	*i*-Pr	*i*-Pr	*i*-Pr	0[b]	77	76
2	**17b**	Et	Et	Et	59	65	77
3	**17j**	Me	Me	Ph	75	17	27
4	**17m**	Ph	Ph	Ph	21	38	53
5	**17s**	*i*-Pr	*i*-Pr	OAlkyl	0[c]	28[d]	32

[a] Yields were determined by ^{1}H-NMR spectroscopy using 1,1,2,2-tetrachloroethane as internal standard. [b] 32% conversion; [c] 20% conversion; [d] isolated yield. Conversions of **17** are >99% unless otherwise specified.

Interestingly, it was also possible to telescope the borylation reaction from silane (**15**) and NHPI-DA (**1a**) in one-pot. Conditions C were proven to be more effective in this context delivering the (borylmethyl)silane in 63% yield, whereas conditions A and B provided 53% and 9% yields, respectively (Scheme 4.8).

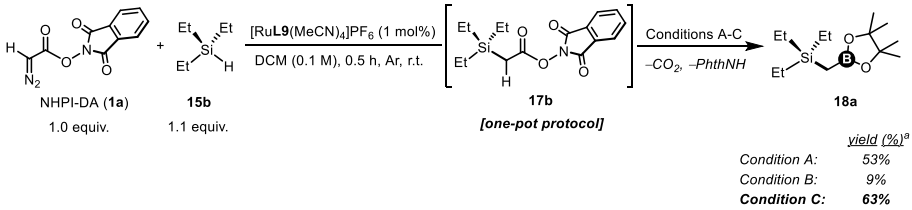

Scheme 4.8: One-pot methylborylation of triethylsilane (**15b**) using NHPI-DA (**1a**). [a] Yields were determined by ^{1}H-NMR spectroscopy using 1,1,2,2-tetrachloroethane as internal standard.

4.4 Scope of the one-pot Methylborylation of Silanes

With suitable conditions in hand for the decarboxylative borylation of the α-silyl redox-active esters, we examined the scope of the one-pot insertion-borylation reaction (Table 4.6). In general, trialkylsilanes exhibited high compatibility in this telescoped insertion-borylation protocol, delivering the (borylmethyl)silanes **18a-c** in good yields. Aliphatics accommodating different functionalities were also tolerated in these reaction conditions, including an alkene (**18e**), chloro (**18f**) and a benzylether (**18g**) substituents. Simple vinylsilane could also be transformed into the corresponding borylmethylated product (**18h**) in moderate yield. It is important to note that the benzylsilane **18d** was obtained in 65% yield, whereas only 35% yield could be obtained

using the previous methods.[69k] Next, this system was applied on different arylsilanes, which include a simple phenyl (**18i**), as well as fluorinated (**18j**), chlorinated (**18l**) and alkynylated (**18m**) (borylmethyl)arylsilanes. Moreover, triphenylsilane (**18n**) and a heteroaryl silane (**18o**) were also tolerated furnishing the respective borylated products in moderate yields. To put these results in perspective, only the product **18k** was previously known and could only be obtained in considerably lower yield.[69k]

Table 4.6: Scope of the one-pot methylborylation of silanes using NHPI-DA (**1a**).[a]

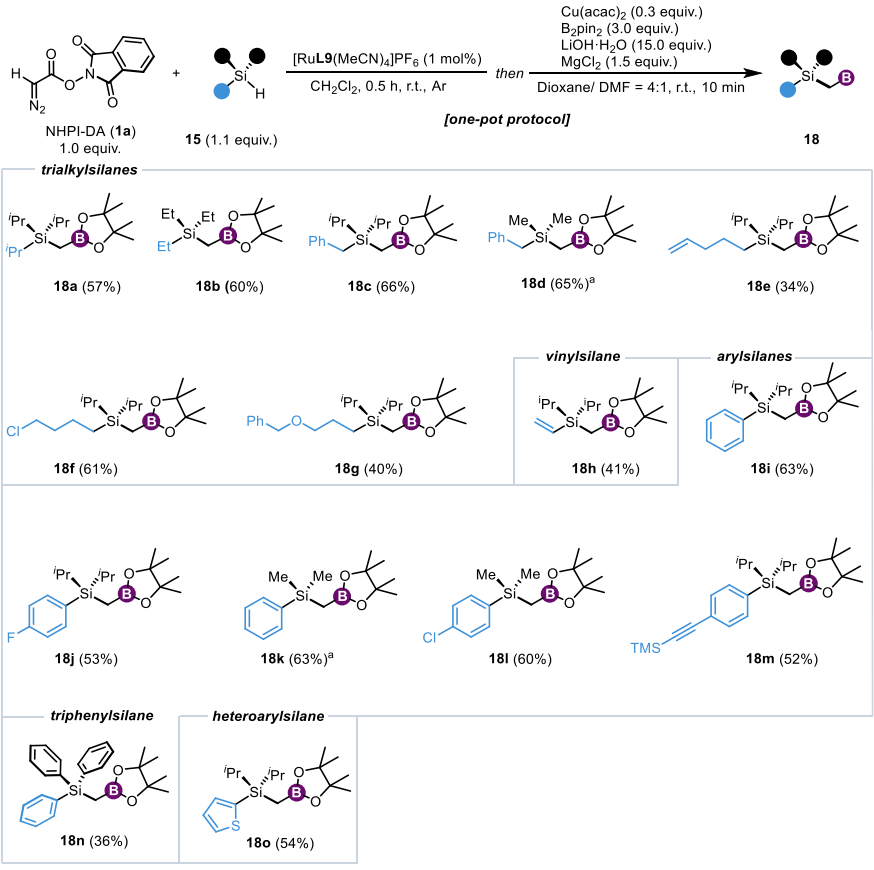

[a] Reaction conditions: **1a** (0.3 mmol), **15** (1.1 equiv.), and [Ru**L9**(MeCN)$_4$]PF$_6$ (1 mol%), CH_2Cl_2 (0.1 M), 0.5 h, r.t., Ar, then Cu(acac)$_2$ (0.3 equiv.), B_2pin_2 (3.0 equiv.), LiOH·H_2O (15.0 equiv.), $MgCl_2$ (1.5 equiv.), Dioxane/DMF = 4:1, 0.1 M, 10 min, r.t., Ar; [a] For the borylation, B_2cat_2 (1.25 equiv.), DMAc (0.1 M), blue LEDs, 14 h then pinacol (4.0 equiv.) and Et_3N (30.0 equiv.) were used.

The synthetic capability of this system was further extended by the evaluation of several alkoxysilanes (Table 4.7). This includes a phenoxy (**18p**), benzyloxy (**18q**) and an aliphatic alcohol fragment **18r**, providing the borylations in modest yields despite their more labile character. It is worth mentioning that this borylation reaction could also be applied on silanes derived from important natural products and pharmacophores, including menthol (**18s**), indole (**18t**) and serine (**18u**). Remarkably, a (borylmethyl)supersilane (**18v**) was also obtained without adjustment or optimization of the standard conditions, despite its high steric bulk. This product illustrates the capacity of the method to rapidly deliver new interesting silaboranes for further exploration of their properties. Moreover, the silanes derived from hydrosilylation of styrene (**18v**) and phenylacetylene (**18w**) could also be engaged in this one-pot borylation protocol hinting at future integration of this method with hydrosilylation reactions. To this end, we explored the scope through the methylborylation of dihydrosilanes, such as diethylsilane and tetramethyldisiloxane, which afforded the *mono*- (**18y**) and *double*-borylated (**18z**) products respectively, albeit in low yields. The *mono*-borylated product (**18y**) likely stems from the competitive hydrogen atom transfer (HAT) to the first α-silyl radical generated, followed by the expected borylation of the second.

Table 4.7: Scope of the one-pot methylborylation of silanes using NHPI-DA (**1a**).[a]

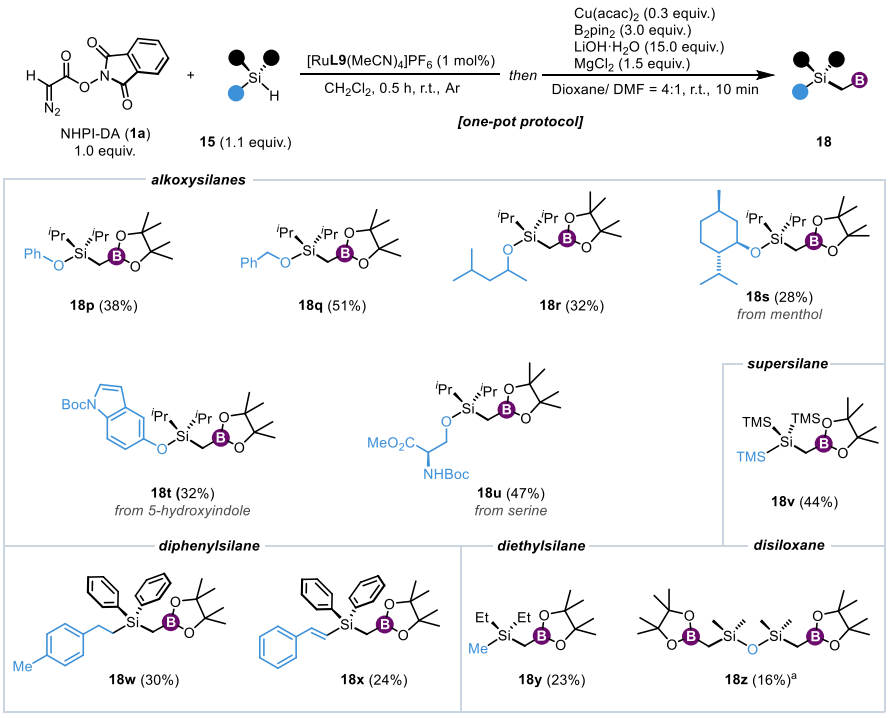

[a] Reaction conditions: **1a** (0.3 mmol), **15** (1.1 equiv.), and [Ru**L9**$(MeCN)_4]PF_6$ (1 mol%), CH_2Cl_2 (0.1 M), 0.5 h, r.t., Ar, then $Cu(acac)_2$ (0.3 equiv.), B_2pin_2 (3.0 equiv.), $LiOH{\cdot}H_2O$ (15.0 equiv.), $MgCl_2$ (1.5 equiv.), Dioxane/DMF = 4:1, 0.1 M, 10 min, r.t., Ar; [a] For the borylation, B_2cat_2 (1.25 equiv.), DMAc (0.1 M), blue LEDs, 14 h then pinacol (4.0 equiv.) and Et_3N (30.0 equiv.) were used.

4.5 Directed *Mono*- And *Di*-functionalization of Allylic Alcohols

4.5.1 Optimization of the Reaction Conditions for the Cascade Decarboxylation-Cyclization

Inspired by the reactivity of the α-silyl redox-active esters towards decarboxylative borylation we started to investigate other cross-coupling reactions associated with these α-silyl radicals, whose chemistry have not been explored in depth (see Section 4.1.3). Unfortunately, we found out that these radicals do not undergo transition or non-transition-metal mediated C−C bond forming reactions. However, complete conversions of these redox-active esters were observed with substantial amount of the HAT product formation of the putative radicals. Interestingly, we found out that the redox-active esters derived from allylic alcohols undergo *5-exo-trig* cyclizations generating oxasilacylopentylmethyl radical which is quenched by a subsequent HAT process. This reactivity is achieved just by irradiating a mixture of the α-silyl redox-active ester and a photoreductant in the presence of blue light. Based on the performance of different photoreductants (**12**) on the photo-Giese reactions (see Chapter 3) we started to experiment with the most relevant ones (**12a,e,f,h**) for the desired decarboxylation (Table 4.8). To our surprise, the dihydronicotinamides (**12a,f**) provided only 11-12% of the desired cyclized product **19a** (Entries 1-2), despite the full conversion of the model substrate **17ab**. These results directly contradicts to the robust performance of the photocoupling reactions with the regular NHPI esters with Michael acceptors, underlining a very different reactivity of the α-silyl redox-active esters. The Hantzsch ester (**12e**) and a benzothiazole derivative **12h**, on the other hand, displayed good reactivity towards the desired product **19a**, with the formation of 5-8% the HAT product (**20a**) using DMA as solvent (Entries 3,4). DMSO proved to be better performing than DMA, rising the yield of **19a** up to 81%, with slight increase in the amount of the HAT product (Entry 5). This types of cascade decarboxylation-cylization reactions are known to perform well at lower concentrations (see publication II). However, lowering the reaction concentration failed to reduce the formation of the HAT product (Entries 6-8). Further screening of the solvents only provided lower yield of the desired product **19a** (Entries 9-11). An optimal yield of 82% of the desired product **19a** was obtained using 2.0 equiv. of the Hantzsch ester in DMSO as solvent (Entries 12-14). Similar yield of **19a** was obtained when irradiated with white LEDs (Entry 15). It is important to highlight that substantial degradation (*ca*. 35%) of the model substrate **17ab** was observed when irradiated in the absence of the photoreductant. Therefore, the yields of **19a** and **20a**, stochiometry of the photoreductants and the concentrations of the reaction media in Table 4.8 are expressed based on 65% (32.5 µmol) of **17ab**.

Table 4.8: Optimization of the reaction conditions.[a]

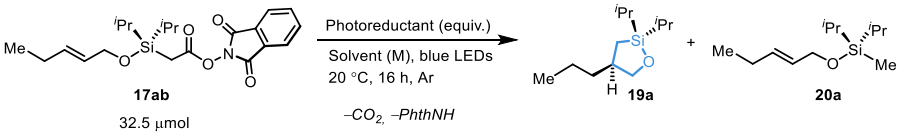

17ab
32.5 μmol

19a

20a

Entry	Photoreductant (equiv.)	Solvent (M)	Yield (19a) %[b]	Yield (20a) %[b]
1	**12a** (3.0)	DMA (0.06)	11	<1
2	**12f** (3.0)	DMA (0.06)	12	<1
3	**12e** (3.0)	DMA (0.06)	63	5
4	**12h** (3.0)	DMA (0.06)	71	8
5	**12h** (3.0)	DMSO (0.06)	81	12
6	**12e** (3.0)	DMSO (0.06)	77	14
7	**12e** (3.0)	DMSO (0.03)	78	12
8	**12e** (3.0)	DMSO (0.006)	77	9
9	**12e** (3.0)	THF (0.03)	52	5
10	**12e** (3.0)	DCM (0.03)	18	<1
11	**12e** (3.0)	MeCN (0.03)	49	6
12	**12e** (2.3)	DMSO (0.03)	78	12
13	**12e** (2.0)	DMSO (0.03)	82	12
14	**12e** (1.5)	DMSO (0.03)	74	11
15[c]	**12e** (2.0)	DMSO (0.03)	77	6

[a] Originally all these experiments were performed in 0.05 mmol. Due to the instability under the blue light irradiation *ca*. 35% of the model substrate **17ab** decomposed; [b] yields were determined by ^{1}H-NMR spectroscopy using 1,1,2,2-tetrachloroethane as internal standard; [c] this experiment was performed using white LEDs.

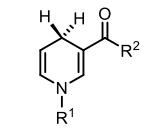

12a R^1 = Bn, R^2 = NH_2
12f R^1 = Bu, R^2 = NH_2

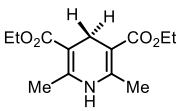

12e

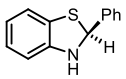

12h

Interestingly, this cascade decarboxylation-cyclization reaction can also be telescoped from silane **15ab** in one-pot. After simple evaporation of DCM the crude α-silyl redox-active ester was irradiated using blue LEDs in the presence of Hantzsch ester and the desired cyclized product **19a** was obtained in 42% yield with 6% HAT of the α-silyl radical before cyclization (Scheme 4.9).

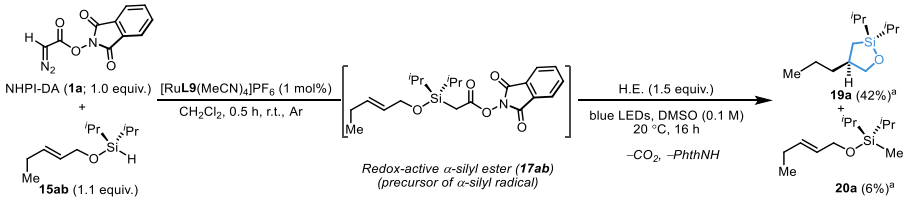

Scheme 4.9: One-pot synthesis of oxasilacyclopentane **19a** from silane **15ab** using NHPI-DA (**1a**). [a] Yields were determined by ^{1}H-NMR spectroscopy using 1,1,2,2-tetrachloroethane as internal standard

4.5.2 Scope of the Cascade Decarboxylation-Cyclization

The scope of this one-pot insertion-cyclization reaction was evaluated with different allylic alcohols (Table 4.9). Using this approach secondary (**19a**) and tertiary (**19b**) carbon-centered radicals were generated after the desired *5-exo-trig* cyclization which after the subsequent hydrogen atom transfer processes provided the corresponding oxasilacyclopentanes in moderate to good yields. A cyclohexane-fused oxasilacyclopentane (**19c**) was synthesized using the silane derived from 2-cyclohexenol in good yield. The silane derived from geraniol could also be engaged in this one-pot protocol allowing for the access to the corresponding cyclized product (**19d**), albeit poor diastereoselectivity. The synthetic usefulness of this system was extended to homoallylic alcohol. A seven-membered oxasilacycloheptane (**19e**) can also be synthesized using this methodology with moderate efficiency. However, using this system we have not observed any cyclization of the α-silyl radical towards the generation of primary carbon-centered radicals.

Table 4.9: Scope of the *mono*-functionalization of allylic and homoallylic alcohols.[a]

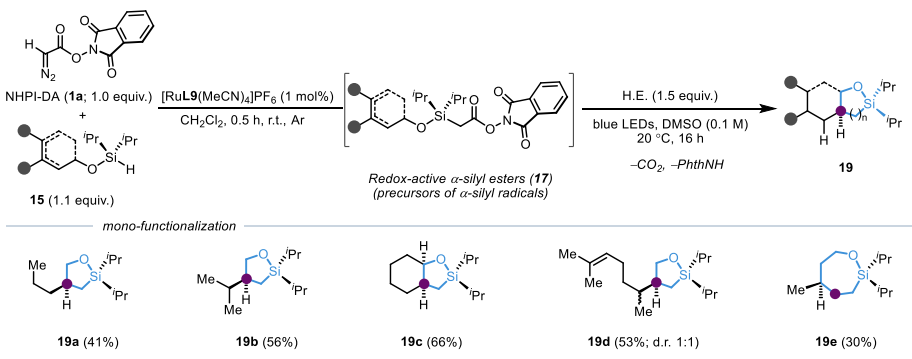

[a] Reaction conditions: **1a** (0.2 mmol), **15** (1.1 equiv.), and [Ru**L9**(MeCN)$_4$]PF$_6$ (1 mol%), CH_2Cl_2 (0.1 M), 0.5 h, r.t., Ar, then H.E. (**12e**; 1.5 equiv.), DMSO (0.1 M), blue LEDs, 16 h, 20 °C.

Giese reactions have enormous applications for the construction of C–C bonds. Based on our experience on the photo-decarboxylative Giese reactions of regular redox-active (NHPI) esters with Michael acceptors (see Chapter 3), we were interested in the reactivity of α-silyl NHPI esters derived from allylic alcohols. As expected, the carbon-centered radicals generated after the cascade decarboxylation-cyclization engage in the C–C bond forming reactions with electron-poor olefins (Table 4.10). The redox-active ester tethered with 2-cyclohexenol moiety was well suited to undergo coupling with Michael acceptors containing different electron-withdrawing substituents. This includes, an ester (**20a**), cyano (**20b**), sulfone (**20c**) and amide (**20d**) functionalities, all providing moderate to good yields of the desired cyclized products in one-pot. Silanes derived from acyclic allylic alcohols (**20e**, **20f**) also participated under this protocol furnishing the products in good efficacy. Additionally, a homoallylic alcohol was also tolerated under this system delivering a seven-membered oxasilacycloheptane derivative (**20g**) in moderate yield *via 7-endo-trig* cyclization of the putative α-silyl radical.

Table 4.10: Scope of the *di*-functionalization of allylic and homoallylic alcohols.[a]

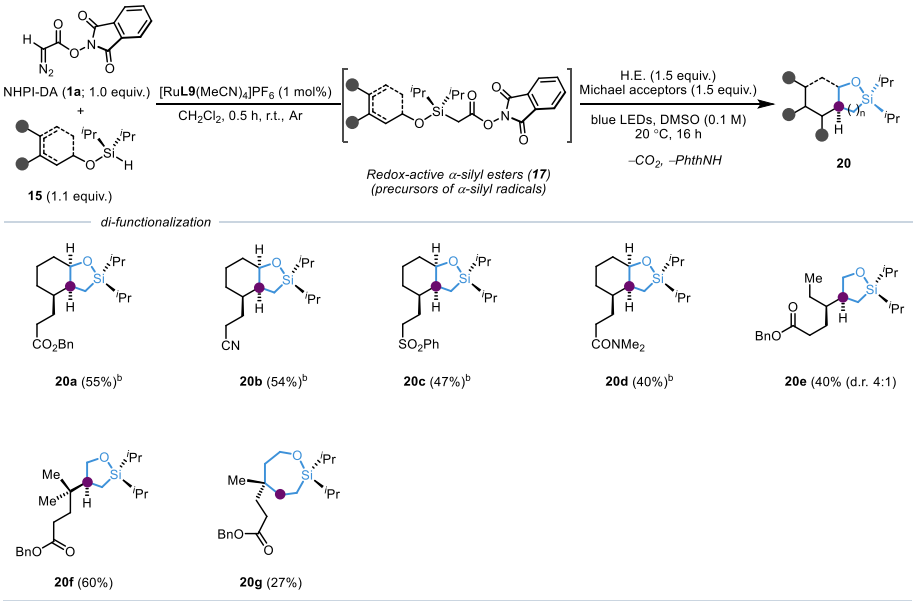

[a] Reaction conditions: **1a** (0.2 mmol), **15** (1.1 equiv.), and [Ru**L9**(MeCN)$_4$]PF$_6$ (1 mol%), CH_2Cl_2 (0.1 M), 0.5 h, r.t., Ar, then H.E. (**12e**; 1.5 equiv.), Michael acceptor (1.5 equiv.), DMSO (0.1 M), blue LEDs, 16 h, 20 °C; [b] single diastereomer.

4.6 Conclusion

In summary, we have developed a one-pot protocol for methylborylation of hydrosilanes using the redox-active diazo compound (NHPI-DA). The key to this development has been the identification of a singularly effective ruthenium catalyst, and a study of different decarboxylative borylation methods in α-silyl redox-active esters. This system allows formal insertion of unstable borymethylidenes into Si−H bond of silanes which is unprecedented as far as we know. Moreover, this established methodology has been applied to many structurally diverse silanes, including alkoxysilanes which have rarely been explored previously. Furthermore, this synthetic route uses minimal excess of the hydrosilane materials and offer a milder approach towards the synthesis of (borylmethyl)silanes compared to previous methods.[61] Overall, considering the current synthetic utility of these organosilaborane products,[60] it is expected that this newly developed insertion-borylation protocol will expedite further advances in their chemistry. In addition, the chemistry α-silyl radicals have been extrapolated through the *mono*- and *di*-functionalization of allylic and homoallylic alcohols merging carbene-catalysis and decarboxylative coupling. The use of Hantzsch ester as the only potential reagent in the blue light promoted decarboxylation step enables cyclization of the α-silyl radicals leading to the access to several five- and seven-membered oxasilacycloalkane derivatives with moderate to good efficiencies.

5. Concluding Remarks

The thesis presented herein describes general C−H and Si−H functionalization methods using a versatile redox-active diazo compound (NHPI-DA) and thereafter decarboxylative coupling of the insertion products. **Chapter 2** of this thesis presents the insertion of NHPI-DA into C−H bond of indoles using ruthenium-metallacycle, delivering redox-active indole products with various types of substituents at the nitrogen atom and in the aromatic rings. Exploiting the rich chemistry of these redox-active esters we have successfully synthesized libraries of C3-alkyl indoles with different functional groups connected by a common methylene unit. Worth mentioning, these products could only be obtained from the insertions of unstable methylidenes, such as borylmethylidenes, benzylidenes, aklylidenes, and alkenylidenes. However, the development of NHPI-DA has allowed the access to these products from a single precursor without the need of custom manipulation of the reagents. **Chapter 3** of this thesis presents Giese-type reactions of redox-active esters with Michael acceptors using biocompatible photoreductants in the presence of blue light. These coupling reactions do not need additional photocatalyst for the activation, which is typical in the photoredox chemistry. The scope of this reaction has been evaluated using different types of 1^{ary}, 2^{ary} and 3^{ary} redox-active esters. Moreover, this reaction can be performed in the presence of free carboxylic acid moieties in both intramolecular and intermolecular fashions. The synthetic usefulness of this methodology has been illustrated *via* the performance of these reactions at diluted and aqueous media. Interestingly, the native biological reductant NADH has also shown high efficacy in these coupling reactions despite its complex structural and photophysical properties. Detailed kinetic studies have been carried out in order to have knowledge about the background of these reactions. The involvement of radical chain mechanism of this photo-coupling reaction has been established through the quantum yield calculation. Further, UV-Vis studies and Stern-Volmer quenching experiments have been performed to have a broad picture about the quenching mechanism involved. **Chapter 4** of this thesis highlights the recent development of a one-pot methylborylation strategy of silanes using the redox-active diazo compound (NHPI-DA) *via* the generation of α-silyl radicals. Once again, Ru-Pheox has proven to be highly effective in the requisite redox-active carbene transfer processes. Using the profound chemistry available for decarboxylative borylation of redox-active esters libraries of (borylmethyl)silanes starting from diversely substituted silanes have been synthesized. The chemistry of these α-silyl radicals has been further extrapolated through a cascade decarboxylation-cyclization of the redox-active α-silyl esters leading to the synthesis of oxasilacyclopentanes, also in one-pot. Moreover, oxasilacyclopentylmethyl radicals after the desired cyclization have been coupled with electron-poor olefins in good stereoselectivity, demonstrating the synthetic usefulness of the NHPI-DA in this context.

Appendix A − Contribution list

I. Took part in the design of the project. Carried out all the experimental works, which includes starting material preparations, optimization of the conditions for the C−H insertion reaction, substrate scope studies and diversification of the products. Assisted in writing the manuscript and wrote the supporting information.

II. Performed 70% of the substrate scope of the photo-Giese reaction. Took part in the kinetic study. Performed the quantum yield calculation, UV-Vis study and Stern-Volmer quenching experiments. Took part in writing the manuscript and wrote 70% of the supporting information.

III. Took part in the design of the project. Performed 90% of the experimental works, including starting material preparations, optimization of catalysts for the Si−H insertion reaction, substrate scope studies and diversification of the products. Wrote the manuscript and the supporting information.

Appendix B − Reprint Permissions

Reprint permissions were granted by the publishers for the publications **I-II**:

I. *Chem. Commun.*, **2021**, *57*, 4532-4535
Copyright © 2021 The Royal Society of Chemistry
Rajdip Chowdhury and Abraham Mendoza* *Chem. Commun*. **2021**, *57*, 4532-4535.

II. *J. Am. Chem. Soc.*, **2020**, *142*, 20143–20151
Copyright © 2020 American Chemical Society
Rajdip Chowdhury,‡ Zhunzhun Yu,‡ My Linh Tong, Stefanie V. Kohlhepp, Xiang Yin and Abraham Mendoza* *J. Am. Chem. Soc.* **2020**, *142*, 20143–20151.

Appendix C − Experimental Data for Chapter 2-4

Full experimental data and supporting information for Chapter 2 can be found at:
https://doi.org/10.1039/D1CC01026C
Raw NMR, HRMS data for Chapter 2 can be downloaded from Zenodo:
DOI: 10.5281/zenodo.4652793.

Full experimental data and supporting information for Chapter 3 can be found at:
https://doi.org/10.1021/jacs.0c09678
Raw NMR, HRMS data for Chapter 3 can be downloaded from Zenodo:
DOI: 10.5281/zenodo.4106400.

The supporting information for Chapter 4 can be downloaded from Zenodo:
https://doi.org/10.5281/zenodo.5888342.

Acknowledgements

First and foremost, my gratitude goes to *Dr. Abraham Mendoza* for giving me the opportunity to pursue doctoral study in your research group and for your supervision during these years. I have learned a lot from you.

I sincerely thank *Prof. Belén Martín-Matute* and my co-supervisor *Prof. Kálmán J. Szabó* for your time to read my thesis and for your valuable remarks. I sincerely thank *Prof. Pher G. Anderson* for reading my half-time report and for your valuable suggestions. I would like to thank all other *PI's* of the Organic Chemistry Department for sharing your research and your valuable comments during SDMs.

I sincerely thank *Prof. Darren Dixon* for being the opponent in my PhD examination. I solemnly thank *Dr. Markus D. Kärkäs* for being the opponent in my half-time seminar. I would like to thank *Prof. Ola Wendt*, *Prof. Eszter Borbas* and *Docent Helena Lundberg* for being the committee in my PhD examination.

I would like to thank the entire administration and the technical staffs (past and present) of the department for your enormous help during my PhD. I sincerely thank *Kristina Romare*, *Martin Roxengren*, *Petra Godin*, and *Dr. Jonas Ståhle* for your very kind help during these years.

I would like to thank *Dr. Shubhankar Bhattacharya* for your help in the popular vetenskaplig sammanfattning.

My sincere thanks to all the members of the Mendoza Lab, past and present. I would like to thank *Dr. Zhunzhun Yu*, *Dr. My Linh Tong*, *Dr. Stephanie V. Kohlhepp* and *Dr. Xiang Yin* for your valuable contribution in the photo-Giese project and for sharing the memorable moments in the lab or outside. I would also like to thank *Dr. Gábor Z. Elek* for your contribution in the silane project. I sincerely thank *Dr. Alberto Abengózar Muñoz* for that amazing one year in Stockholm, this time will always be special to me. I sincerely thank to *Dr. Matteo Costantini*, you have been a great co-worker and a friend throughout these years. To, *Emanuele Silvi* and *Beatriz Meana Baamonde* thank you for being very nice co-workers and friends, I wish I had the chance to spend more time with you guys. To, *Dr. Marc Montesinos Magraner, Dr. Stefano Parisotto, Alba H. Pérez Jimeno, Xandro Vidal, Lara Lavrenčič, Carolin Kalff, Jesper Schwarz, Catarina Santos, Dr. Kilian Colas, Dr. Elisa Martinez de Castro, Dr. Rodrigo Ramirez, Dr. Michael Muratore and Zainab Alsaman*, thank you for sharing the lab with me and the time that we spent together at some point and thanks for all the scientific discussions that we had.

I would like to thank *Dr. Biswanath Das, Dr. Srimanta Manna, Dr. Shobhan Mondal, Dr. Kumar Bhaskar Pal, Dr. Jayarajan Ramasamy, Dr. Gurpreet Kaur, Dr. Kiran Reddy Baddigam, Dr. Ramesh Veleru, Dr. Sudipta Ponra, Dr. Rahul Watile* and *Dr. Nagaraju Molleti* for building up all fun moments during our stay in the department.

To all of my friends, *Jianping Yang* (almost doctor), *Luca Massaro, Bram Peters, Dr. Haibo Yu, Vu Duc Ha Phan, Víctor García Vázquez* (almost doctor), *Alba Carretero Cerdán* (almost doctor), *Aitor Bermejo López* (almost doctor), *Alexandru Postole, Dr. Alessandro Ruda, Axel Furevi* (almost doctor), *Kevin Manuel Dorst, Dr. Qiang Wang, Tautvydas Kireilis, Dr. Sybrand Jonker and Dr. Dong Wang*, whom I have met during last four years, thank you for making this time meaningful.

Finally, I would like to thank my wife, *Mrs. Priya Dutta* for being with me always, specially during one of the toughest time in my life.

References

1. (a) Schreiber, S. L. *Science* **2000**, *287*, 1964-1969; (b) Schreiber, S. L. *Chem. Eng. News.* **2003**, *81*, 51-61; (c) Burke, M. D.; Schreiber, S. L. *Angew. Chem. Int. Ed.* **2004**, *43*, 46-58; (d) Galloway, W. R.; Isidro-Llobet, A.; Spring, D. R. *Nat. Commun.* **2010**, *1*, 80.
2. (a) Cui, W.-G.; Zhang, G.-Y.; Hu, T.-L.; Bu, X.-H. *Coord. Chem. Rev.* **2019**, *387*, 79-120; (b) Desmons, S.; Fauré, R.; Bontemps, S. *ACS Catal.* **2019**, *9*, 9575-9588; (c) Hurst, T. E.; Deichert, J. A.; Kapeniak, L.; Lee, R.; Harris, J.; Jessop, P. G.; Snieckus, V. *Org. Lett.* **2019**, *21*, 3882-3885; (d) Sakakura, T.; Choi, J. C.; Yasuda, H. *Chem. Rev.* **2007**, *107*, 2365-2387; (e) Touqeer, S.; Castoldi, L.; Langer, T.; Holzer, W.; Pace, V. *Chem. Commun.* **2018**, *54*, 10112-10115; (f) Touqeer, S.; Ielo, L.; Miele, M.; Urban, E.; Holzer, W.; Pace, V. *Org. Biomol. Chem.* **2021**, *19*, 2425-2429; (g) Luescher, M. U.; Vo, C. V.; Bode, J. W. *Org. Lett.* **2014**, *16*, 1236-1239; (h) Vo, C. V.; Luescher, M. U.; Bode, J. W. *Nat. Chem.* **2014**, *6*, 310-314; (i) Cory, R. M.; McLaren, F. R., *J. Chem. Soc., Chem. Commun.* **1977**, 587-588; (j) Ma, X.; Su, J.; Zhang, X.; Song, Q. *iScience* **2019**, *19*, 1-13; (k) Mesters, C. *Annu. Rev. Chem. Biomol. Eng.* **2016**, *7*, 223-238; (l) Liu, Q.; Wu, L.; Jackstell, R.; Beller, M. *Nat. Commun.* **2015**, *6*, 5933; (m) Li, H.; Zhang, Y.; Yan, Z.; Lai, Z.; Yang, R.; Peng, M.; Sun, Y.; An, J. *Green Chemistry* **2022**, *24*, 748-753; (n) Fu, M.-C. Conversion of Formic Acid in Organic Synthesis as a C1 Source. In *Studies on Green Synthetic Reactions Based on Formic Acid from Biomass*, *Springer*: Singapore, **2020**, 1-26; (o) Beydoun, K.; Thenert, K.; Wiesenthal, J.; Hoppe, C.; Klankermayer, J. *ChemCatChem* **2020,** *12*, 1944-1947.
3. For reviews and book chapters on metal–carbene chemistry: (a) de Frémont, P.; Marion, N.; Nolan, S. P. *Coord. Chem. Rev.* **2009,** *253*, 862-892; (b) Schubert, U. *Coord. Chem. Rev.* **1984**, *55*, 261; (c) Doyle, M. P.; Duffy, R.; Ratnikov, M.; Zhou, L. *Chem. Rev.* **2010,** *110*, 704-724; (d) Doyle, M. P.; Ratnikov, M.; Liu, Y. *Org. Biomol. Chem.* **2011,** *9*, 4007-4016; (e) Zhu, S.-F.; Zhou, Q.-L. *Acc. Chem. Res.* **2012,** *45*, 1365-1377; (f) Ford, A.; Miel, H.; Ring, A.; Slattery, C. N.; Maguire, A. R.; McKervey, M. A. *Chem. Rev*. **2015**, *115*, 9981-10080; (g) Cheng, Q. Q.; Deng, Y.; Lankelma, M.; Doyle, M. P. *Chem. Soc. Rev.* **2017**, *46*, 5425-5443; (h) Moss, R. A.; Platz, M. S.; Jones, M., Jr., Eds. Reactive Intermediate Chemistry; *Wiley-Inter science: New York*, **2004**; (i) Liu, M. T. H. Chemistry of Diazirines; CRC Press: Boca Raton, FL, **1987**; Vols.1 & 2; (j) Davies, H. M.; Hedley, S. J. *Chem. Soc. Rev.* **2007**, *36*, 1109; (k) Xiao, Q.; Zhang, Y.; Wang, J. *Acc. Chem. Res.* **2013**, *46*, 236; (l) Zhang, Y.; Wang, J. *Chem. Commun.* **2009**, *2009*, 5350.
4. (a) A.Hermann, M.; *Liebigs Ann. Chem.* **1855**, *95*, 211; (b) Nef, J. U. *Ann.* **1897**, *298*, 202.
5. (a) Doering, W. V. E.; Knox, L. H. *J. Am. Chem. Soc.* **1953**, *75*, 297; (b) Doering, W. V. E.; Hoffmann, A. K. *J. Am. Chem. Soc.* **1954**, *76*, 6162.

6. (a) Fischer, E. O.; Maasböl, A. *Angew. Chem. Int. Ed.* **1964**, *3*, 580−581; (b) Schrock, R. R. *J. Am. Chem. Soc.* **1974**, 96, 6796−6797; (c) Xia, Y.; Qiu, D.; Wang, J. *Chem. Rev.* **2017**, *117*, 13810-13889.
7. Greuter, F.; Kalvoda, J.; Jeger, O. *Proc. Chem. Soc.* **1958**, *349*.
8. (a) Jia, M.; Ma, S. *Angew. Chem. Int. Ed.* **2016,** *55*, 9134-9166; (b) Goudreau, S. R.; Marcoux, D.; Charette, A. B. *J. Org. Chem.* **2009,** *74*, 470-473; (c) Muller, P. *Acc. Chem. Res.* **2004,** *37*, 243-251.
9. (a) Li, A. H.; Dai, L. X.; Aggarwal, V. K. *Chem. Rev.* **1997,** *97*, 2341-2372; (b) McGarrigle, E. M.; Myers, E. L.; Illa, O.; Shaw, M. A.; Riches, S. L.; Aggarwal, V. K. *Chem. Rev.* **2007,** *107*, 5841-5883; (c) Burtoloso, A. C. B.; Dias, R. M. P.; Leonarczyk, I. A. *Eur. J. Org. Chem.* **2013,** *2013*, 5005-5016.
10. (a) Crabtree, R. H. *The organometallic chemistry of the transition-metals*, John Wiley & Sons, Inc., Hoboken, New Jersey, **2014**; (b) Zhu, D.; Chen, L.; Fan, H.; Yao, Q.; Zhu, S. *Chem. So.c Rev.* **2020,** *49*, 908-950.
11. (a) Nguyen, S. T.; Johnson, L. K.; Grubbs, R. H. *J. Am. Chem. Soc.* **1992**, *114*, 3974-3975; (b) Schwab, P.; France, M. B.; Zillerr, W.; Grubbs, R. H. *Angew. Chem. Int. Ed*. **1995**, *34*, 2039- 2041.
12. Maas, G. *Chem. Soc. Rev.* **2004**, *33*, 183-190.
13. (a) Yu, Z.; Mendoza, A. *ACS Catal.* **2019**, *9*, 7870-7875; (b) Montesinos-Magraner, M.; Costantini, M.; Ramírez-Contreras, R.; Muratore, M. E.; Johansson, M. J.; Mendoza, A. *Angew. Chem. Int. Ed.* **2019**, *58*, 5930-5935.
14. (a) Barton, D. H. R.; George, M. V.; Tomoeda, M. *J. Chem. Soc.* **1962**, 1967-1974; (b) Barton, D. H. R.; Crich, D.; Motherwell, W. B. *J. Chem. Soc., Chem. Commun.* **1983**, 939-941; (c) Barton, D. H. R.; Garcia, B.; Togo, H.; Zard, S. Z. *Tetrahedron Lett.* **1986**, *27*, 1327-1330; (d) Barton, D. H. R.; Jaszberenyi, J. C.; Theodorakis, E. A. *Tetrahedron* **1992**, *48*, 2613-2626; (e) Wiberg, K. B.; Lowry, B. R.; Colby, T. H. *J. Am. Chem. Soc.* **1961**, *83*, 3998; (f) Eaton, P. E.; Cole, T. W. *J. Am. Chem. Soc.* 1964, 86, 3157; (g) Meinwald, J.; Shelton, J. C.; Buchanan, G. L.; Courtin, A. *J. Org. Chem.* **1968**, *33*, 99.
15. Nefkens, G. H. L.; Tesser, G. I. *J. Am. Chem. Soc.* **1961**, *83*, 1263.
16. (a) Okada, K.; Okamoto, K.; Oda, M. *J. Am. Chem. Soc*. **1988**, *110*, 8736-8738; (b) Okada, K.; Okamoto, K.; Morita, N.; Okubo, K.; Oda, M. *J. Am. Chem. Soc*. **1991**, *113*, 9401-9402; (c) Okada, K.; Okubo, K.; Morita, N.; Oda, M. *Tetrahedron Lett.***1992**, *33*, 7377−7380.
17. (a) Wilson, C. V. *Org. React.* **1957**, *9*, 332. (b) Sheldon, R. A.; Kochi, J. K. *Org. React.* **1972**, *19*, 279; (c) Ruivila, H. G. *Synthesis* **1970**, 499; (d) Della, E. W.; Patney, H. K. *Synthesis* **1976**, *8*, 251; (e) Barton, D. H. R.; Crich, D.; Motherwell, W. B. *Tetrahedron Lett.* **1983**, *24*, 4979.
18. (a) Yi, H.; Zhang, G.; Wang, H.; Huang, Z.; Wang, J.; Singh, A. K.; Lei, A. *Chem. Rev.* **2017**, *117*, 9016-9085; (b) Guo, S.-r.; Kumar, P. S.; Yang, M. *Adv. Synth. Catal.* **2017**, *359*, 2-25; (c) Bell, J. D.; Murphy, J. A. *Chem. Soc. Rev.* **2021**, *50*, 9540-9685.
19. (a) Cornella, J.; Edwards, J. T.; Qin, T.; Kawamura, S.; Wang, J.; Pan, C. M.; Gianatassio, R.; Schmidt, M.; Eastgate, M. D.; Baran, P. S. *J. Am. Chem. Soc.* 2**016**, *138*, 2174-2177; (b) Li, C.; Wang, J.; Barton, L. M.; Yu, S.; Tian, M.; Peters, D. S.; Kumar, M.; Yu, A. W.; Johnson, K. A.; Chatterjee, A. K.; Yan,

M.; Baran, P. S., *Science* **2017**, 356, eaam7355; (c) Edwards, J. T.; Merchant, R. R.; McClymont, K. S.; Knouse, K. W.; Qin, T.; Malins, L. R.; Vokits, B.; Shaw, S. A.; Bao, D. H.; Wei, F. L.; Zhou, T.; Eastgate, M. D.; Baran, P. S. *Nature* **2017**, *545*, 213-218; (d). Qin, T.; Cornella, J.; Li, C.; Malins, L. R.; Edwards, J. T.; Kawamura, S.; Maxwell, B. D.; Eastgate, M. D.; Baran, P. S. *Science* **2016**, *352*, 801-8055; (e) Fawcett, A.; Pradeilles, J.; Wang, Y.; Mutsuga, T.; Myers, E. L.; Aggarwal, V. K. *Science* **2017**, 357, 283-286; (f) Candish, L.; Teders, M.; Glorius, F. *J. Am. Chem. Soc* .**2017**, *139*, 7440-7443; (g). Huihui, K. M.; Caputo, J. A.; Melchor, Z.; Olivares, A. M.; Spiewak, A. M.; Johnson, K. A.; DiBenedetto, T. A.; Kim, S.; Ackerman, L. K.; Weix, D. J. *J. Am. Chem. Soc.* **2016**, *138*, 5016-5019; (h) Cheng, W. M.; Shang, R.; Fu, Y. *Nat. Commun.* **2018**, *9*, 5215; (i) Koy, M.; Sandfort, F.; Tlahuext-Aca, A.; Quach, L.; Daniliuc, C. G.; Glorius, F. *Chem. Eur. J.* **2018**, *24*, 4552-4555; (j) Wang, G. Z.; Shang, R.; Fu, Y., *Org. Lett.* **2018**, *20*, 888-891; (k) Liu, X. G.; Zhou, C. J.; Lin, E.; Han, X. L.; Zhang, S. S.; Li, Q.; Wang, H. *Angew. Chem. Int. Ed.* **2018**, *57*, 13096-13100; (l) Mao, R.; Frey, A.; Balon, J.; Hu, X. *Nat. Catal.* **2018**, *1*, 120-126; (m) Mao, R.; Balon, J.; Hu, X. *Angew. Chem. Int. Ed.* **2018**, *57*, 13624-13628; (n) Proctor, R. S. J.; Davis, H. J.; Phipps, R. J. *Science* **2018**, *360*, 419-422; (o) Ni, S.; Garrido-Castro, A. F.; Merchant, R. R.; de Gruyter, J. N.; Schmitt, D. C.; Mousseau, J. J.; Gallego, G. M.; Yang, S.; Collins, M. R.; Qiao, J. X.; Yeung, K. S.; Langley, D. R.; Poss, M. A.; Scola, P. M.; Qin, T.; Baran, P. S. *Angew. Chem. Int. Ed.* **2018**, *57*, 14560-14565; (p) Huang, H.-M.; Koy, M.; Serrano, E.; Pflüger, P. M.; Schwarz, J. L.; Glorius, F. *Nat. Catal.* **2020**, *3*, 393-400; (q) Tlahuext-Aca, A.; Candish, L.; Garza-Sanchez, R. A.; Glorius, F. *ACS Catal.* **2018**, *8*, 1715-1719; (r) Tlahuext-Aca, A.; Garza-Sanchez, R. A.; Schafer, M.; Glorius, F. *Org. Lett.* **2018**, *20*, 1546-1549; (s) Wang, J.; Cary, B. P.; Beyer, P. D.; Gellman, S. H.; Weix, D. J. *Angew. Chem. Int. Ed.* **2019**, *58*, 12081-12085; (t) Xue, W.; Oestreich, M. *Angew. Chem. Int. Ed.* **2017**, *56*, 11649-11652; (u) Qin, T.; Malins, L. R.; Edwards, J. T.; Merchant, R. R.; Novak, A. J.; Zhong, J. Z.; Mills, R. B.; Yan, M.; Yuan, C.; Eastgate, M. D.; Baran, P. S. *Angew. Chem. Int. Ed.* **2017**, *56*, 260-265; (v) Fu, M. C.; Shang, R.; Zhao, B.; Wang, B.; Fu, Y. *Science* **2019**, *363*, 1429-1434; (w) Liu, C.; Shen, N.; Shang, R. *Org. Chem. Front.* **2021**, *8*, 4166-4170.

20. Niu, P.; Li, J.; Zhang, Y.; Huo, C. *Eur. J. Org. Chem.* **2020,** *2020*, 5801-5814.
21. (a) McCarver, S. J.; Qiao, J. X.; Carpenter, J.; Borzilleri, R. M.; Poss, M. A.; Eastgate, M. D.; Miller, M. M.; MacMillan, D. W. C. *Angew. Chem. Int. Ed.* **2017,** *56*, 728-732; (b) Wang, J.; Lundberg, H.; Asai, S.; Martín-Acosta, P.; Chen, J. S.; Brown, S.; Farrell, W.; Dushin, R. G.; O'Donnell, C. J.; Ratnayake, A. S.; Richardson, P.; Liu, Z.; Qin, T.; Blackmond, D. G.; Baran, P. S. *Proc. Natl. Acad. Sci.* **2018,** *115*, E6404−E6410; (c) Phelan, J. P.; Lang, S. B.; Sim, J.; Berritt, S.; Peat, A. J.; Billings, K.; Fan, L.; Molander, G. A. *J. Am. Chem. Soc.* **2019,** *141*, 3723-3732; (d) Badir, S. O.; Sim, J.; Billings, K.; Csakai, A.; Zhang, X.; Dong, W.; Molander, G. A. *Org. Lett.* **2020,** *22*, 1046-1051; (e) Badir, S. O.; Lipp, A.; Krumb, M.; Cabrera-Afonso, M. J.; Kammer,

L. M.; Wu, V. E.; Huang, M.; Csakai, A.; Marcaurelle, L. A.; Molander, G. A. *Chem. Sci.* **2021**, *12*, 12036-12045.
22. (a) Leitch, A. J.; Bhonoah, Y.; Frost, C. G. *ACS Catal.* **2017**, *7*, 5618−5627; (b) Kaushik, N. K.; Kaushik, N.; Attri, P.; Kumar, N.; Kim, C. H.; Verma, A. K.; Choi, E. H. *Molecules* **2013**, *18*, 6620-6662.
23. Humphrey, G. R.; Kuethe, J. T. *Chem. Rev.* **2006**, *106*, 2875-2911.
24. (a) Evans, B. E.; Rittle, K. E.; Bock, M. G.; DiPardo, R. M.; Freidinger, R. M.; Whitter, W. L.; Lundell, G. F.; Verber, D. F.; Anderson, P. S.; Chang, R. S. L.; Lotti, V. J.; Cerino, D. H.; Chen, T. B.; Kling, P. J.; Kunkel, K. A.; Springer, J. P.; Hirshfield, J. *J. Med. Chem.* **1988**, *31*, 2235; (b) Horton, D. A.; Bourne, G. T.; Smythe, M. L. *Chem. Rev.* **2003**, *103*, 893.
25. Sandtorv, A. H. *Adv. Synth. Catal.* **2015**, *357*, 2403-2435.
26. Cacchi, S.; Fabrizi, G. *Chem. Rev.* **2005,** *105*, 2873-2920.
27. Bansal, R. K. *Heterocyclic Chemistry **2015***, Ch. 7, 272.
28. (a) Fischer, E.; Jourdan, F. *Ber. Dtsch. Chem. Ges.* **1883**, *16*, 2241−2245; (b) Gassman, P. G.; Bergen, T. J. V.; Gruetzmacher, G. *J. Am. Chem. Soc.* **1973**, *95*, 6508–6509; (c). Wang, Z. *Comprehensive Organic Name Reactions and Reagents* **2010**, page no. 1791−1794; (d) Bartoli, G.; Palmieri, G.; Bosco, M.; Dalpozzo, R. *Tetrahedron Letters* **1989**, *30*, 2129–2132; (e) Gribble, G. W. *Indole Ring Synthesis: From Natural Products to Drug Discovery* **2016**, *Chapter 23*, 249−259; (f) Batcho, A. D.; Leimgruber, W. *Org. Synth.* **1985**, *63*, 214–220; (g) Larock, R. C.; Yum, E. K. *J. Am. Chem. Soc.* **1991**, *113*, 6689–6690.
29. (a) Putra, A. E.; Takigawa, K.; Tanaka, H.; Ito, Y.; Oe, Y.; Ohta, T. *Eur. J. Org. Chem.* **2013**, 28, 6344-6354; (b) Johnson, H. E.; Crosby, D. G. *J. Org. Chem.* **1963**, *28*, 1246-1248; (c) De Rosa, M.; Soriente, A. *Eur. J. Org. Chem.* **2010**, *32*, 1029-1032; (d) Soni, V.; Khake, S. M.; Punji, B. *ACS Catal.* **2017**, *7*, 4202-4208.
30. (a) Hock, K. J.; Knorrscheidt, A.; Hommelsheim, R.; Ho, J.; Weissenborn, M. J.; Koenigs, R. M. *Angew. Chem. Int. Ed.* **2019**, *58*, 3630-3634; (b) Vargas, D. A.; Tinoco, A.; Tyagi, V.; Fasan, R. *Angew. Chem. Int. Ed.* **2018**, *57*, 9911-9915; (c) Sarkar, M.; Daw, P.; Ghatak, T.; Bera, J. K. *Chem. Eur. J.* **2014**, *20*, 16537-16549; (d) Delgado-Rebollo, M.; Prieto, A.; Pérez, P. J. *ChemCatChem* **2014**, *6*, 2047-2052; (e) Chen, W.; Gaisina, I. N.; Gunosewoyo, H.; Malekiani, S. A.; Hanania, T.; Kozikowski, A. P. *ChemMedChem* **2011**, *6*, 1587-1592; (f) Yadav, J. S.; Reddy, B. V. S.; Satheesh, G. *Tetrahedron Lett.* **2003**, *44*, 8331-8334; (g) Brandenberg, O. F.; Chen, K.; Arnold, F. H. *J. Am. Chem. Soc.* **2019,** *141*, 8989-8995.
31. (a) Ciszewski, L. W.; Durka, J.; Gryko, D. *Org. Lett.* **2019,** *21*, 7028-7032; (b) Gibe, R.; Kerr, M. A. *J. Org. Chem.* **2002**, *67*, 6247-6249; (c) Johansen, M. B.; Kerr, M. A. *Org. Lett*. **2010**, *12*, 4956-4959.
32. (a). Boruta, D. T.; Dmitrenko, O.; Yap, G. P. A.; Fox, J. M. *Chem. Sci.* **2012**, *3*, 1589-1593; (b) Cai, Y.; Zhu, S.-F.; Wang, G.-P.; Zhou, Q.-L. *Adv. Synth. Cat.* **2011**, *353*, 2939-2944; (c) DeAngelis, A.; Shurtleff, V. W.; Dmitrenko, O.; Fox, J. M. *J. Am. Chem. Soc.* **2011**, *133*, 1650-1653; (d) Fraile, J. M.; Le Jeune, K.; Mayoral, J. A.; Ravasio, N.; Zaccheria, F. *Org. Biomol. Chem*.

2013, *11*, 4327–4332; (e) Gao, X.; Wu, B.; Huang, W. X.; Chen, M. W.; Zhou, Y. G. *Angew. Chem. Int. Ed.* **2015**, *54*, 11956-11960; (f) Lian, Y.; Davies, H. M. L. *Org. Lett.* **2012**, *14*, 1934-1937; (g) Liu, K.; Xu, G.; Sun, J. *Chem. Sci*. **2018**, *9*, 634-639; (h) Singh, R. R.; Liu, R.-S. *Chem. Commun.* **2017**, *53*, 4593-4596; (i) Zhang, X.-J.; Liu, S.-P.; Yan, M. *Chin. J. Chem*. **2008**, *26*, 716-720; (j) Dasgupta, A.; Babaahmadi, R.; Slater, B.; Yates, B. F.; Ariafard, A.; Melen, R. L. *Chem* **2020,** *6*, 2364-2381; (k) Yang, Z.; Moller, M.; Koenigs, R. M. *Angew. Chem. Int. Ed.* **2020**, *59*, 5572-5576; (l) Jana, S.; Li, F.; Empel, C.; Verspeek, D.; Aseeva, P.; Koenigs, R. M. *Chem. Eur. J.* **2020,** *26*, 2586-2591; (m) Wood, J. L.; Stoltz, B. M.; Dietrich, H.-J.; Pflum, D. A.; Petsch, D. T. *J. Am. Chem. Soc.* **1997**, *119*, 9641–9651; (n) Jurberg, I. D.; Davies, H. M. L. *Chem. Sci.* **2018**, *9*, 5112-5118; (o) Li, M.; Guo, X.; Jin, W.; Zheng, Q.; Liu, S.; Hu, W. *Chem. Commun.* **2016**, *52*, 2736-2739.

33. (a) Ghorai, J.; Chaitanya, M.; Anbarasan, P. *Org. Biomol. Chem.***2018**, *16*, 7346-7350; (b) Chan, W.-W.; Yeung, S.-H.; Zhou, Z.; Chan, A. S. C.; Yu, W.-Y. *Org. Lett.***2010**, *12*, 604-607; (c) Dhole, S.; Chiu, W. J.; Sun, C. M. *Adv. Synth. Catal.* **2019,***361*, 2916-2925.
34. (a) Ghorai, J.; Anbarasan, P. *Org. Lett.* **2019**, *21*, 3431−3435; (b) Song, M.-P.; Niu, J.-L.; Zhang, X.; Du, C.; Zhang, H.; Li, X.-C.; Wang, Y.-L. *Synthesis* **2018**, *51*, 889-898; (c) Ozuduru, G.; Schubach, T.; Boysen, M. M. *Org. Lett.* **2012**, *14*, 4990-4993; (d) Hedley, S. J.; Ventura, D. L.; Dominiak, P. M.; Nygren, C. L.; Davies, H. M. L. *J. Org. Chem*. **2006**, *71*, 5349-5356; (e) Gnad, F.; Poleschak, M.; Reiser, O. *Tetrahedron Lett*. **2004**, *45*, 4277-4280.
35. (a) Benoit, G.; Charette, A. B. *J. Am. Chem. Soc.* **2017**, *139*, 1364-1367; (b) Barluenga, J.; Quiñones, N.; Tomás-Gamasa, M.; Cabal, M.-P. *Eur. J. Org. Chem.* **2012,** *2012*, 2312-2317; (c) Greb, A.; Poh, J. S.; Greed, S.; Battilocchio, C.; Pasau, P.; Blakemore, D. C.; Ley, S. V. *Angew. Chem. Int. Ed.* **2017**, *56*, 16602-16605; (d) Rulliere, P.; Benoit, G.; Allouche, E. M. D.; Charette, A. B. *Angew. Chem. Int. Ed.* **2018**, *57*, 5777-5782; (e) Herle, B.; Holstein, P. M.; Echavarren, A. M. *ACS Catal.* **2017**, *7*, 3668-3675.
36. Chanthamath, S.; Thongjareun, S.; Shibatomi, K.; Iwasa, S. *Tetrahedron Lett.* **2012**, *53*, 4862-4865.
37. Wang, J.; Shang, M.; Lundberg, H.; Feu, K. S.; Hecker, S. J.; Qin, T.; Blackmond, D. G.; Baran, P. S. *ACS Catal.* **2018**, *8*, 9537-9542; (b) Cheng, W.-M.; Shang, R.; Zhao, B.; Xing, W.-L.; Fu, Y. *Org. Lett.* **2017**, *19*, 4291-4294; (c) Hu, D.; Wang, L.; Li, P. *Org. Lett.* **2017**, *19*, 2770-2773.
38. (a) Giese, B. *Angew. Chem. Int. Ed.* **1983,** *22*, 753-764; (b) Giese, B.; González-Gómez, J. A.; Witzel, T., *Angew. Chem. Int. Ed.* **1984,** *23*, 69-70; (c) Millet, A.; Lefebvre, Q.; Rueping, M. *Chem.* **2016,** *22*, 13464-13468; (d) Ramirez, N. P.; Gonzalez-Gomez, J. C. *Eur. J. Org. Chem.* **2017,** *2017*, 2154-2163; (e) Chu, L.; Ohta, C.; Zuo, Z.; MacMillan, D. W. *J. Am. Chem. Soc.* **2014**, *136*, 10886-10889; (f) El-Hage, F.; Scholl, C.; Pospech, J. *J. Org. Chem.* **2020**, *85*, 13853-13867; (g) Gant Kanegusuku, A. L.; Roizen, J. L. *Angew. Chem. Int. Ed.* **2021**, *60*, 21116-21149.
39. (a) Pratsch, G.; Lackner, G. L.; Overman, L. E. *J. Org. Chem.* **2015**, *80*, 6025-36; (b) Zheng, C.; Wang, G. Z.; Shang, R. *Adv. Synth. Catal.* **2019**, *361*, 4500-4505.

40. (a) Kölmel, D. K.; Loach, R. P.; Knauber, T.; Flanagan, M. E. *ChemMedChem* **2018,** *13*, 2159-2165; (b) Bloom, S.; Liu, C.; Kölmel, D. K.; Qiao, J. X.; Zhang, Y.; Poss, M. A.; Ewing, W. R.; MacMillan, D. W. C. *Nat. Chem.* **2018**, *10*, 205-211; (c) Brandhofer, T.; Mancheño, O. G., *ChemCatChem* **2019**, *11*, 3797-3801; (d) Schwarz, J.; König, B. *Green Chem.* **2016,** *18*, 4743-4749; (e) Müller, D. S.; Untiedt, N. L.; Dieskau, A. P.; Lackner, G. L.; Overman, L. E. *J. Am. Chem. Soc.* **2015**, *137*, 660-663; (f) Jamison, C. R.; Overman, L. E. *Acc. Chem. Res.* **2016**, *49*, 1578-1586; (g) Yang, J.; Zhang, J.; Qi, L.; Hu, C.; Chen, Y. *Chem. Commun.* **2015**, *51*, 5275-5278; (h). Chen, T. –G.; Barton, L. M.; Lin, Y.; Tsien, J.; Kossler, D.; Bastida, I.; Asai, S.; Bi, C.; Chen, J. S.; Shan, M.; Fang, H.; Fang, F. G.; Choi, H. –W.; Hawkins, L.; Qin, T.; Baran, P. S. *Nature* **2018**, *560*, 350-354.
41. (a) Aycock, R. A.; Pratt, C. J.; Jui, N. T. *ACS Catal.* **2018,** *10*, 9115-9119; (b) Kölmel, D. K.; Meng, J.; Tsai, M.-H.; Que, J.; Loach, R. P.; Knauber, T.; Wan, J.; Flanagan, M. E. *ACS Comb. Sci.* **2019**, *21*, 588-597; (c) Garreau, M.; Le Vaillant, F.; Waser, J. *Angew. Chem. Int. Ed.* **2019**, *58*, 8182-8186; (d) Bottecchia, C.; Noël, T. *Chem. Eur. J.* **2019**, *25*, 26-42.
42. Li, H.; Breen, C. P.; Seo, H.; Jamison, T. F.; Fang, Y.-Q.; Bio, M. M. *Org. Lett.* **2018**, *20*, 1338-1341.
43. Fukuzumi, S.; Inada, O.; Suenobu, T. *J. Am. Chem. Soc.* **2003**, *125*, 4808−4816.
44. Kim, J.; Lee, S. H.; Tieves, F.; Paul, C. E.; Hollmann, F.; Park, C. B. *Sci. Adv.* **2019,** *5*, eaax0501.
45. (a) Brewster, M. E.; Simay, A.; Czako, K.; Winwood, D.; Farag, H.; Bodor, N. *J. Org. Chem.* **1989**, *54*, 3721− 3726; (b) Paul, C. E.; Gargiulo, S.; Opperman, D. J.; Lavandera, I.; Gotor-Fernandez, V.; Gotor, V.; Taglieber, A.; Arends, I. W. C. E.;´ Hollmann, F. *Org. Lett.* **2013**, *15*, 180−183.
46. Martens, F. M.; Verhoeven, J. W.; Gase, R. A.; Pandit, U. K.; de Boer, T. J. *Tetrahedron* **1978,** *34*, 443-446.
47. (a) Fukuzumi, S.; Mochizuki, S.; Tanaka, T. *J. Chem. Soc., Perkin Trans. 2* **1989**, 1583-1589; (b) Fukuzumi, S.; Hironaka, K.; Tanaka, T. *J. Am. Chem. Soc.* **1983**, *105*, 4722-4727; (c) Fukuzumi, S.; Koumitsu, S.; Hironaka, K.; Tanaka, T. *J. Am. Chem. Soc.* **1987**, *109*, 305-316.
48. (a) van Leeuwen, T.; Buzzetti, L.; Perego, L. A.; Melchiorre, P. *Angew. Chem. Int. Ed*. **2019,** *58*, 4953-4957; (b) Buzzetti, L.; Prieto, A.; Roy, S. R.; Melchiorre, P. *Angew. Chem. Int. Ed.* **2017**, *56*, 15039-15043; (c) Bonet, A. G.; Tellis, J. C.; Matsui, J. K.; Vara, B. A.; Molander, G. A. *ACS Catal.* **2016**, *6*, 8004-8008.
49. Scott, T. G.; Spencer, R. D.; Leonard, N. J.; Weber, G. *J. Am. Chem. Soc.***1970**, *92*, 687−695.
50. (a) Alnajjar, M. S.; Kuivila, H. G. *J. Org. Chem.* **1981**, *46*, 1053−1057; (b) Walborsky, H. M.; Topolski, M. *J. Am. Chem. Soc.* **1992**, *114*, 3455−3459; (c) Wong, P. C.; Griller, D. *J. Org. Chem.* **1981**, *46*, 2327−2329.
51. Hoye, T. R.; Eklov, B. M.; Ryba, T. D.; Voloshin, M.; Yao, L. J. *Org. Lett.* **2004**, *6*, 953−956.

52. Buzzetti, L.; Crisenza, G. E. M.; Melchiorre, P. *Angew. Chem. Int. Ed.* **2019**, *58*, 3730−3747.
53. Cismesiaa, M. A.; Yoon, T. P. *Chem. Sci.* **2015**, *6*, 5426-5434.
54. (a) Rosokha, S. V.; Kochi, J. K. *Acc. Chem. Res.* **2008**, *41*, 641−653; (b) Lima, C. G. S.; Lima, T. M.; Duarte, M.; Jurberg, I. D.; Paixao, M. W. *ACS Catal.* **2016**, *6*, 1389−1407; (c) Foster, R. *J. Phys. Chem.* **1980**, *84*, 2135−2141.
55. Cao, Z.-Y.; Ghosh, T.; Melchiorre, P. *Nat. Commun.* **2018**, *9*, 3274.
56. Lakowicz, J. R. *Principles of Fluorescence Spectroscopy*, *Plenum:* New York, 1983, Chapter 9; (b) Fraiji, L. K.; Hayes, D. M.; Werner, T. C. *J. Chem. Educ.* **1992**, *69*, 424−428.
57. (a) Pac, C.; Ihama, M.; Yasuda, M.; Miyauchi, Y.; Sakurai, H. *J. Am. Chem. Soc.* **1981**, *103*, 6495−6497; (b) Lackner, G. L.; Quasdorf, K. W.; Overman, L. E. *J. Am. Chem. Soc.* **2013**, 135, 15342−15345; (c) Ito, Y.; Kimura, A.; Osawa, T.; Hari, Y. *J. Org. Chem.* **2018**, 83, 10701−10708.
58. Martens, F. M.; Verhoeven, J. W.; Varma, C. A. G. O.; Bergwerf, P. J. *Photochem.***1983**, *22*, 99−113.
59. Prasad, H., *Resonance* **2002,** *7*, 48-64.
60. (a) Ramesh, R.; Reddy, D. S., *J. Med. Chem.* **2018,** *61*, 3779-3798; (b) Mills, J. S.; Showell, G. A. *Expert Opin Investig Drugs* **2004,** *13*, 1149-57; (c) Liu, B.; Gai, K.; Qin, H.; Wang, J.; Liu, X.; Cao, Y.; Lu, Q.; Lu, D.; Chen, D.; Shen, H.; Song, W.; Mei, J.; Wang, X.; Xu, H.; Zhang, Y *J. Med. Chem.* **2020**, *63*, 5312-5323; (d) Franz, A. K.; Wilson, S. O. *J. Med. Chem.* **2013,** *56*, 388-405; (e) Barraza, S. J.; Denmark, S. E. *J. Am. Chem. Soc.* **2018,** *140*, 6668-6684.
61. (a) Zhang, S.; Zhang, X.- M.; Bordwell, F. G. *J. Am. Chem. Soc.* **2002**, *117*, 602-606; (b) Hopkinson, A. C.; Lien, M. H. *J. Org. Chem.* **2002**, *46*, 998-1003.
62. (a) Connolly, J. W.; Urry, G. *Inorg. Chem.* **1963**, *2*, 645-646; (b) Wilt, J. W.; Kolewe, O. *J. Am. Chem. Soc.* **1965**, *87*, 2071-2072; (c) Yamamoto, K.; Nakanishi, K.; Kumada, M. *Journal of Organometallic Chemistry* **1967**, *7*, 197-202; (d) Wilt, J. W.; Kolewe, O.; Kraemer, J. F. *J. Am. Chem. Soc.* **1969**, *91*, 2624-2631; (e) Shih, C.; Fritzen, E. L.; Swenton, J. S. *J. Org. Chem.* **1980,** *45*, 4462-4471; (f) Mayon, P.; Chapleur, Y. *Tetrahedron Lett.* **1994**, *35*, 3703-3706.
63. (a) Goh, K. K.; Kim, S.; Zard, S. Z. *J. Org. Chem.* **2013,** *78*, 12274-12279; (b) Lo, J. C.; Kim, D.; Pan, C. M.; Edwards, J. T.; Yabe, Y.; Gui, J.; Qin, T.; Gutierrez, S.; Giacoboni, J.; Smith, M. W.; Holland, P. L.; Baran, P. S. *J. Am. Chem. Soc.*, **2017**, 139, 2484-2503; (c) Yang, N.; Fang, Y.; Xu, F.; Zhou, R.; Jin, X.; Zhang, L.; Shi, J.; Fang, J.; Wu, H.; Zhang, Z. *Org. Chem. Front.*, **2021,** *8*, 5303-5309.
64. Advances in Silicon Science, Hydrosilylation, *Springer*, **2009**.
65. Thomas, N. R. *Silicon* **2010,** *2*, 187-193.
66. (a) Organosilicon Chemistry: Novel Approaches and Reactions, eds., Hiyama, T.; Oestreich, M. Wiley-VCH, *Weinheim*, **2020**; (b) Silicon in Organic, Organometallics, and Polymer Chemistry, Ed., Brook, M. A. Wiley-

Interscience Publication, **2000**; (c) Cuenca, A. B.; Shishido, R.; Ito, H.; Fernandez, E. *Chem. Soc. Rev.*, **2017**, *46*, 415−430; (d) Lee, V. Y.; *Organosilicon Compounds*, Academic Press, **2017**.

67. (a) Bols, M.; Pedersen, C. M. *Beilstein J. Org. Chem.* **2017,** *13*, 93-105; (b) Pétursson, S. *J. Chem. Edu.* **1997**, *74*.
68. For the application of (borylmethyl)silanes; (a) Matteson, D. S.; Majumdar, D. *J. Chem. Soc., Chem. Commun.* **1980**, 39-40; (b) Matteson, D. S.; Majumdar, D. *Organometallics* **2002**, *2*, 230-236; (c) Zou, G.; Reddy, Y. K.; Falck, J. R. *Tetrahedron Lett.* **2001**, *42*, 7213-7215; (d) Molander, G. A.; Yun, C. S.; Ribagorda, M.; Biolatto, B. *J. Org. Chem.* **2003**, *68*, 5534-5539; (e) Molander, G. A.; Ham, J.; Seapy, D. G. *Tetrahedron* **2007**, *63*, 768-775; (f) Ueno, S.; Chatani, N.; Kakiuchi, F. *J. Am. Chem. Soc.* **2007**, *129*, 6098-6099; (g) Murray, S. A.; Luc, E. C. M.; Meek, S. J. *Org. Lett.* **2018**, *20*, 469-472; (h) Yang, Y.; Tsien, J.; David, A. B.; Hughes, J. M. E.; Merchant, R. R.; Qin, T. *J. Am. Chem. Soc.* **2021**, *143*, 471-480.
69. For synthesis of (borylmethyl)silanes; (a) Allais, C. *Encyclopedia of Reagents for Organic Synthesis*, Trimethylsilylmethylboronic Acid, **2016**; (b) Whitmore, F. C.; Sommer, L. H. *J. Am. Chem. Soc.* **1946**, *68*, 481; (c) Peterson, D. *J. Org. Chem.* **1968**, *33*, 780; (d) Matteson, D. S.; Majumdar, D. *J. Chem. Soc., Chem. Commun.* **1980**, 39; (e) Matteson, D. S.; Majumdar, D. *Organometallics* **1983**, *2*, 230; (f) Helal, C. J.; Magriotis, P. A.; Corey, E. J. *J. Am. Chem. Soc.* **1996**, *118*, 10938; (g) Ihara, H.; Ueda, A.; Suginome, M. *Chem. Lett.* **2011**, *40*, 916-918; (h) Ohmura, T.; Torigoe, T.; Suginome, M. *J. Am. Chem. Soc.* **2012**, *134*, 17416-17419; (i) Ohmura, T.; Torigoe, T.; Suginome, M. *Organometallics* **2013**, *32*, 6170-6173; (j) Torigoe, T.; Ohmura, T.; Suginome, M. *J. Org. Chem.* **2017**,*82*, 2943-2956; (k) Shu, C.; Noble, A.; Aggarwal, V. K. *Nature* **2020**, *586*, 714-719.
70. Kramer, K. A. W.; Wright, A. N. *J. Chem. Soc.* **1963**, 3604.
71. For review about Si−H insertion; Keipour, H.; Carreras, V.; Ollevier, T., *Org. Biomol. Chem.* **2017,***15*, 5441-5456.
72. For Si−H insertion with acceptor diazocompond; (a) Bagheri, V.; Doyle, M. P.; Taunton, J.; Claxton, E. E. *J. Org. Chem.*, **1988**, *53*, 6158; (b) Andrey, O.; Landais, Y.; Planchenault, D. *Tetrahedron Lett*. **1993**, *34*, 2927; (c) Andrey, O.; Landais, Y.; Planchenault, D.; Weber, V. *Tetrahedron*, **1995**, *51*, 12083; (d) Kan, S. B. J.; Lewis, R. D., Chen, K; Arnold. F. H. *Science* **2016**, *354*, 1048-1051.
73. For Si−H insertion with donor-acceptor diazocompond; (a) Landais, Y.; Planchenault, D. *Tetrahedron Lett.* **1994**, *35*, 4565; (b) Landais, Y.; Planchenault, D. *Tetrahedron* **1997**, *35*, 4565; (c) Buck, R. T., Coe, D. M.; Drysdale, M. J.; Ferris, L.; Haigh, D.; Moody, C. J.; Pearson, N. D.; Sanghera, J. B. *Tetrahedron Asymmetry* **2003**, *14*, 791; (d) Ge, M.; Corey, E. J. *Tetrahedron Lett.* **2006**, *47*, 2319; (e) Hrdina, R.; Guénéé, L.; Moraleda, D; Lacour, J. *Organometallics*, **2013**, *32*, 473; (f) Sambasivan, R.; Ball, Z. T. *J. Am. Chem. Soc.* **2010**, *132*, 9289; (g) Davies, H. M. L.; Hansen, T.; Rutberg, J.; Bruzinski, P. R. *Tetrahedron Lett.* **1997**, *38*, 1741; (h) Hyde, S.; Veliks, J.; Liégault, B.; Grassi, D.; Taillefer, M.; Gouverneur, V. *Angew. Chem. Int. Ed.*, **2016**, *55*,

3785; (i) Yasutomi, Y.; Suematsu, H.; Katsuki, T. *J. Am. Chem. Soc.* **2010**, *132*, 4510; (j) Keipour, H.; Ollevier, T. *Org. Lett.* **2017**, *19*, 5736.
74. Nakagawa, Y.; Chanthamath, S.; Fujisawa, I.; Shibatomi, K.; Iwasa, I. *Chem. Commun.* **2017**, *53*, 3753.
75. (a) Kidonakis, M.; Stratakis, M. *Org. Lett.* **2018**, *20*, 4086-4089; (b) Tseberlidis, G.; Caselli, A.; Vicente, R. *Journal of Organometallic Chemistry* **2017**, *835*, 1-5.
76. Robertson, J.; O'Connor, G.; Sardharwala, T.; Middleton, D. S. *Tetrahedron* **2000,** *56*, 8309-8320.
77. Wang, J.; Cary, B. P.; Beyer, P. D.; Gellman, S. H.; Weix, D. J. *Angew. Chem. Int. Ed.* **2019,** *58*, 12081-12085.